Challenges related to storage and transfer of solar energy with a case study on long distance power transfer

Master of Science Thesis in Theoretical physics and energy physics

Eirik B. Kvernevik

Institute of physics and technology
University of Bergen

June 21, 2010

Contents

Acknowledgements

I would like to thank my supervisor Jan S. Vaagen for introducing me to the subject of energy and energy related issues through several interesting debates conducted by EnergiForum (EF) the last two years. He has introduced me to valuable information regarding current energy debate and given me important perspectives on how policy, economy and physics together form the energy industry we see today, and in the future.

I would also like to express my gratitude to my fellow students which have been giving me both social and academic input the last two years. A special thanks goes to my fellow student Anders Thomassen from Departement of Mathematics for helping me with various technical issues regarding programming in Matlab and Latex. Interesting science-related topics have also been dicussed with passion and curiosity. At last I would like to thank my parents and relatives for encouraging and supporting me.

Abstract

The challenges that will be discussed in this thesis are two-fold; the problems related to transmission of power over long distances, and the need for energy storage, especially at night. Both of the issues are accentuated by solar power where the distance between production cite and consumer may become large. The need for storage is a consequence of the intermittent nature of solar power, which relies upon the presence of the sunlight. These two concerns differ clearly from the storage and production advantage of power generation from coal power plants which are not dependent on energy storage since its power source is always available. The transition from fossile fuels to other ways to generate electric power is partly driven by increasing fuel costs reflecting gradual depletion of natural resources, and partly by environmental concerns - recently the possibility of an irreversible climate change due to fossil burning in particular. More and more countries are dependent on oil import as the production of oil gradually is relying on fewer countries. In this regard, solar power has potential to be a important contributor for hydrogen production for a possible future hydrogen based transportation sector. The possibility of chemical storage will also be discussed.

The electric grid is becoming a growing challenge with an increasing power fraction coming from renewables. A proposed alternative to energy storage is a more modern grid which can control fluctuations in the grid more efficiently. This includes construction of high voltage transmission interconnections between geographically distant regions. A recent report published by the European Climate Foundation (ECF) presents how the European electric grid should be changed to maintain europe's energy security when a large fraction of the total energy comes from renewables. This report will also be assessed.

Energy units

Throughout the text, different energy units has frequently been used.

Definitions

- **Joule**
  1 Joule is the work done by a force of one newton in moving an object a distance of one meter.

- **Watt**
  the rate of which energy is being used; 1 W = 1J/s

- **Watt-hour**
  One watt-hour is the amount of energy used if work is done at an average rate of one watt for one hour

Joule and watt hour have the same SI-units but with different magnitude,the table below shows how to convert between them

	symbol	SI-units	Joule	watthour
Joule	J	kgm^2/s^2	1	$2{,}778*10^{-4}$
Watt hour	Wh	kgm^2/s^2	3600	1

This means that one watt-hour equals 3600 joule and one joule equals $2{,}778*10^{-4}$ Wh.

The SI prefixes used in the text are listed below

SI prefixes		
Prefix	Symbol	magnitude
nano	n	10^{-9}
micro	μ	10^{-6}
milli	m	10^{-3}
centi	c	10^{-2}
kilo	k	10^{3}
mega	M	10^{6}
giga	G	10^{9}
tera	T	10^{12}
peta	P	10^{15}

Example: 1 kWh = 1000 Wh = 3600*1000 J

If a 60 Watt light bulb is on for 24 hours, the following energy is being consumed by the lightbulb:

60 W * 24h = 1440 Wh = = 1,44 kWh = 3600*1440 J

Number convention

Throughout the text I have used comma when writing decimals, for instance:
2,45 = 245*10^{-2} with this convention.
When writing big numbers i write, for instance,
300 000 or 3*10^5
In America you often see the number 3*10^5 be written like 300,000 and 3*10^8 like 300,000,000 , however, this convention is not used in this thesis. 300,000 would be equal to 300 or 3*10^2 with my comma convention.

remark: I have used two different multiplication notations in the text. Many places I have used *, but some places $\times$ is used.

Physical constants and quantities found in the text

Physical constants and quantities		
Name	Symbol	Value (SI-units)
Avogadros number	N_A	6,02214199*10^{23} mol^{-1}
Boltzmann constant	k	1,3806503*10^{-23} J/K
Charge of an electron	q	1,602176462*10^{-19} C
Plancks constant	h	6,62606876*10^{-34} Js
Speed of light in vacuum	c	2,99792458*10^8 m/s
Permittivity of free space	ϵ_0	8,854187818*10^{-12} F/m
Permeability of free space	μ_0	4π*10^{-7} F/m
Stefan-Boltzmann constant	σ	5,670400*10^{-8} W/m^2K^4
Solar Luminosity	L_0	3,839*$10^2$6 W
Solar constant	S	1367 W/m^2
mean sun-eart distance	AU	1,49598*10^{11}m

where one Farad (F) in SI-units are $\frac{A^2s^4}{m^2kg}$

Programs used in the thesis

1. Matlab - used to produce the graphs in the thesis and for various calculations. Webpage: www.mathworks.com

2. Mayura draw - for simple illustrations. Webpage: www.mayura.com

3. the plugin texclipse in combination with Eclipse - for writing the document. Webpage: http://texlipse.sourceforge.net/ and http://www.eclipse.org/

Chapter 1

Motivation

A key issue of renewable energy sources is that they generally need a large area because of their low energy density. This is true for wave, wind and solar power. To cope with this problem in a crowded world the best solution may be to import the electricity from another place, a place where huge land areas can be utilized for electricity production. For solar power, a region which fits this description is the deserts, near the equator in particular. In the deserts, the sun shines strong most of the day and there are huge open areas available for energy extraction. Several companies and scientific communities today believe that solar power from deserts can make a significant contribution to the total energy demand in future. The German Aeorospace center (DLR) recently made a report on the possibilities for a Trans-Mediterranean Interconnection for concentrated solar power from the Sahara desert in Africa to a European supergrid[1]. The potential for solar power are big. But, there are several issues related to storage and transmission of power that must be solved[1].

The other motivation is a search for alternative energy sources to the fossil fuels. Today, we are facing substantially depleted carbon resources (oil) and environmental problems due to fossil fuel burning (coal and oil). This includes a potentially critical climate problem, an issue of current debate. The burning of fossile fuel has caused the carbon dioxide concentration in the atmosphhere to rise. Carbon dioxide is a so-called greenhouse gas, and increases of green house gases in the athmosphere, affect the average global temperature. The reason for this chain of events is that greenhouse gases absorb and re-emit infrared radiation, which radiates out from the earth. The Intergovernmental Panel on Climate Change (IPCC) concludes in its report in 2007 that most of the temperature increase observed since the middle of the last century is caused by increasing concentrations of greenhouse gases due to human activity such as depletion of rainforests and the fossil fuel burning[2]. According to [3], coal production have increased steadily since the industrial revolution. [4] have calculated that from 1769 to 2006, the world annual coal production has increased 800-fold, and coal production is still increasing today. With Chinas fast running industrialization, where they raise a new coal power plant every week, [5], the coal production will still increase for years to come.

While the resources for coal still are substantial and can last for another 150 years, the conventional oil production are expecting to peak soon. WEO 2008 claims that conventional oil production will peak around 2020[6]. This must not be mistaken for being the total oil

[1] Political and economical challenges will always be there due to huge investments over many years and needed cooperation of many different countries with different needs. However, these challenges are not in the scope of this thesis.

production. The total oil production includes more unconventional ways to extract the oil, such as oilsand etc. With this in mind, the total oil production may peak 10 years later, around 2030. This number is highly debated and there are many variables related to the number. Offcourse, the oil peak can further be delayed by improving technology of extraction, and discoveries of new unknown oil reservoirs.

If the goal for the world is to reduce CO_2 emission it is crucial that we find alternatives to the fossil fuels. We have today no single realistic inheretor that can take the place of the fossile energy, and it is quite unlikely that such a replacement by one single source will take place. The most realistic scenario in the future will probably be a combination of different energy sources. In this energy mix, solar power can be an important contributor. David MacKay has given some plausible scenarios of possible energy plans, based on a goal of zero CO2 emission, for the world in his recent book[4]. A mix of different sources is also assumed to be a fundament for the future European energy security in the report published by the European Climate Foundation (ECF)(roadmap 2050) which will be discussed in the thesis.

1.1 Overview

In **Chapter 2** the theoretical limits for how much power that can be extracted from solar radiation will be analysed. We start with the energy flux at the surface of the sun and then finds the energy flux density outside the earht's atmosphere. further on, the interactions with the atmosphere will be considered and the distribution of radiation as a function of latitude and season. In **Chapter 3** and **4** I will go through the physics behind the two main technologies for solar electricity generation. In **Chapter 3** I will identify the main components which defines the power output of a solar cell. In **Chapter 4** the discussion is dedicated to concentrated solar power (CSP). The different technologies are presented before I go in further detail about the parabolic trough technology. Here, the efficiency of the different components of the plant are discussed. An overview of the cost components and the levelized energy costs (LEC) will be given. The discussion of storage possibilities for CSP starts in **Chapter 5**. An overview of current storage technologies and calculation of their capacities are presented. A comparision between 4 different thermal storage systems are given, one of them the storage system in use on the recent built CSP plants in Spain. A calculation of needed amount of material for the four systems is given and also an overview of the cost. In **Chapter 6**, the roadmap 2050 report is assessed and main results are pointed out. **Chapter 7** is dedicated to long distance power transfer, where AC and DC power are compared against each other. An example calculation of the losses in the NorNed cable between Norway and the Netherlands are given. In **Chapter 8** we do a case study on the possibility of transferring solar power from Africa to Europe based on two reports made by DLR. In **Chapter 9**, needed modifications on the model used in chapter 8 are pointed out.

Chapter 2

Theoretical limits for solar energy extraction

The sun provides our earth with an enormous amount of energy, but it is not an infinite amount of energy. The earths finite size, its distance from the sun and its athmosphere gives us the possibility to calculate a clearly defined maximum theoretical value for the solar power that can be used by humans at the surface.

It all starts at the center of the sun. In the extreme conditions with temperatures of more than $40 * 10^6 K$ that exists at it's center, the nuclear reactions that eventually give planet earth its energy, take place. The minimum temperature at which fusion reactions can occur is about 10^7 K, [7]and luckily for us the sun‘s core is slightly hotter. The energy can therefore be released in the fusion of hydrogen nuclei into helium nuclei in which matter is converted into energy.

The surface of the sun that we can see is called the photosphere, and the temperature here is about 6000 K. The gases at this particular temperature emit a characteristic spectrum of light intensities at different wavelengths. The rediation spectrum from the sun can be approximated by a black body with black body temperature 5780 K. At this temperature, the spectrum can be very well approximated by the blackbody radiation spectrum given by Planck's law (Appendix B) (the earth can also be assumed to radiate like a black body with a black body temperature T $\sim$ 300K) [8]

The amount of power produced by the sun is $3,9 * 10^{26}$ W. This energy flux is called the solar luminosity and its symbol is L_0. Because we consider the sun as a blackbody the relation between the energy flux and surface temperature are governed by Stefan-Boltzmanns law given by

$$P = A\sigma T^4 \tag{2.1}$$

where P is the total emitted power from a black body, and equals L_0 in the case of the sun. T is the absolute blackbody temperature at the surface, A is the surface area and σ is Stefan-Boltzmann constant. Note that the black body-equvalent temperature for the sun is $\sim$ 5780K.

As the radiation gets farther and farther away from the sun, it is spread out in an uniform way over a larger and larger spherical area. Because of this, only a very small fraction of the intial amount of energy falls on earth. In fact, each square meter of surface normal to the incident solar radiation at earth's mean orbital distance from the sun receives an annual

mean value of 1367 W, as measured by satellites. This number wil be defined as the solar constant below.

The energy balance of the earth is given by the first law of thermodynamics, which states that energy is conserved. The first law can be formulated in the following way " the heat added to a system is equal to the change in internal energy minus the work done by the system on the environment" In mathematical symbols we have[1]:

$$\delta Q = \delta U - \delta W$$

The mass flux of energy delivered to earth is negligible, so we can to good approximation say that the transmission of energy from sun to earth is entirely radiative. The work done by earth on its environment is also negligible. So, to calculate the approximate energy balance of earth, we need only consider radiative energy exchanges. This means that the climate on earth is almost entirely dependent on this exchange of radiation. Knowing this, it is clearly very important to have a good overview on how the energy from the sun varies over time to give a true picture of how much the climate is changed by human activities and what is caused by the sun itself. This has been researched and discussed by IPCC in later years. The Intergovernmental panel in climate changes (IPCC) third assessment report states that the measured magnitude of recent solar varitation is much smaller than the effect due to the increase in greenhouse gases in the atmosphere[9]. Measurements done by satelittes since 1979 confirm that the sun itself is not the entire cause of global warming [10].

However, there are various known periodic weather phenomena on earth that cause variations in the climate. For example, the year 2008 was measured to have the lowest global mean temperature since 2000. This was ascribed to the periodic climate pattern La Nina, and it caused abnormal cold weather in january 2008. Trenberth[11] argues that it is not a sufficient explanation to say that a year with abonormal temperature variation is a result of natural variable weather phenomena. There must instead be a closed energy budget than can account for where the radiative forcing from the top of the athmosphere has gone. There are currently no sufficiently accurate methods to measure and track where the energy that is added to the climate system goes, and this inability to properly track the energy, limits the possibilities to plan and solve issues related to climate changes.

It is possible to track changes in net radiation at the top of the athmosphere. The energy budget has been estimated in the period 2000-2004 and the imbalance between incoming solar radiation and reflected solar radiation together with the outgoing longwave radiation at the top of the athmosphere have been estimated to be $0,9 \pm 0,5$ W/m^2.[11]. So there is a netto energy absorption in the earth system.

From 1993 to 2003 the global energy budget can reasonable well be accounted for in terms of change in ocean heat content and melting of glaciers and arctic sea ice. But after 2003 the net radiation absorbed by the earth does not longer coincide with the change in ocean heat content and ice melting. Measurement shows that CO_2 concentrations have further increased since 2003 which should result in an increasing heat absorption. Still, measurements of ocean temperature from 2004 to 2008 indicate that the increase in the ocean heat content has been

[1]We have here chosen the convention that the work δW is negative when the system (earth in this case) does work on the environments

slowed down significantly. It can be shown that melting ice is a factor of 40 to 70 times more effective than thermal expansion of the oceans in terms of raising the sea level. From this one finds that the sea level rise would have been considerable more dramatic than what we see today, if all the net energy had gone into melting land ice. One can also calculate that there would not be enough sea ice in the world to account for the energy. One must therefore conclude that the observed sea level rise and heat content does not account for the measured energy imbalance at the top of the athmosphere and therefore, current observations cannot account for the recent energy variability. The energy must have gone somewhere else.

Trenberth concludes in his article that "To better understand and predict regional climate change, it is vital to be able to distinguish between short-lived climate anomalies, such as caused by El Nino or La Nina events, and those that are intrinsically part of climate change, whether a slow adjustment or trend, such as the warming of land surface temperatures relative to the ocean and changes in precipitation characteristics."

2.1 The solar constant

The solar constant is defined as the solar energy density (W/m^2) at normal incidence outside the earth's atmosphere. It is dependent on the solar luminosity L_0 and the sun-earth distance. Because the sun-earth distance vary over one orbit, The solar constant is actually not a constant, but a variable depending on earth's position in hte orbit relative the sun and the variations in the the solar luminosity. Therefore it is usually the mean value averaged over one orbit that is being referred to. The mean value recently measured by satellites is 1367 W/m^2.

According to [12], the solar constant can be given as a function of day number in the following way:

$$S = 1367(1 + 0,033cos(2\pi * \frac{d}{365}))W/m^2 \tag{2.2}$$

where d = 1 = January 1'st and d = 365 = December 31. From this we see that when the earth is closest to the sun, around the 1'st of January, S = 1412 W/m^2 and deviates $\sim$ 3,2% from the mean value. The earth is farthest away from sun around the first of July and at that date the value is 1322 W/m^2, here it also deviates $\sim$ 3,2% from the mean value.

Satelite measurements from 1980 to 2009 show that the annual mean value of the solar constant has varied between 1354 W/m^2 and up to about 1374 W/m^2[13]. This variation is mostly due to the solar cycles; a periodic phenomenon with an average length of about 11 years where different solar activities are observed to occure with different frequency and magnitude i.e number of sunspots visible on the photosphere, which can affect the solar luminosity.

The mean value of S can also be calculated to good approximation by using the mean sun-earth distance over one orbit (one year) and by using a constant solar luminosity :

As earlier mentioned, the fusion processes in the sun delivers an energy flux that we call the solar lumonisity. This energy flux varies very slightly and can be assumed constant, its value is $L_0 \sim 3,9 * 10^{26}W$ [14]. The average flux density on the photosphere can then be calculated by dividing the solar luminosity by the area of the photosphere:

$$\text{Flux density}_{photo} = \frac{L_0}{Area_{photo}} = \frac{L_0}{4*\pi*r^2{}_{photo}} = \frac{3{,}9*10^{26}}{4*\pi*[6{,}96*10^8]^2} = 6,4*10^7\ W/m^2$$

The space between the photosphere and the atmosphere of the earth can be considered to be a vacuum. If this is true then the amount of energy passing through any sphere with the sun at its centre should be equal to the solar luminosity. If we now assume that the flux density is uniform over a sphere of radius d with the sun at its center, we obtain following formula :

$$L_0 = S_d * 4 * \pi * d^2 \text{ , where } S_d \text{ is the flux density at distance d.}$$

Thus, we see that the flux density is inversely proportional to the square of the distance to the sun. The flux density S_d is the solar constant at distance d from the centre of the sun. In the case for the solar constant at earth's distance we drop the subscript d and we then obtain the solar constant for earth, knowing that the mean earth-sun distance is $1,5 * 10^{11}$ m:

$$S = \frac{3{,}9*10^{26}W}{4*\pi*[1{,}5*10^{11}m]^2} = 1379W/m^2$$

We see that this theoretical value is slightly bigger than the actual satelite measured value, mostly because of the round-off values used for the mean earth-sun distance and the solar luminosity. Exact values like this do not apply in the real world.

2.2 Interactions with the atmosphere

We found in the last section that when the photons from the sun have reached earth, the energy flux density that was initially $6,4 * 10^7\ W/m^2$ at the photosphere has decreased to about 1367 W/m^2 when reaching the top of the atmosphere of earth. The amount of solar radiation reaching the earth is called the *insolation*, short for "incident solar radiation".

Now, when the photons finally have reached the atmosphere, they will meet some resistance. Before the radiation reaches earth's surface, a fraction of it will be reflected back to space and some will be absorbed by the different compounds in the atmosphere. In fact, only around 50% of the total radiation wil reach the surface (depends somewhat on wheather conditions). The figure 2.1 gives a good view of the situation.

The smooth dotted line in the figure is the radiation spectrum from a blackbody, and is given by Planck's radiation law. The actual radiation spectrum from the sun at the top of earth's atmosphere almost coincides with the blackbody spectrum for infrared wavelengths (0,8 μm and above). There are some bigger differences between the two graphs for the UV and visible wavelengts. Furthermore, we see from the figure that about 9% of the radiation is ultraviolet, 40% is in the visible region, and about 50% is infrared.

The fraction of light reflected back to space from the atmosphere is called the *albedo*, and the earth has an albedo of 30%. Another 20% is absorbed in the atmosphere or scattered back to space. Much of the ultraviolet radiation is absorbed by oxygen, nitrogen and ozone in the upper atmosphere, this part of the atmosphere is known in public as the Ozone layer. Some of the infrared radiation is selectively absorbed and scattered by water vapor and carbon dioxide in the lower atmosphere.(This part depends very much on weather conditions).

The remaining 50% of the incident solar energy reaches the surface and is almost all absorbed. The reason for the relatively constant temperature of the earth is a result of the

Figure 2.1: Spectrum of solar radiation at the top of the atmosphere and at ground level. The minima in the ground level spectrum are a result of the absorption by water vapor, CO_2, O_2, N_2 and O_3 (Ozone) [15]

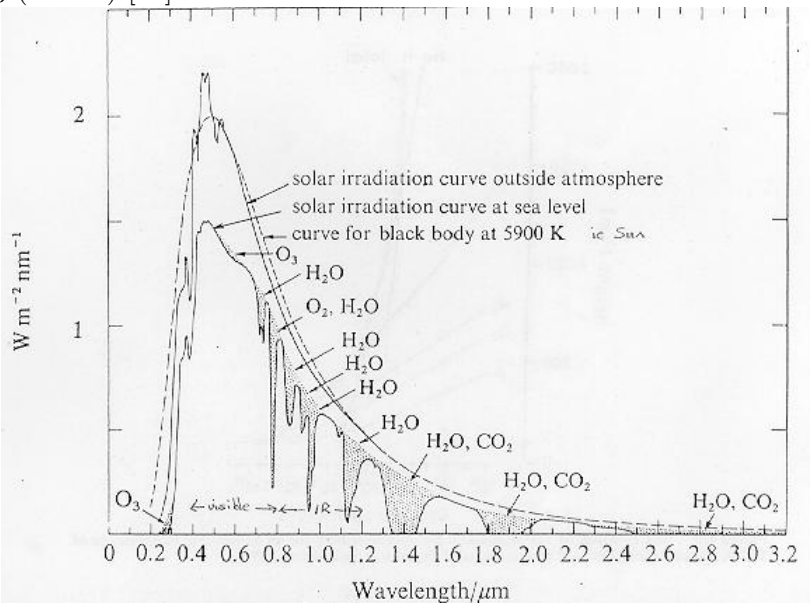

energy balance between the incoming solar radiation and the energy radiated by earth. As mentioned earlier the earth can approximately be considered as a blackbody, and Planck's law may therefore be applied. From this we find that earth radiates primarily infrared radiation, and from Wien's displacement law we see that the radiation spectrum is consentrated around 10 μm. Most of this infrared radiation emitted from earth is absorbed by CO_2 and H_2O in the atmosphere and some reradiates back to earth. This reradiation back to earth is known as the atmospheric greenhouse effect, and it maintains the surface temperature of the earth about 40K higher than it would be if there were no absorption. It can be calculated that the average surface temperature would be rather cold, about 258K, if we had no atmosphere. Today, as a result of fossil burning, the amount of CO_2 in the atmosphere is increasing, resulting in the problem that the greenhouse effect is working "too well" and thus heating up the earth.

Before we take a closer look at the factors that determine the amount of insolation on different regions at the surface, I will calculate the average energy flux (power) over the entire surface.

First we must appreciate the fact that only half of the earth will recieve solar radiation at any time of day. Now, the sunny side of earth would receive just as much solar radiation if it were flat, with the same radius. So, by taking the ratio between the cross section through the center and the entire surface area of earth and multyplying this with the insolation would give us the average we are looking for [12];

$$1367W/m^2 \times 0,7 \times \frac{\pi R^2}{4\pi R^2} \sim 240W/m^2 \tag{2.3}$$

The factor $0,7$ comes in because the albedo of earth is $0,3$. This means that the formula above also accounts for what is absorbed and/or scattered in the atmosphere in addition to

the surface.

The remaining insolation that is reaching earths surface contains two different components. One part is the direct sunbeam from the sun, this component is the one that can be used in electricity production, and with the use of two main technologies: Photovoltaic and consentrated solar power systems. Secondly we have a diffuse component. This is radiation that is first absorbed by the atmosphere and then scattered over the entire sky. This component can be used for thermal heating systems, but also photovoltaic systems.

2.3 The distribution of insolation over the surface

Lets take a closer look on the factors that control how much insolation different regions are recieving on the earths surface.

The average insolation calculated above is not always a good approximation of the solar radiation in many regions, In fact, the amount of insolation received at any particular location on earth's surface may vary between 0 and $\sim$ 1050 W/m^2, depending on the latitude, the season, time of day and the degree of cloudiness. The first three factors are a result of the geometry of earth's orbit around the sun.

Figure 2.2: Earths orbit around the sun

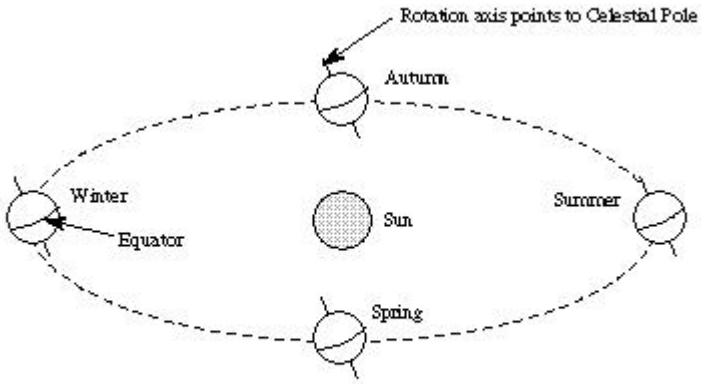

Earth's orbit around the sun is elliptic with an eccentricity near zero, this is why we use a mean value of the earth-sun distance when calculating the solar constant. In addition, the axis about which the earth itself spins is tilted relative to the orbital plane of motion at an angle of $23,5°$. Consequently, the North pole is tilted towards the sun during the northern hemisphere's summer and away from the sun in the winter. The exact opposite happens for the southern hemisphere. The northern hemisphere is, because of this, exposed to more hours of sunlight in the summer, and the amount of solar radiation striking a horizontal surface is greatest in this season. In the winter, the insolation is spread over a larger horizontal area due to the tilt angle and the sunrays must pass through a larger amount of the atmosphere resulting in that less radiation reach the surface of earth because of absorption and scattering from the atmosphere.

The angle the sun is making with the vertical (relative observer) is called the solar azimuth angle θ_z . The solar azimuth at a particular location and a particular instant of time on earth is a function of several different angles (explained in the appendices). Generally, the farther north, the higher is the value of θ_z, and the lower in the sky the sun will be. This is clearly observed in Norway, north of the polar circle where the sun is found under the horizon most of the time during winter.

The tilt angle also explains the location of the tropics, where the sun appears directly overhead at solar noon[2] in a given season. In other words the solar azimuth will be 0°. The tropic of capricorn is located $23,5$ degrees south, here the sun is found overhead at noon in December. In June, the location where the sun is directly overhead at noon has moved to the tropic of Cancer, which is located $23,5$ degrees north. In March and September the sun is directly overhead at solar noon at the Equator. Because of it's locations the solar insolation is greatest in between the two tropics with equator at the center.

Figure 2.3: Global distribution of solar irradiation averaged over one year, given in watt per square meter.[16]

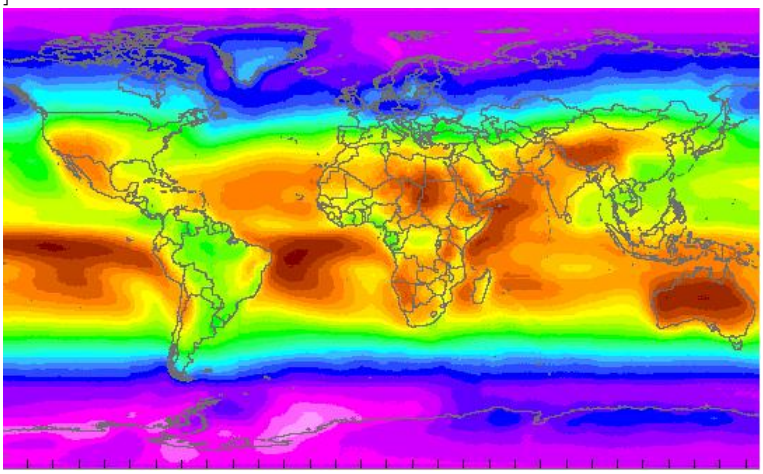

In the world map of figure 2.3, we see the global distribution of solar irradiation over one year, given in watt per square meter. The colors purple, blue, light blue and up to green represents low irratiation densities (zero to about 170 W/m^2).The middle colors from light green up to dark red represents high irradiation densities (180 to about 290 W/m^2)[3] We observe that the most sunny regions indeed lies in between the two tropics. The region stretches from the middle parts of Australia and southern parts of Africa up to the southern part of Spain and the USA. We can convert the average power to total annual radiation energy, by multiplying the average power with the number of hours in the year(8760h). We find that the annual insolation in the region with the highest power densities, lies between $\sim$ 1600 and 2600 kWh/m^2.

If we go further north in Europe, for example up to Germany, the insolation is about half of what it is near the tropics. Despite this fact, Germany is today, togheter with Spain,

[2]Solar noon is the time of day when the sun has its lowest azimuth angle, that is, is highest in the sky

[3]Irradiation values are very dependent on how they are measured, the particular values in this map are the irradiation striking a horizontal surface over one year. For a surface that can track the sun over the sky, the values will be higher

installing more large scale photavoltic power than any other country in the world. The installed PV power in Germany increased to 5.3 GW by the end of 2008, with $1,5$ GW new capacity installed[17]. This shows that even regions with far less solar insolation than the tropical regions can utilize solar power on a large scale. Small scale installations can be used everywhere in the world, even in Norway.

An interesting observation is that two of the regions with the highest insolation densities in the world have at the same time one of the lowest population densities, namely the Sahara desert in North Africa and Australia. One may think at first that this is a negative coincidence when thinking about solar energy extraction, and that it would be optimal if the electricity were made were it is needed. This is in general true because of transmission costs etc. But one of the problems with solar energy and other renewables is the need for huge areas because of the relatively low energy density. This problem can be overcome in these regions. The problem will then be to transport the electricity to needed areas. We will take a look at this problem in a later chapter.

Lets calculate how much power one could produce in theory if these two regions were filled with a mix of different solar power installations.

The area of mainland Australia is about $7,6$ million square kilometres. The area of the Sahara desert is about $9,1$ million square kilometres. One could ofcourse, even in theory, never use the entire area for solar power. Let us therefore say that in theory one could use 10% of the land area. We assume that each square meter of collector surface needs 3 m^2 of land area. Therefore, 3,3% of the total land area will harvest the solar energy.

So, we will then have left 250800 km^2 in Australia and 300300 km^2 in Sahara for solar power installations. Based on the irradiation map we assume the average insolation density in the region to be 290 W/m^2(It is higher for systems that can track the sun). Further, we assume that the effiency from heat to electricity is 15% . We will then have :

$P_{tot} = (250800 + 300300)10^6 m^2 * 290 W/m^2 * 0,15 = 2,397 * 10^{13} W$

Thus, the power delivered in this theoretical calculation amounts to about 24 TW of power. The global energy consumption in 2006 was, in comparison, about 15 TW[18].

This calculation indeed shows, that in theory, solar power alone has the potential to meet global energy demands.

This chapter have shown the theoretical limits for solar power , and in the next chapter we will take a look on the different solar power technologies that can produce electricity from this theoretical solar potential.

Chapter 3

Physics behind solar power technologies

There are a number of different ways to harvest the energy in solar radiation. To decide which technology to use, one must first know what the energy shall be used for. If the purpose is to heat up buildings or do some mechanical work to run, for instance, a refrigerator, it may not be nescessary to convert the heat into electricity first. If electricity is the goal then it is important to decide whether it is important to have the opportunity to store the energy for later use, storage at night for instance. Some technologies are better fit for energy storage than others. When choosing technology one must also think about the economical aspects. The different technologies can be divided into three main categories:

1. Solar thermal energy systems
2. Photovoltaic Power
3. Concentrated Solar Power

There is an additional category called Concentrated Photovoltaic Power. This technology concentrates sunlight towards high efficiency solar cells. This is a very interesting combination with some attractive features such as high efficiency and reduced land area. The main problem is the high cost of the needed solar cells.

3.1 Solar thermal energy systems

This category consists of systems that collect the solar energy to produce heat. The heat produced can be used to drive a heat engine that converts the thermal energy to some mechanical work. The heat can also be used directly, to heat up buildings or to boil water. There are different ways to collect this heat, dependent on how high the work temperatur is needed to be.

To maintain temperatures in buildings one usually use collectors in the low-temperature scale. These collectors can use water or air to transfer the heat where it is needed. Other examples are solar chimneys that heat up air and circulate the air around in a building.

When higher temperature is needed one needs a system that concentrates the incoming solar radiation to a smaller area. Lenses or mirrors constructed in parabolic shape are usually

Figure 3.1: Flat plate collector

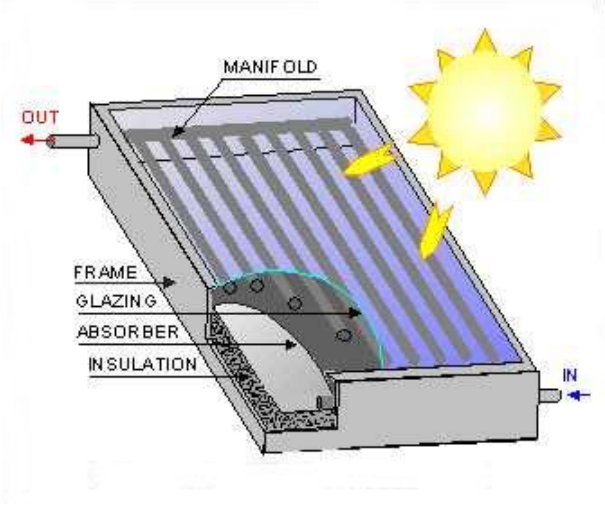

used to obtain the high temperatures. The high temperature will then boil water or some other liquid to generate steam. This principle is also used in electricity generation, only then another step is needed: the steam must then go through a turbine to produce electricity.

3.2 Photovoltaic power

The potovoltaic power system consist of a group of single cells connected togheter to form a module. As the term "photovoltaic" implies (photo = light and voltaic = electricity), each cell converts solar radiation directly into electricity.

The process that generates electricity in the solar cell was observed already in 1839 by the french experimental physicist Edmond Becquerel who found that some materials would generate small amounts of electric current when exposed by light. Despite this early discovery, the process behind the phenomenon wasn't understood until Albert Einstein, in 1905, in his paper on the photoelectric effect, explained the particle-view of light. According to his theory, light is composed of discrete quantities with certain discrete energies. Later, these quanta got the name "photons".

While the photovoltaic effect is based on the same physical fundament as the photoelectric effect, the two processes have different outcomes: In the photoelectric effect, the photons hits the electrons in the material, causing the electrons to leave the surface of the material and hitting a plate behind where they can be detected. In the photovoltaic effect the photon-electron collisions cause the electrons not to leave the material, but rather to move around within the material, which then can contribute to an electrical current when an electric field is formed.

3.3 The power output of a solar cell

The power output of a solar cell is determined by three main factors: $P_e = P_s \eta A_{eff}$ where P_s is the solar intensity, η is the efficiency and A_{eff} is the effective area of the solar cell. We will in the following find out how to determine these three factors. First we will do some calculations for the ideal case.

3.3.1 The ideal solar cell

The p-n jucntion in the solar cell can in the ideal case be thought of as a diode, in which current can move only one way. The solar cell will then be equvalent with the circuit in figure 3.2.

Figure 3.2: The solar cell equvalent circuit [19]

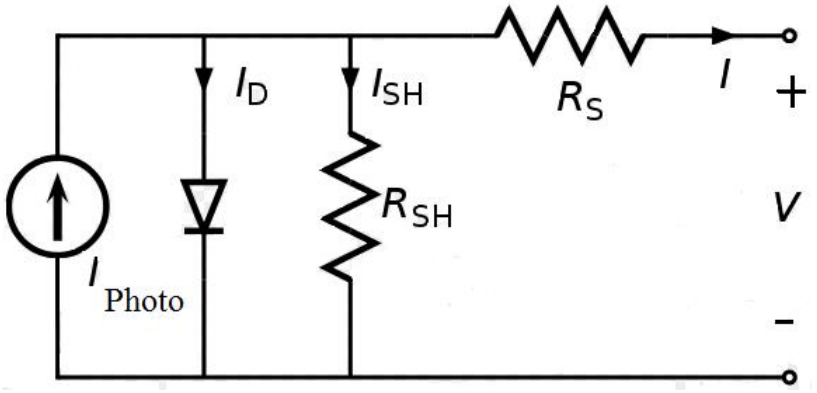

I_{photo}, the photocurrent,is proportional to the incident light intensity and originates from the photon-electron collisions in the n-type semiconductor. I_D is the ideal diode current. R_S is the series resistance from ohmic losses in the front surface and the shunt resistance, R_{sh}, also called the parallell resistance, comes from leakage currents due to recombinations in the p-n junction, in the sence that when $R_{sh} = \infty$ we will have no leakage currents. Because R_S usually has much more impact on the efficiency than R_{sh}, especially at high light intensities, we assume $R_{sh} = \infty$ in the following.The shunt current can also be neglected. Produced PV cells have R_{sh} from 300Ω and up to laboratory quality around 1000Ω[20].

The power generated from a circuit is given by the product of the net current running through it and the potential difference between the teminals, known as the voltage, that is, P = IV. Therefore it would be nice if we could express the current as a fuction of the voltage. For a diode this can be done through the Shockley diode equation [20]:

$$I_D = I_s(e^{\frac{qV_{tot}}{nkT}} - 1) \tag{3.1}$$

where I_s is the diode saturation current which depends on semiconductor properties. Here, n is the ideality factor (n=1 for an ideal diode), k is Boltzmann's constant, q is the charge of an electron and T is the absolute temperature.
In the case of solar cells this equation describes a solar cell which is not exposed to any solar illumination, I_D is therefore often called the dark current of the solar cell.

To apply the results to a solar cell with an arbitrary area we define the current density J = I/A

The net current density of a solar cell exposed to light will then be given by

$$J = J_{photo} - J_s(e^{\frac{qV_{tot}}{nkT}} - 1) \tag{3.2}$$

Here, $V_{tot} = V + Jr_s$, where r_s is the specific resistance (Ω m^2). J_{photo} , by convention, is defined to be in the positive direction. Because of this, the I-V characteristics is obtained in the first quadrant of the I-V plane[21].

A plot of an example I-V characteristic resulting from this equation is given in Figure.3.3

Figure 3.3: I-V characteristics for an ideal solar cell

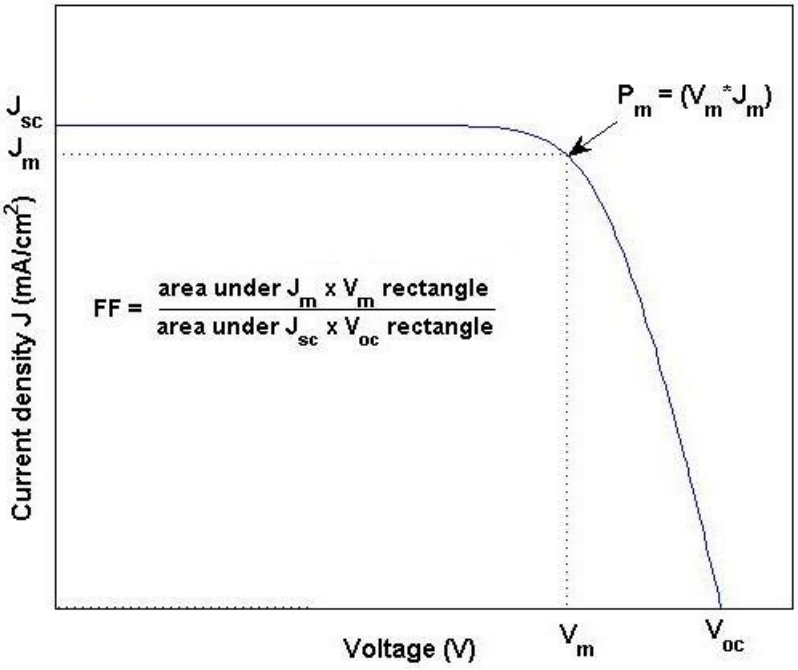

We can now define two quantities illustrated in Figure 3.3:

1. V_{oc} - the open circuit voltage, that is, when no current is running through the circuit.
2. J_{sc} - the short circuit current density, measured when the two terminals are connected to each other, that is, with zero voltage.

By introducing these two quantities we can find an upper bound for the maximum power output per unit area:

$$P_m = J_m V_m < J_{sc} V_{oc} \tag{3.3}$$

P_m can be found directly from the graph.[1] It is the area of the largest possible rectangle that can be drawn inside the graph.(Called the maximum power rectangle)

[1] P_m can also be found mathematically by considering V to be a function of I; P = JV(J), then finding the solution to $\frac{dP}{dJ} = 0$

We can from the figure define yet another quantity, known as the Fill Factor, FF. It is defined to be the ratio between the maximum power rectangle and the product $J_{sc}V_{oc}$:

$$FF = \frac{J_m V_m}{J_{sc} V_{oc}} \tag{3.4}$$

The bigger FF is, the more power is produced by the solar cell.

We can calculate J_{sc} and V_{oc} directly from (3.2) by setting, respectively, V_{tot} and J to zero:

$$J_{sc} = J_{photo} - J_s(e^{\frac{qI_{sc}r_s}{kT}} - 1) \tag{3.5}$$

where, r_s is the specific series resistance (units Ω m^2)

$$V_{oc} = \frac{kT}{q} ln(\frac{J_{photo}}{J_s} + 1) \tag{3.6}$$

3.3.2 Photovoltaic efficiency η_{photo}

Now, we return to the efficiency we initially were interested in. The maximum efficiency is given by the maximum power output by the solar cell divided by the power input from incoming radiation:

$$\eta_{photo} = \frac{P_m}{P_s} = \frac{J_m V_m}{P_s} = \frac{FF * J_{sc} V_{oc}}{P_s} \tag{3.7}$$

So, to maximize the efficiency one must maximize FF, J_{sc} and V_{oc}. We see from Equations (3.5) and (3.6) above that they are all dependent on J_{photo} and J_s . J_s depends on material properties and typically increases with temperature. This will result in a decrease in V_{oc} . Therefore, all in all, an increase of cell temperature will decrease the efficiency.

Below is a table showing some example values of the quantities describing the efficiency for various materials.

Figure 3.4: I-V characteristics for an ideal solar cell [21]

Cell Type	Area (cm^2)	V_{oc} (V)	J_{sc} (mA/cm^2)	FF	Efficiency (%)
crystalline Si	4.0	0.706	42.2	82.8	24.7
crystalline GaAs	3.9	1.022	28.2	87.1	25.1
poly-Si	1.1	0.654	38.1	79.5	19.8
a-Si	1.0	0.887	19.4	74.1	12.7
$CuInGaSe_2$	1.0	0.669	35.7	77.0	18.4
CdTe	1.1	0.848	25.9	74.5	16.4

The values are measured under standard conditions with $P_s = 1000W/m^2$ and cell temperature 25°C.

While what we have done here obviously is a very simplified approach to the real solar cell, we have been able to discuss the main factors that are involved in the determination of the efficiency.

In the general case, the efficiency is dependent on several different material properties of the

semiconductor [20]; the saturation current, depends on temperature, and the amount of holes and electrons in p-type and n-type regions. Maybe the most important one is the photocurrent, that is how many electrons per incoming photons are contributing to the current. This quantity is highly dependent on the band gap for the given semiconductor. The efficiency also depends on the series resistance, which is dependent on the junction depth, impurity concentrations in the p-type and n-type regions, and the construction of the electrical wires at the front surface.

3.3.3 Solar cell area

These electrical wires will also affect the effective area on the solar cell available for the incoming solar radiation.

To absorb all the electrons into the electrical circuit one must put electrical wires all over the surface of the solar cell, so that as many electrons as possible can jump into the circuit before they can recombinate with its ionized atom. Because of this, around 5% of the surface of a typical solar cell is shaded by the wires.

If we are taking into consideration the ratio between the effective area where the solar radiation hits the solar cell and the actual physical area the PV module takes on the ground, the efficiency will decrease as a function of this ratio. The total power output of a solar cell can now be written as

$$P_e = P_s * \eta_{photo} * A_{phys} * \beta, \tag{3.8}$$

where $\beta = \frac{A_{eff}}{A_{phys}}$

Its important to be aware of this factor, because if the efficiency has been measured with the effective area, but the total area of the power plant in the calculation is given with the physical area, then this will give a wrong picture of the total power output from the plant. It may also give a wrong estimate on how much area a power plant may need in order to extract a certain amount of energy.

β also decreases if the solar cells are tilted relative the earth's surface, in the sense that each PV module then needs more physical area to avoid shading effects on the modules behind it.

3.4 Standard test conditions

When one reads about efficiencies for solar cells in different media it is important to know where the efficiency is measured and under what conditions it is measured. In laboratories the efficiency is almost always measured under the AM1, 5 conditions. It is an abbreviation for Air mass 1, 5 and it represents the atmospheric path length relative to the minimum path length when the sun is directly overhead. AM1, 5 means that the light must travel 1, 5 meter for every vertical meter. It can be characterized by the angle between the sun and the vertical, that is the solar azimuth angle θ_z. The AM0 condition represents the solar spectrum outside the atmosphere.

The standard test conditions also include an insolation of $1000W/m^2$ and a cell temperature of 25°C

The difference in the efficiencies measured at the site of power production and that in the laboratory is partly because of these idealized conditions described above, but it is also caused by an effect called the Staebler-Wronski effect, which is a light induced degradation of the semiconductor. This means that defects in the solar cell material arise as the cell is exposed to light during its first $\sim$ 1000 hours of operation. This decreases the power output from its initial production level to a stable, lower power output. Alot of research is going on to solve this, but so far the reasons behind this effect are not fully understood.

3.5 Current technology and future improvements

Up to now silicon based solar cells have been the standard for commercial PV modules with single cystalline silicon (sc-Si) as the most efficient (up to $\sim$ 25 laboratory efficiency) but most expensive, and polycrystalline Silicon (pc-Si) as the least efficient(record 17% laboratory efficiency) but with the lowest cost. These solar cells are produced with help of silicon wafers. These wafers account for about half the total cost of the cells. Therefore, research today aims towards methods of reducing the thickness of the wafers, and also making the production more efficient with lower loss of material due to dust accumulation etc.[22].

Other materials than silicon have been proven to be eighter too expensive or too inefficient, but intense research in recent years have been given some breakthroughs in new, cheaper materials with reasonable efficiencies. Examples of promising materials are organic materials and CIGS solar cells[2]. The organic materials are much cheaper than the Silicon as they can be produced efficiently in large scale with printable semiconductors. However, the organic based solar cells are still suffering from low efficiencies. Other materials are Gallium Arsenide (GaAs) which is one of the most promising compounds in multijunction solar cells and they have today the efficiency record at 41%[3][23]. Also, research aims towards development of thin-film photovoltaic, referred to as "second generation" solar cells and the goal is to replace the wafer cells with these. Because the material used for the thin films can be significantly reduced compared to the conventional wafers they have a potential of reducing the total cost of the solar cell. In addition, potential efficiency improvements can be achieved since the bandgaps related to the thin films can be better fitted to the solar spectrum [24]. In 2010, German researchers achieved a record efficiency for thin film solar cells (CIGS technology). The new record efficiency was measured to $20,1\%$[25]. Also in 2010, a record 17% efficiency for multicrystalline silicon cells was achieved.[26]. The old record was $16,5\%$ and the improvement was made by moving the conductor wires to the back of the cell which increased the surface area available to capture the incoming photons.

It is important to emphasize that the efficiency-values that are published are the values measured under standard, idealized conditions in laboratories. Efficiencies of commercial modules used in the field are typically only half of these official "champion cell" values.

The photovoltaic technology has in the last years been the fastest growing global power source. $5,4$ GW of new grid connected capacity was installed in 2008 increasing the total grid connected PV power to 13 GW. This makes a 70% increase from 2008 to 2009[27]. If this increase continues at the same rate it may soon come to a point where the reliability of the electric grid might be in danger. Since the photovoltaic technology is an intermittent

[2]solar cells based on a compound of copper, indium, gallium and selenium

[3]This efficiency was achieved with a concentration ratio of 500, and has not yet been commercialized

power source with no economical large scale storage technology available (also true for wind energy which also is growing rapidly), it will be crucial that the electricity grid can adapt to an increasing fraction of intermittent power sources to stabilize local fluctuations. How this can be done will be discussed in Chapter 6.

Chapter 4

Concentrated solar power

When you were a kid, you may have tried to fry an ant by holding a magnifying glass towards direct sunlight. What happens is that when the incident sunrays hit the outer surface of the magnifier, the convex shape of the glass are directing all the incoming sunlight onto a much smaller area at the focal point on the other side. This will effectively produce a greater energy density, and eventually the ant will be fried.

Figure 4.1: Concentrating sunlight with the aid from a magnifying glass

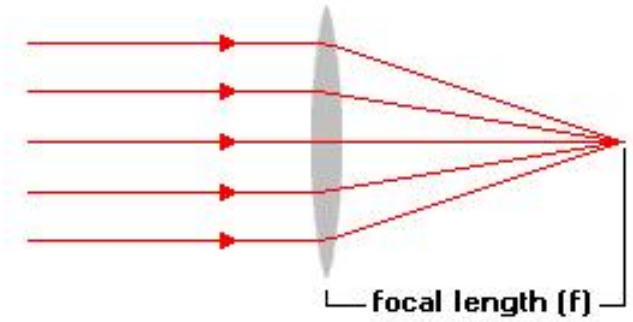

This simple (and brutal) experiment shows the potential power in sunlight and describes the basic idea behind concentrated solar power (CSP): By gathering the incident sunlight that reaches a large area and focusing it onto a smaller area, one can reach high energy densities at one single point, called the focal point.[1] If a receiver containing a fluid is placed at the focal point, the high energy density can effectively heat up the fluid and reach high temperatures. The high temperatures can produce steam which in turn can run a steam turbine to produce electricity.

There are several different technologies available which utilize the principle of concentration, but they all must go through some similar steps to produce the electricity; All the systems includes a concentrator, a receiver, a heat transportation fluid (HTF) (execpt the parabolic dish which use an engine). Some of the systems have also the possibility to integrate energy storage to be used when there is no sunlight. The last component of the systems will

[1] Since the sun is not a perfect point source the sunrays are not perfectly parallell, this puts a limit on the maximum achievable concentration ratio, see appendix D for more

be a steam/gas turbine and an electricity generator. Because the CSP technology requires direct sunlight to operate, some kind of system to track the sun during the day is crucial.

We can immediately conclude that there are many similarities between a solar thermal power plant and a conventional power plant (fossile fuel or nucler power plant) The main diference is how the heat, which is used to run the turbines, is produced. This fact gives the opportunity to combine, for example, fossile fuel and solar power in one single hybrid power plant, which may give some advantages both from an economical viewpoint and for a more reliable plant.

4.1 The parabolic dish

The parabolic dish is constructed as a stand alone unit, and is very similar to a satellite dish. The surface of the concentrator has the shape of a paraboloid and is covered by reflective mirrors which focus light towards the focal point where a receiver is placed. The receiver contains a heat engine, usually a Stirling engine. The fluid in the engine is heated by the sunlight and the Stirling engine converts this heat into mechanical power. The mechanical power then runs a generator to produce electricity. The dish has also an integated tracking system to keep the dish in an optimal position towards the sun during the day.

Figure 4.2: Parabolic dish [28]

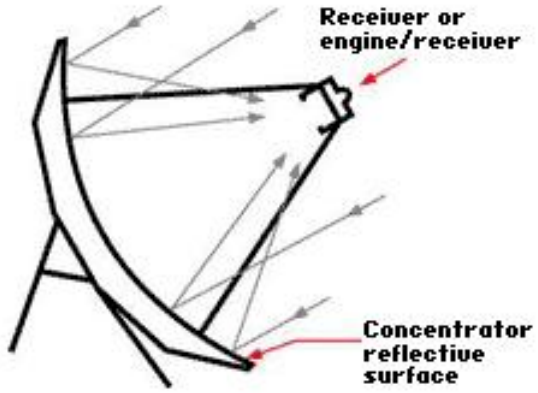

Because all the components needed for electricity production is placed at the unit, there is no need for a heat transfer fluid (HTF). It can be shown that the maximum concentration ratio for a paraboloid shaped concentrator is $\sim$ 46000 (see appendix D). The typical concentration ratios are significantly below this maximum (between 300 and 2000). The high temperature that can be reached and no need for heat transfer fluid makes the parabolic dish more efficient than systems based on linear concentrators.

The disadvantage is the expensive technology used for tracking the sun accurately during the day and the costly materials in the concentrator itself. Because there are no heat transfer fluid, this technology is not very suitable when energy storage is needed.(We will discuss a

possible storage method in Chapter 5) Because of this and the modular nature of the technology, the parabolic dish may have a larger potential as a decentraliced power source,especially in developing countries with high solar intensities, than as a large scale centralazed power plant. With the standard technology up to this date, one single unit can produce up to $25kW_e$ of electricity at peak levels.[29] Lets say it produces a mean value of 20 kW during sunlight. If one family uses 500 W of electricity on average, one dish is enough to give electricity to 40 families in the village, during sunlight.

Recently, two large scale projects are developing in USA. One of them a 450 MW size plant and the other a 750 MW size plant.[30]

4.2 The central tower

In a central tower installation (also called power tower), there are a large number of concentrator units distributed around a central receiver. The concentrators are flat mirrors which tracks the sun dynamically (heliostats). The central reciever is located at the top of a tower.

Figure 4.3: central tower [28]

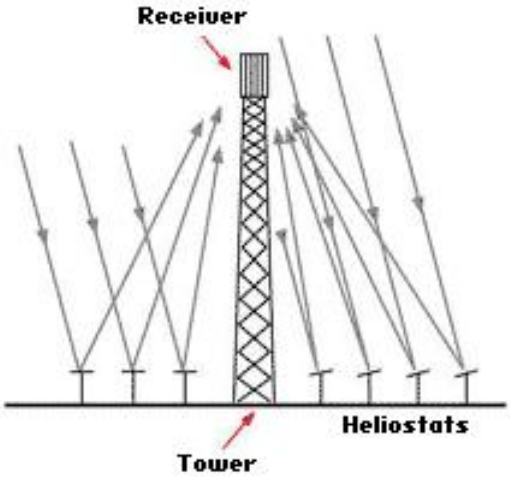

The receiver contains a HTF which absorbs and transport the heat to the power block where steam is produced. The steam runs a turbine to produce electricity in a generator. The standard HTF is usually oil, but lately there has been research on other HTF‘s, for instance molten salt.

Central receiver plants are today considered to be further away from commercialisation than parabolic trough systems. However, they have good longer-term projcetions for higher conversion efficiencies. Medium scale Projects are under construction in Spain (20 MW), and larger plants under development in USA and South Africa[31].

4.3 Linear concentrator systems

The concentrators in these systems consists of long line of mirrors in different shapes that tracks the sunlight togheter as one single unit and reflects the sunligt towards a linear receiver

located at the focal line in front of the mirrors. A fluid in the reciever absorbs the energy and the heated fluid is then transfered through tubes and used to boil water to produce steam to run a conventional steam turbine. There are two main types of linear concentrator systems in use today:

4.3.1 Parabolic troughs

This is the type of plants that where built in the Mojave desert in California between 1984 and 1991[2][32]. The parabolic troughs consists of modular parabolic shaped mirrors mounted on a support structure connected to each other in long rows. The mirrors can track the sun along one axis of rotation, usually a north-south axis, and then trach the sun from east to west (in the northern hemisphere). Each row of mirrors (called a Solar Collector Assembly (SCA)) tracks the sun as one single unit. A receiver is placed along the focal line, located directly above the saddelpoint of the parabola. This receiver consists of a black coated tube containing a heat transfer fluid, which transfers the heat to the power block of the plant. Maximum achievable concentration ratio are ~ 220, typical values are around 80.

Figure 4.4: Parabolic trough [28]

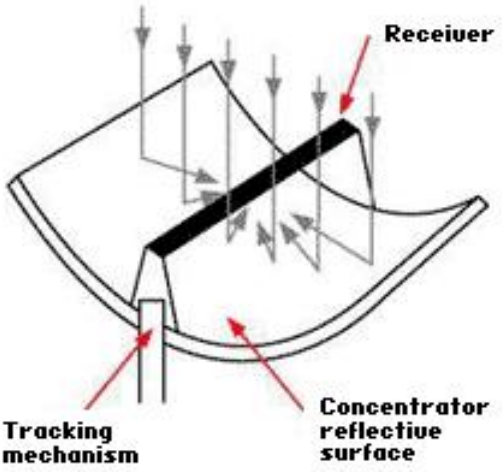

Today, several $50 - 100$ MW projects are under construction and under development in Spain. There are also plants that already have gone online. In china the plans for a 2000 MW plant is being developed. In the USA, a 64 MW plant went online in 2009.

4.3.2 Linear Fresnel reflector systems

Here, one receiver is positioned above several mirrors to allow the mirrors greater mobility in tracking the sun. The reflective mirrors used are nearly flat. This simple mirrorshape can lower the cost of production, and because the receiver can be in an arbitrary distance away from the reflectors, one can use long focal lengths which means one can use more conventional materials such as flat glass[33]. All this will reduce the investments and operation costs due to maintenance. Unfortunately there is, as always a backside: Because of the cheaper materials

[2]These plants will later in the text be called the SEGS (Solar Energy Generating systems).It was nine plants in all, named SEGS I to IX

used for reflection and lower concentration factor , the optical performance will be reduced and one will therefore not reach the same temperatures as for the parabolic troughs and thus the power output becomes lower. Still, if research shows that the reduction in performance is less than the reduction in costs, this may not be a a very huge problem after all.

In the following I will discuss three important factors for the solar plants, namely the overall solar-to-electric efficiency , the overall costs and the plant size/MW capacity, these threee factors are related to each other in the way that when the efficiency increases, the plant size as function of area needed for a given MW capacity decreases and thus the overall costs also decreases.

4.4 Efficiencies - Parabolic trough

Here I go in greater detail on the Parabolic trough technology because this is the technology which has been in operation for the longest time and thus the technology with the most reliable data collection to study. Much of the discussion in this section can be transferred to the central power tower.

To find a number for the overall solar-to-electric efficiency of a power plant one need to know the energy losses in every part of the plant. The example numbers given throughout these sections are found from the operation of the SEGS IV plant in California. (It was built in 1989, but the data here are from 1999) I will also give some numbers from the Andasol power plants that went online in march 2009, but because of the recent startup, detailed efficiencies for the different parts are not available. The data is retrieved from the Sunlab and Sargent & Lundy (S&L) report published in 2003 as a response to the Departement of Energy's (DOE) need for an objective assesement of the CSP technology[34].

Figure 4.5: Parabolic trough power plant

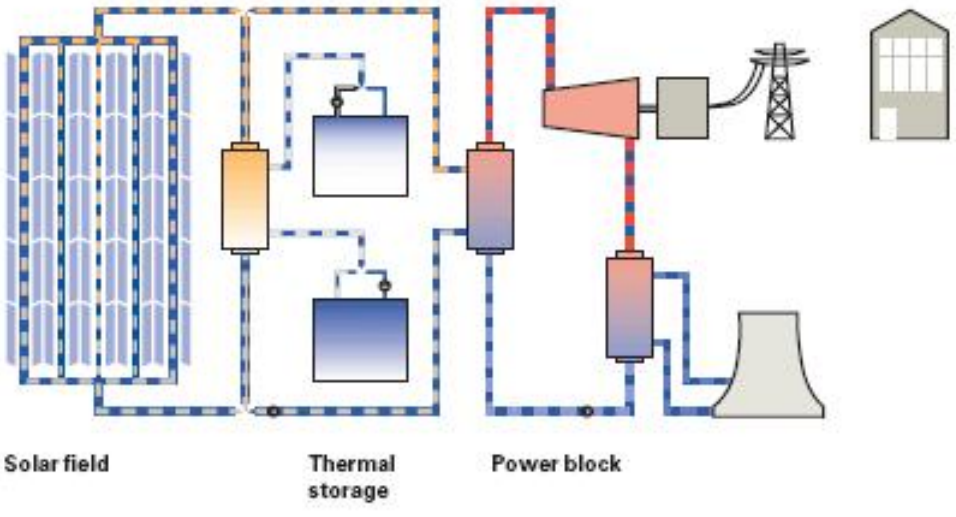

A parabolic trough power plant consists of 3 main parts (see Figure 4.5):

1. The solar field: its constituents are the concentrator (support structure, mirrors and tracking system), the reciever pipes, the HTF within and glass envelope.
2. The power block: consists of the rankine type steam cycle, turbine and the generator.
3. The thermal storage system.

4.4.1 The solar field efficiency η_{SF}

The solar field efficiency is determined by the losses related to different parts in the concentrator and the receiver.

The concentrator‘s curvature is basically described by the formula

$$z = \frac{x^2}{4f} \tag{4.1}$$

where f is the distance of the focal point from the vertex. This parabolic curvature assures, given two conditions, that all the incident light rays are reflected and focused at one single line in space. The two conditions are the following:

1. The sunrays travelling towards the parabolic collector are parallell to a line drawn from the focal point to the vertex. (this line is called the optical line.
2. The surface of the concentrator is covered by a perfect smooth layer of a 100% reflective material.

Figure 4.6: The receiver is located at the focal point F, a distance a from the vertex.

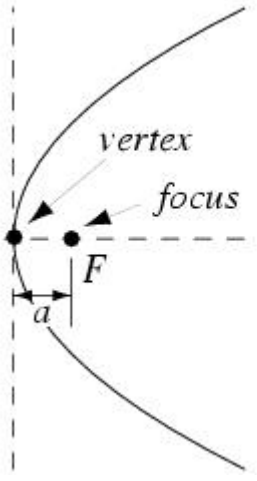

Any deviation from these two conditions will result in a scattering of sunrays and some of them may not hit the receiver. It is therefore important that the receiver has a cross sectional area large enough to receive all the incoming sunrays. It is also important to make sure that the parabolic shape of the mirrors which these two conditions relies upon is being maintained.

With the two conditions above in mind, important parts of the concentrator efficiency must include tracking system accuracy, geometric accuracy of the concentrator, incident angle modifier (ratio between the incident angles that can be collected by the concentrator and the total spectrum of incident radiation angles during the day)[3], mirror reflectivity and mirror cleaningness.

The remaining solar energy which is not lost in the concentrator is directed towards the receiver. The losses in the receiver must be related to each of the components of the receiver: a black coated absorber tube, the HTF within, and a protective glass envelope surrounding the tube. The space between the aborber tube and the envelope should be in vacuum to protect the antireflective material that covers the tube. The vacuum is maintained by bellows covering the tube on each interconnection. Bellow shadowing will therefore result in a loss. Other factors are transmissivity of glass envelope, receiver tube absorption, receiver thermal efficiency ($0,729$ for SEGS VI) and thermal losses in the pipes.

One must also take into account losses related to row to row shadowing, end losses due to light which is reflected off the ends of each collector and the solar field availability, which is the percentage of total time during sunlight the plant is operating. (99% at SEGS VI)

The losses mentioned above related to the concentrators and receivers can be summarized into one single factor: the Solar Field efficiency (η_{SF}). For the SEGS IV plant this efficiency was $0,373$ For the andasol plants in Spain, official numbers show a $0,5$ Solar field efficiency[35].

4.4.2 Thermal storage efficiency η_{TS}

The SEGS plants did not have thermal storage, but the two Andasol plants in Spain do, together with many of the plants under construction, and here one must take into account the losses related to this. With the available storage systems today, such as systems with molten salt, the overall loss are claimed to be one percent. Thermal storage will in addition remove most of the startup/shutdown losses for the plant, and thus, the introduction of a Thermal Storage system may potentially give the plant a positive increase in overall efficiency.

4.4.3 Power block efficiency η_{PB}

This is the overall efficiency of the Rankine steam cycle and the turbine/generator together. The power block availability and the parasitic losses[4] are here also integrated into this power block efficiency.

4.4.4 Overview

In the following table the efficiencies for the two plants is given.

[3] this factor is not easy to improve as this depends as much on the availability of the sun itself as the position of the concentrator, in fact, both Sunlab and S&L is operating with no improvements at all on this number in their future projections up to 2020. Experience from the SEGS(Solar Energy Generating system) plant in California, 1999 gave this factor the number $0,873$

[4] This is the losses related to the electric energy the plant needs to operate properly (For pumping, cooling etc.) It also includes startup/shutdown losses

	SEGS VI	Andasol 1 & 2
η_{SF}	0,377	0,5
η_{TS}	1,00	0,99
η_{PB}	0,284	0,3
η_{tot}	0,106	0,15

From the table we see that the Andasol plants has a solar-to-electric efficiency of about 15% and the SEGS IV plant a efficiency of $10,6\%$. The increase in efficiency is, as we can see, mainly from improvements in the solar field efficiency, which has increased from $37,5\%$ to 50%[5]

4.5 Efficiency improvements in future

In the table below the efficiency improvements for differents parts of the plant projected by Sunlab and S&L is shown.[34]

		projected cases			
		SEGS VI 1999	2004	2010	2020
η_{SF}	Sunlab	0,377	0,470	0,493	0,497
	S&L	0,377	0,461	0,446	0,447
η_{TS}	both	1,000	0,991	0,996	0,996
η_{PB}	both	0,284	0,307	0,347	0,349
η_{tot}	Sunlab	0,107	0,162	0,17	0,172
	S&L	0,107	0,14	0,154	0,155

4.5.1 Comments about the sunlab and S&L projections

We observe that S&L and Sunlab have different values for their projected values of η_{SF}. Most of this difference is the different values they have on the future receiver thermal efficiency which lies inside the η_{SF}. For instance, in 2004 Sunlab projected the thermal efficiency for the reciever to be $0,859$. S&L's value is $0,843$. Both have increased significantly from the SEGS value $0,729$. The reasons for differences in η_{SF} between Sunlab and S&L are due to their different assumptions they made as a base for their projections.

Sunlab assumed a more intensive technology development than S&L, which had a more conservative approach with only modest research and development in the period. The S&L improvements was mostly due to small evolutionary "learningcurve" improvements based on an assumed deployment rate and increases in plant sizes.

Being in the year 2010 we can compare the projected values with actual numbers from recently built plants in Spain and USA.
Given that the efficiencies published by Andasol 1 & 2 is correct, ($\eta_{SF} = 0,5$) then we observe that Sunlab's projections is closest to this value. It is interesting to observe that this value

[5]Because the Andasol plant is very new, the details about the different parts of the plant is still confidential to the public, and the values presented here might still not be representative for the long run operation of the plant

is achieved without the deployment rates and plant sizes assumed in the projections. In fact, Andasol 1 & 2 togheter with Nevada Solar One in USA, that went online in 2007 and 2009, respectively, are the first commercial parabolic trough plants built since the last SEGS plant was built in 1991. Andasol 1 & 2 has each a 50 MW capacity, while Nevada Solar one has a 64 MW capacity. The conclusions must be that even with the small/non existing deployment rates, improvements in efficiencies has happend, this must mean that there has been some research and development between 1991 and 2006. We will take a look at some specific improvements in the end of the chapter.

From the Sunlab projections we also observe that η_{SF} seems to converge towards $0,5$ with smaller and smaller improvements. This may indicate that we allready are very close to the maximum theoretical value of η_{SF}.

Further, we observe that the projected increase in the power block efficiency, η_{PB} is the same for both Sunlab and S&L. This is because the improvements in the power block is not very dependent on deployment rates and plant sizes as it is for the solar field. The power block is typical a conventional Rankine steam cycle used in conventional power plants and thus is a mature technology. However, there are a significant improvement potential for η_{PB}; Today in conventional power plants turbines can reach an 45% efficiency and in combined cycle power plants with gas turbines they can reach even higher[36]. To reach these high efficiencies it is important that the steam temperatures is high enough, because according to the Carnot eficiency the maximum theoretical efficiency of a system is entirely dependent on the temperature of the heat source and the temperature of the sink. Because the temperature of the sink usually is limited by the temperature of the earth one must increase the temperature of the heat source to increase the efficiency. Today, the steam temperatures in a CSP plant are limited by the maximum temperature of the HTF , and today, the standard HTF is syntetic oil which has a maximum outlet temperature of 393°C. This is about the same that was used in the SEGS plants.

Some of the reasons for the higher η_{PB} projections to Sunlab and S&L than we see today is that they have assumed the introduction of molten salts as HTF at an earlier stage than what we actually see today. Molten salt can reach significantly higher temperatures than synthetic oil, around 500°C, and therefore the Carnot efficiency of the system will increase.

The small increase in η_{PB} from SEGS to Andasol is mostly due to a decrease in the parasitic losses due to shutdown/startup, and also due to more efficient pumping. The big improvements, however, will not happend before the introduction of a HTF that can hold higher temperatures in its liquid state. Alternatively ,with the introduction of Direct Steam Generation (DSG), one does not need a HTF at all.(In a DSG system the power block and solar field will be in a closed loop without the need for heat exchangers)

4.6 Overview of the plant costs

Improvements in efficiency is not enough to make CSP competetive. Research and development aiming at cost reductions is just as important. An improvement of the solar field efficiency will reduce the size of the solar field and thus reduce materials needed. Unfortunately, this does not necessarely mean a reduction in cost, because if the materials needed for the efficiency improvements is more expensive than the savings due to reduction in plant

size, then we have no overall improvement.

As mentioned in the previous section it seems that R&D(Research and Development) is closing in on the maximum solar field efficiency, but thare is still a lot of potential cost reductions to search for. For instance, by moving from todays standard of thick glass mirrors towards lightwweight, thin front-surface reflectors with integrated surface coating one can potentially reduce cost of mirrors in half.[37] The challenge then will be to maintain the high efficiency.

The table below shows the most important cost categories for the parabolic solar power plant. The percentages is projections(year 2004 case) made by S&L for a 100 MW_e capacity plant with 12 hours of thermal storage.[34]

Component	percentage of total cost
Solar field	58%
Thermal Storage	23%
Power block	14%
other(preparing site etc)	5%

Wee see that the solar field, for this plant size, counts for over half of the total cost of the plant, and for bigger plant sizes the solar field becomes an even bigger part of the total cost.

The cost of the solar field is distributed over the solar fields different components in the following way:

Component of Solar field	percentage of total solar field cost
Metal support structure	29%
mirrors	19%
Receiver	20%
other(HTF, electronics etc)	32%

So, the mirrors, support structures and recievers counts for almost 70% of total costs of the Solar field.

These three components will therefore be the most important components to reduce costs on, especially when the plants gets bigger.

The direct factors that defines the cost of the components are

- Type of material
- Amount of material per unit
- Production method
- Transport
- Mass prdouction

To calculate total costs one must also include the labor costs related to assembling and erecting the units on-site. The lifetime together with operation & maintenance costs during its lifetime is also important but will not be analyzed here. It is a common assumption that the O&M costs does not increase significantly with increased plant size. Standard economical lifetime for the CSP plants are $25 - 30$ years.

In the two next sections, an overview of the current status for two of the most important cost components in the solar field are given. We will examine whether or not there are competion between different producents and if cost reductions are within reach.

4.6.1 Mirrors - current status and future development

First, we take a look in the past. The mirrors used at the SEGS VI plant in 1999 had a cost of around $40\$/m^2$. They where made from thick ($4mm$) glass with cobber back layers. The mirrors developed at that time had already reached high reflectivity ($0,93 - 0,94$) and was one of the most reliable components at the SEGS plants. The mirrors showed, in general, no degradation of efficiency when cleaned, and today, mirrors that have operated in 20 years still shows good optical properties.[32] However, the costs of the mirrors where high, due to the material used and the amount of material used (thickness).

Going over to the current mirror standard we can take a look at the recent built plants in USA and spain. What we see at these plants (Nevada Soalar One and Andasol 1 & 2) is that the same type of mirrors that where used at the SEGS plants still is in use here. The material is the same with the same cost, reflectivity and thickness. In fact, it was the only reflector in use at current commercial parabolic trough plants until 2008[6], and it came from the same producent (Flabeg).[38]

In light of the experiences at the SEGS plants and the current plants it should be clear that is is in cost reductions, and not efficiency improvements, the biggest potential lies. Offcurse, when looking for cost reductions, one usually need new materials with different optical properties, and therefore effeciency improvements comes togheter with cost reductions.

Today, there are several different mirror alternatives, some at the test stage (per 2007) and some ready for commercializing:

Reflector type	Reflectance	Cost ($/m^2)	Status/issues
Thick,glass	0,93-0,94	40-45	Standard reflector/ breakage and cost.
Aluminized reflector	0,90-0,92	20 - 25	testing finished in 2008/reflectance and durability
Silverized polymer on aluminum substrate	0,93-0,94	<30	testing fin ished/Durability
Thin Glass (<1 mm)	0,93-0,96	15-43	on-site testing in 2008/breakage
Advanced coatings/superthin glass	>0,95	<11	experimental stage/durability

The information in the table above is taken from a paper from 2007[38] and partly from a paper written in 2004[39]. it is also based on information gained from reflector companies.

From the table we see that the main property which need to be proven for the new technologies is their durability in harsh outdoor weather conditions, that is, how long will their lifetimes be, and how will their optical properties be changed during their lifetime.

Reflector supplier Reflectech and NREL has togheter developed a thin silver-polymer film reflector. According to Reflectech (a subsidiary of collector supplier Skyfuel Inc) the films has the same efficiency and durability as the glass mirrors currently in use, but with a lower cost and weight. Reflectech and Skyfuel believes that 30% cost reductions for the total solar

[6] there has been installations of new types of collectors before 2008 for various testing loops

collector assembly[7] is possible. Up to this date, ReflecTech has been eight years in commercial use and it has demonstrated that it has less than $0,5$ percent loss in reflectivity during this time. [40]

However, A DLR report named "Optical Characterisation of Reflector Material for Concentrating Solar Power Technology" [41] demostrated that polymer films with a silvered reflective layer had, indeed, a hemispherical reflectance comparable with the silvered glass mirrors but, with a 5% lower direct reflectance[8] (Silvered glass mirrors where shown to have both direct and hemispherical reflectance at 94%)

The 30% cost reduction from the current $40 - 45\$/m^2$ for glass mirrors results in a price at around 30 $\$/m^2$. At their homepage the cost is listed as $18\$/m^2$ [42], but this price only includes the polymer film. One also need a rigid substrate to maintain its shape. I.e if using an aluminum substrate this would cost around $9\$/m^2$. The total price will therefore be about 29 $\$/m^2$.

Besides The polymer films the table also shows Aluminized reflectors and here the German company Alanod-solar is currently in front. The same DLR report showed that Alanods metal based mirrors achieved competetive direct reflectivity and durability ($1 - 2\%$ loss in reflectivity over an accelerated test equivalent of $7,5$ years.) The problem with these Metal based reflectors has usually been their low abrasion ressitance.[39] This means that they do not respond well to the current cleaning methods and they experience abrasions from these maintenance requirements, this was also confirmed in the DLR report.[41]

Despite these facts it is clear that the polymeric films and the metal based reflectors has the advantage that they do not break that easily as glass. As a response to this, the glas manufacturers have been developing laminated glass mirrors for the CSP industry, with Guardian Industries in the front.[43] The advantages with this lamination is that there is less chance for breakage, and if the glass should break it would still be relatively functional.

At last, the thin glass mirrors must be mentioned. They have typically a higher Reflectance then the conventional tick glass, and also a lower material cost. The problems that up to now has been experienced with these reflectors is their low resistance to breakage, and this increases the replacements that has to be made togheter with handling costs)

4.6.2 Support structure - current status and future development

In the following only the cost of the support structure itself is discussed. The cost of the tracking system and other electronic equipment comes under a different category.

We start the discussion with a list that covers the most important factors when discussing the cost of the structure.

- **Weight**

  Often given as kg/m^2 , where the area is the amount of ground surface the structure occupies. The weight of structure is first found and then distributed over the occupied ground area. the cost is often given as \$/tonnes or per kg, or \$/kW. A light weight construction will not only reduce the direct manufacturing costs, but also reduce labor costs for assembling and erecting.

[7] The Solar collector assembly (SCA) is the rows of independently tracking parabolig troughs. Its component is the support structure, mirrors and the receiver tubes togheter with trackingsystem and electronic controls

[8] For CSP applications the direct reflectance gives the amount of solar irradiance concentrated onto the receiver and is therefore the most relevant reflectance parameter.

- **Material properties**
  This will often dictate the weight of the structure. But the best material cannot only have lightweight properties, it must also be able to withstand severe outdoor weather conditions during a standard lifetime of 30 years] Stiffness properties is especially important to help maintain its parabolic shape during relatively strong wind loads and to make it possible to construct units with longer lengths to reduce interconnection costs etc

- **Simplicity of manufacturing**
  For the manufacturing to be as cost efficient as possible it is important that the structure has a very simple design and few separate parts. It is also important that the design makes it possible to transport the structure as efficient as possible to the site where it is assembled and erected.

- **Future cost components**
  Includes expected lifetime for the construction and operation and maintenance costs during its lifetime.

The first commercial support structures where developed by the company Luz in 1982 and where used at the SEGS plants. Luz went bankrupt in 1991, right after the ninth SEGS plant was built, main reason was that the Levelized energy costs (LEC) where too high to compete with the fossil fuels. The SEGS plants were later sold to investors as independent power projects and is still in operation, and today, they are claimed to have a LEC at $0,12-$,14. [32]

Luz made two improved versions of their original Structure: LS-2 and LS-3. LS-3 were used at the plants made at the end of the 80‘*s* and their improvements where based on operational experiences from the first plants. At the end of the 90‘*s* two new support structures developed. In Europe, a group of European companies and research laboratories developed a troughdesign called Eurotrough. At the same time the american project called Duke Solar developed. The two projects had some fundamental differences in designs.

Eurotroughs approach was a steel structure with a square Torque box design. The main part was a 12 meter long space frame made of steel with a square cross section. This box was the fundament for the support arms helding the parabolic mirrors. The benefits of the Torque box was a structure with exellent stiffness properties that allowed the SCA length to be increased form 100 for the LS-3 to 150 meters and in addition allowed the collectors to operate more accurate under higher wind loads. The structure had only four steel parts which simplified manufacturing and on-site labor costs. The design also gave more efficient packing which reduced transportation costs.[44] However, one of the main goals for the project was to reduce the weight of the structure, this was to some extent successful (14 % weight reduction compared to LS-3 however, LS-2 actually had a 12% lower weight than LS-3), but the choice of steel as material laid limitations for big weight reductions.

Duke Solar‘s approach was a Aluminum space frame that was developed directly from the LS-2 design. The new structure had reduced weight, better corrosion resistance and easier manufacturing and installation. However, with Aluminum, the Stiffness properties could not be improved and there was no increase in the SCA units.

Up to the year 2007 when Nevada Solar one came into operation, there was only the Luz collectors that was in operation at commercial plants. Today, we have mainly four different

collector designs in commercial operation. Collectors from Acciona Solar power (former Duke Solar) are installed at Nevada Solar One, collectors from Flagsol(one of the companies that developed Eurotrough) are installed at the Andasol plants, and in june 2009 the company Skyfuel inc signed an agreement with Sunray Energy Inc. to install their support structures, togheter with Reflectech mirrors at Sunray's 43 MW parabolic trough plant in California. (Earlier known as SEGS 1 and 2) The installations where finished in early 2010[45].

The tables below provides available information about the main properties of the four commercialized structures. There are other structures from other companies commercial available(in various test loops at different plants) but they are not considered here. The numbers are found from [46] and the different companies own pages.

	LS-3	Flagsol	Acciona	Skyfuel
Structure	V-truss	Torque box	space frame	space frame
Material	Steel	Steel	aluminum	aluminum
Length per SCA	99	148,5	100	115
Aperature area pr. drive (m^2)	545	817,5	470	656
Geometric concentration	82:1	82:1	82:1	75:1
Weight (kg/m^2)	33	33	22	18

From this table we observe that there is a big difference in weight between the steel structures and the aluminum structures. If the numbers from Skyfuel is correct the weight of their collectors is around 18 kg/m^2 which is a 45% weight reduction from LS-3 . The question will then be if the weight reduction alone will be enough to reduce the costs. If the aluminum used at skyfuel is not more than 45% more expensive than the steel used at Flagsol, then we have a cost reduction when we only look at the cost per kg.

However, the steel structures have typically better stiffness properties and therefore allows for longer total length of SCA's and thus reduce the number of needed drives. One typically use one drive per SCA. One could also reduce the number of receivers in a SCA but the number of receivers is more or less independent of the length of the SCA's and does not give an immediately cost reduction when the SCA length increases. The table below shows how the number of drives changes with different SCA lengths for a given plant size: (the 50 meter collector is the LS-2 used at the first SEGS plants)

SCA length	50	100	115	150	200
SCA width	5	5,75	6	,5,75	5,75
SCA area	235	545	654	817	1092
Number of SCA's relative to the 100 SCA	130%	100%	85%	67%	50%
Number of drives	130%	100%	85%	67%	50%

So, by double the SCA length one can reduce the cost of the drives by 50%. This will probably give some savings in the OM costs also. It is interesting to observe that Skyfuels aluminum based modules actually are 2 meters longer than the steel structures used at other plants (14 meters against 12 meters). These lengths does not mean that the aluminum structures have better stifness properties. The standard 12 meter length is more for convenience under manufacturing and transportation.

4.6.3 Summary of the status for the two components

There is an ongoing "battle" between the glass producers and the manufacturers of metal-based,- and polymeric reflectors. Today it seems that the glass manufacturers still have the upper hand when it comes to reliability and optical properties, but the metal-based and polymeric reflectors are closing in. What is currently going in the favour for the polymeric and metal based reflectors are their lower cost. However, all the reflectors have the potential to greatly reduce their price, the glass reflectors with advanced super-thin glass currently at experimental stage and the polymer films with a possible all-polymeric reflector. For the support structures there is a battle between the producents of support structures made of steel and aluminium. The steel structures features better stiffness properties which is important under harsh weather conditions, while the aluminuum structures features lower weight and a possible lower prize. Up to very recently there was a very limited selection in both reflectors and support structures for commercial CSP applications. Keeping in mind that there has been no construction of new commercial parabolic trough plants between 1991 and 2007 this cannot come as a shock. However, the CSP industry have gotten a new start due to new policy incentives and subsidies and in the last two years more manufacturers have found their way into the commercial buisness and this will, most probably, lead to further cost reductions due to competition and increased mass production if the deployment rate of new plants increases.

4.6.4 Estimates on the total cost of the solar field

In most scientific papers it is the solar field capital cost as a whole that is given an estimat for and the estimates today is typically in the range $190 - 220$ euro, or $250 - 300$\$.[47] [48] [34]. Sunlab's estimate of the solar field costs for the SEGS VI plant in 1999 was 250\$. This value may be to low, as we shall see. It is difficult to obtain detailed cost breakdowns for the plants, but what we do know is that there were no thermal storage at the SEGS VI so the total capital costs would be divided between the solar field and the power block. The total Capital cost of the plant was in 1997 estimated to be $\$119,2$ million. Knowing that the plant had a peak capacity at 30 MW and a solar field area at $188000m^2$ this gives $\$634/m^2$ or \$3973/kW. If we assume the percentage cost breakdowns estimated by Sunlab and S&L is representative. then the cost breakdowns for a Parabolic trough power plant without thermal storage are:

Solar field : 80% Power block: 15% Other: 5%

80% of 3973 is 3178 which is very close to the number published by Solarpaces (\$3048/kW). So this cost distribution seems to be representative. 80% of $\$634/m^2$ is around $\$500/m^2$, the double of what Sunlab and S&L estimated. Actually, the $\$500/m^2$ seems to be comparable to the recent built plants in Spain and Nevada.

Name	SEGS VI	Andasol 1	Nevada
Country	USA	Spain	USA
Solar resource (kWh/m^2-year)	2725	2136	2606
Electricity generation (GWh/yr)	89,4	158	134
Fossil Backup	34%	12%	none
Production started	1989	2008	2007
Peak turbine capacity (MW)	30	50	72
Thermal Storage (hours)	none	7,5	0,5
Total capital cost ($\$10^6$)	119	400	260
Solar field Aperture area (m^2)	188000	510120	357000
Total cost per m^2	\$634	\$784	728
Total cost per kw	3972	8000	3611
Solar field cost pr m^2	500	450	500

The data in the table above is found from [46] The solar field costs in the last row is found by using the cost breakdowns estimated by S&L and sunlab. Because S&L and sunlab's reference plant was a $100MW$ plant with 12 hours of thermal storage I have made a interpolation between the cost breakdown for a plant with no thermal storage and a plant with 12 hour of thermal storage for Nevada solar one with ony $0,5$ hours of thermal storage.

We can calculate how much of the total cost would be in the solar field if we assume solar field cost of $\&250/m^2$:

Name	SEGS VI	Andasol 1	Nevada Solar One
percentage of total cost	39	32	34

This percentage is way below any cost breakdown estimates found in literature.

One possible answer to this is that the cost components that the total costs of the plants is based upon vary from source to source. In the cost estimates I have only accounted for the direct capital costs needed for the construction of the plant. The annual Operation and maintenance costs is not taken into account, nor is the indirect costs such as contigencies and insurance. Therefore it may be that the total costs for Andasol and Nevada solar one listed in [46] has taken these costs into account and because of this gives a higher cost estimate than other sources, but still, it is peculiar that this would result in a doubling of estimated costs. On the other hand, the current plant sizes is still small, relatively, and one would quite possible see a siginficant cost reduction per square meter when the plant sizes increases.

4.7 Levelized energy cost

The Levelized Energy Cost (LEC) is alfa and omega when discussing costs of power plants. The LEC of a plant is what it all comes down to when deciding whether a plant can compete in the electricity market or not.

The Levelized energy costs is defined to be the value($/kWh) the generated elecricity must be sold for such that the present value of the total investments over the economical lifetime for the plant becomes zero. The total investments include the direct initial investments, annual operation and maintenance costs and annual cost of fuel. The cost is levelized in the sence that it is adjusted to account for the impact of inflation over the economical lifetime of the plant. This constant, levelized cost value makes it easier to compare different energy alternatives against each other.

The Levelized energy cost in its most detailed form is calculated with both fixed costs and costs that vary annually, and the costs are then summated over the entire lifetime of the plant in the following way[49]:

$$\sum_{i=1}^{n} \frac{CE_i}{(1+r)^i} = \sum_{i=1}^{n} \frac{c_i}{(1+r)^i} \tag{4.2}$$

where C = LEC , c_i is the annual $/kWh investment costs in the year i and can be divided into four parts: OM_i - the Operation and maintenance costs in the year i, IC_i - investment costs in the year i FC_i - Fuel costs in the year i and LC_i - Land lease cost in the year i . r = the discount rate also called the interest rate. This discount rate depends on the balance between debt-financing and equity-financing, and an analysis of the financial risks in the project. The assumed inflation is also baked into the formula. E_i = Generated electricity in the year i and n is the economical lifetime of the plant

For simplification one could assume total annual costs of equal magnitude each year and a constant annual electricity production. Unfortunately, Equation 4.2 does not apply under this simplification as the discount rate r will be eliminated from the equation.

For the simplification that all the costs are constant for each year and with one initial capital investment another approach is available. The following model is widely used as a alternative to the more detailed cash flow model, and was initially provided by the NWTC for the wind industry[50].

Instead of the discount factor in Equation 4.2 a Fixed Charge Rate (FCR, which consist of a standard set of financial assumptions, is being used. The FCR distributes the initial costs of the plant over the lifetime. The FCR includes construction financing, financing fees, return on debt and equity, detailed lender requirements, economical lifetime, income tax, property tax, and insurance. A typical value of FCR for the parabolic trough technology is around 10%. The formula is given by

$$LEC = \frac{FCR * C_{invest} + C_{O\&M} + C_{fuel}}{E_{net}} \tag{4.3}$$

where C_{invest} is the total cost of construction, $C_{O\&M}$ the annual operation & maintenance costs (includes staff wages, material replacements etc.,) C_{fuel} the annual cost of fuel and E_net is the net annual electricity production.

We can now use this model to calculate the Levelized costs for the SEGS VI plant, Andasol and Nevada solar one.

Name	SEGS VI	Andasol 1	Nevada Solar One
Electricity generation (GWh/yr)	89,4	158	134
Fossil Backup	34%	12%	none
Total capital cost ($\$10^6$)	119	400	260
$C_{O\&M}$ ($\$10^6$)	3,2	3,5	3,5
C_fuel ($\$10^6$)	2	2	0
FCR	10%	10%	10%
LEC ($/kwh)	0,19	0,28	0,22

The operation and maintenance costs togheter with fuel cost are based on actual data from the SEGS VI plant.[32] It has an annual O&M cost at $107/kW and fuel cost of $\$0,022$/kWh. O&M (Operation and Maintenance) cost for the other plants are based on the assumption that O&M costs does not increase significantly with increased plant size.

These numbers must be taken with reservations as there are some uncertainities related to the numbers for the total capital cost and the FCR value. In addition, the FCR model do not include factors such as production tax credits, state credits etc. These type of incentives depends on the project location and where the power is sold.These factors are discussed in a section below. Nevertheless, the LEC calculeted here at least give us a indication of the magnitude of the energy cost for the parabolic trough technology.

A more detailed calculation of the LEC where made by IEA in 2005.[51] They calculated the LEC for a 100 MW parabolic trough power plant in USA with 15% capacity factor. Assuming the discount rate to be 5 and 10% they found the LEC to be $0,165 and $0,27 respectively. For comparision the LEC for a coal fired power plant in USA was found to be $0,027 and $0,036 with 5 and 10% discount rate, respectively. For a nucler power plant the LEC was 0,031 and 0,047.

It should be mentioned that the 15% capacity factor assumed by IEA can, with existing technology be increased to around 50%(in principle it can approach 100%) when thermal storage are included. The dispatchability will also be increased.

When comparing the LEC for the Parabolic trough power plant with the LEC for nuclear power plants and coal fired plant it seems to be a long way for the parabolic trough technology to reach market competetive values. It is a common belief that if the CSP technology want to compete with the conventional power plants the CSP plants must reach a LEC value around $0,060.

Increased deployment rates and bigger plants might reduce costs due to mass production and “learning curve” improvements of technology. The problem is, someone must pay for this deployment rate and the bigger plants before the technology reach market competetive LEC values. It is at this point that policies and incentives comes into picture.

4.8 Policy- governmental incentives and subsidies

No new commercial CSP plants has been built between 1991 ans 2006. Why is that so, one might ask. One of the most important reasons for this lack of deployment is that there has not been attractive for private investors to put their capital into CSP plants. The simple reason for this is that the cost of electricity from the plants still are too expensive to compete in the electricity market.

The plants built between 1984 and 1991 in California was built because the government in California provided attractive tax credits and other forms of incentives to attract investors[32].

This is a key issue for CSP and any other technology for that matter. Without the correct incentives to make it attractive for investors to invest, the industry will stay dormant, and with lack of deployment and experience, cost reductions becomes harder for the industry to achieve.

It is therefore important for governments to give these incentives, as they act as a start booster to get the industry going and that way give it a chance to eventually stand on its own feet.

Two ilustrative examples on how governmental incentives make a difference is the current situation in Germany and Spain.

Germany, located in northern Europe and consequently has a modest insolation density, are currently the country which is installing most photovoltaic panels in the world. One of the reasons has been the incentives provided by the government. One of the most important incentives was presented in 2006, when the socalled Renewable Energy Act (EEG) was introduced. The EEG included subsidies for producers of renewable energy, for example, producers of solar power received 43 eurocents for each kWh generated[52].

In Spain, a first incentive for CSP plants was introduced in 2002. This guranteed 12 eurocents per kWh produced. However, this incentive was found to be too small to give investors the needed security, and in 2004, the incentive was increased to 18 eurocents per kWh. This increase was the starting point in Spain where CSP for the first time was made economical attractive for investors, and they made the development of the Andasol plants, that was constructed in 2008, possible. The incentives boosted the construction of new plants in several ways: [53]

1. the same incentives was given for PV and CSP for installations from 100 kW up to 50 MW

2. An extra subsidy was given for the first 200 MW of CSP built (give a total of 0,21 eurocents per kWh.)

The incentives are annually adapted to the current electricity price, and the plants are allowed to use 12-15% in natural gas back-up.
[53]

In august 2005 the 200 MW limit was raised to 500 MW. This is the reason why there are so many 50 MW plants under development and under construction in Spain today. Actually, 12 50 MW plants are eighter under construction or under development.[46] (The plants does not exceed the 50 MW size due to the incentives that only are given for plants up to that size)

From this we can conclude that incentives like them given in Germany and Spain are an efficient way of increasing deployment rates of solar power plants. However, incentives like this cannot go on forever; eventually it must come to a point where the CSP industry should be able to stand on its own feet.

4.9 Paths towards a competetive LEC

Besides increasing of deployment rates and plant sizes due to gevernmental incentives, there are two main paths the solar industry can follow to make the solar energy competetive to

other sources.

The first is to spesialize the solar power plant to produce peak load power during hours when the sun is shining. One of the ways to do that is to built a solar power plant with eighter a small percentage of fossil fuel backup, or, with a smalll thermal storage system, each of the systems can be used to keep power production stable during short weather transitions. Another approach is to integrate a solar field into a conventional power plant in a socalled Integrated Solar Combined Cycle (ISCC). The ISCC is is a hybrid fossil-solar power plant which uses the solar field to heat up excess heat from the gas turbine to be runned in a steam turbine. This alternative requires only a solar field and no thermal storage.

There are several potential benefits regarding cost reduction here. For a solar power plant with a small percentage of fossil backup, the cost of a thermal storage system can be eliminated completely. With introduction of Direct Steam Generation (DSG) it is also possible to eliminate the cost of the HTF and heat exchangers and make the power block cycle considerably simpler with fewer parts. The power production from CSP plants typically reach peak power generation at the time of day when electricity consumption is at its highest, that is when electricity cost is at its highest. This peak load electricity is more expensive to produce by the base load power plants because the base load producing power plants have to use additional generators to generate the electricity. With a ISCC it is possible to increase the efficiency for the fossil power plant, beacuse one then can use the solar field to heat up the waste heat from the turbine and then use it in a gas turbine during peak load.

The second path one can follow is to construct base load solar power plants. These plants can have a high capacity factor. In this category it seems that the Power tower has the highest potential where high temperatures can be produced and energy storage becomes more effective. One must here develop a system that can use a high temperature HTF, which also can be used as energy storage. Another way is to use thermochemical storage where one uses the thermal energy to produce chemical compunds that can be stored easily and later used to produce electricity through an electrochemical device such as a fuel cell or a battery. (i.e hydrogen, methanol or ammonia). This apporach will be essential if the solar technology is going to be a source for fuel to transportation in future.

In the next chapter we will look at the approach where different types of energy storage is used to increase the capacity factor of the plant, eighter to produce electricity at night or to transport the energy from the plant for other uses.

Chapter 5

Energy Storage

Introduction of energy storage is an important step towards a competive LEC for a large scale centralized CSP power plant, and the only way for a solar-only power plant to produce base load power at any hour of the day.

The new Andasol plant in Spain is the only CSP plant in operation today with a significant thermal storage capacity, and althought, according to my calculation, the LEC has been increased at Andasol compared to the other plants in operation, the thermal storage concept has potential to reduce the LEC in the future. One must remember that the thermal storage system at Andasol is the first molten salt storage system ever built for a commercial CSP plant, and the next plants with the same technology will probably benefit from the experiences gained form the design and construction at Andasol. Also, there are other alternatives to thermal storage which is interesting and may be introduced at future solar power plants.

Below we will give an overview of the various storage methods available and then present in some detail the most promising methods for CSP.

5.1 Mechanical energy storage

The idea behind mechanical energy storage comes from the principle of energy concervation.

In this category we find one of the most common storage methods today, namely pumped storage.

5.1.1 Pumped Storage

Here, one uses the produced electricity to pump water uphill to a reservoir where it can be stored for later use. It can often be economical beneficial to do this during periods with low electricity prices and then produce electricity from this storage during peak energy prices.

It is the potential energy from the water which is utilized to produce electric energy trough hydroelectric turbines with high efficiencies.

The potential energy of a body of water with mass m and height h above the turbine is given by

$$E = mgh = \rho V g h \tag{5.1}$$

where ρ is the density of water and V is the volume of the water body.

The theoretical maximum electrical power output for a water turbine will then be, assuming water is incompressible, :

$$\frac{dE}{dx} = P_w = \rho g h \frac{dV}{dt} = \rho g h q \eta_w \tag{5.2}$$

where $q = \frac{dV}{dt}$ is the volume flow of water directed towards the turbine, and η_w is the efficiency of the turbine and generator combined.

The power needed for the pump to pump a given volume flow of water uphill a height h is given by.

$$P_{pump} = \frac{\rho g h q}{\eta_{pump}} \tag{5.3}$$

where q here must in practice be restricted by the volume flow capacity of the pump. η_{pump} is the pump efficiency, the friction factor for the tubes is also included in this efficiency.

The ratio between power extracted from the water and the power needed to pump the water uphill is then

$$r = \frac{P_w}{P_{pump}} = \eta_w \eta_{pump} \tag{5.4}$$

This means that for every kWh of energy delivered to the pumps for pumping the water uphill one will get the number r back in electricity. Usually, r lies between $0,7$ and 0,85[54].

Lets introduce a variable C_{pump} representing the price of electricity at the time the water is pumped uphill. Let C_w represent the price the electricity must be sold for when the water is released to the turbine, for the storage method to break even.

Assuming $C_{pump} = \$0,10$, C_w and r = 0,7 gives

$$C_w = \frac{C_{pump} * 1kWh}{r * kWh} = \frac{\$0,10 * 1kWh}{0,7kWh} = \$0,143 \tag{5.5}$$

which means that the electricity price at the time when the water turbine is generating electricity must be 43% higher than the price when the water was pumped uphill.

Since a CSP plant is producing most of its electricity during daytime/afternoon, when the market electricity price is at its peak, pumped storage may not be the best choice for a CSP plant. Also, the method is dependent on elevations in the terrain around the power plant which will limit possible locations for a CSP plant that wants to use pumped storage.

5.1.2 Compressed air

Another interesting storage possibility is to compress air in an underground reservoir, for instance in a depleted mine.

The theoretical limits for energy storage in a gas is governed by the laws of thermodynamics.

We assume in the following an ideal gas compressed underground in an reversible isothermal process in which the gas is compressed under constant temperature. The first law of thermodynamics is, in its most general form given by

$$\delta U = \delta Q + \delta W \tag{5.6}$$

The gas will here be compressed under constant temperature, this means that the heat gained from compression must be transferred and stored in the environments. Therefore, the gas loses an amount of heat to the environments and for a reversible process this heat will be returned when the gas expands again.

The internal energy of an ideal gas cannot be changed at constant temperature so in this case we must have $\Delta U = 0$ From Equation (5.6) we must have then that the work done during the compression is transferred to the environent in form of heat. However, to obtain an expression for the usefull work for the process one must subtract the volume work against the constant athmospheric pressure.

We will then obtain an expression for the total useful work for the process, also known as the exergy:[12]

$$W - p_o \Delta V = \Delta Q = -T_o \Delta S \tag{5.7}$$

The ideal gas law relates the intensive state quantities to each other in the following way:

$$pV = NkT \tag{5.8}$$

where N is the particle number and k is Boltzmann‘s constant.

We would like to find the mass of the air within the reservoir, given in kilograms.

Knowing that dry air at 300 K has $28,965$ g/mol and N_A is Avogadros number(Number of particles in one mole), then N can be written as

$$N = \frac{M_{air} N_A}{28,965 * 10^{-3} kg/mol} \tag{5.9}$$

where M_{air} is the total mass of air in reservoir after compression.

the total mass can then be found from the ideal gas law:

$$N = \frac{M_{air} N_A}{28,965 * 10^{-3} kg/mol} = \frac{p_1 V_{res}}{kT_1} \Longrightarrow M_{air} = 28,965 * 10^{-3} kg/mol * \frac{p_1 V_{res}}{N_A k T_1} \tag{5.10}$$

where, V_res is the volume of the compressed air in the reservoir.

The useful work from the compression is found from Equation (5.7):

$$W_{useful} = p_0 dV - T_0 dS \tag{5.11}$$

We can now introduce the enthalpy H = U + pV and the totalt differential of the enthalpy dH = TdS+Vdp. Rearranging the terms gives:

$$dS = \frac{dH}{T} - \frac{V dp}{T} = C_p \frac{dT}{T} - \frac{Nk}{p} dp \tag{5.12}$$

In the last equality we used the relation dH = C_pdT , where C_p is the heat capacity under constant pressure, and the substitution V = $\frac{NkT}{p}$

Integration between initial- and end state yields:

$$dS = p_0 \int_{S_0}^{S_1} dS = (S_1 - S_0) = \Delta S = C_p \int_{T_0}^{T_1} \frac{1}{T} dT - Nk \int_{p_0}^{p_1} \frac{1}{p} dp = 0 - Nkln(\frac{p_1}{p_0}) \quad (5.13)$$

where we have assumed C_p constant and that $T_1 = T_0$.

Thus, the expression for T_0dS becomes

$$- T_0 Nkln(\frac{p_1}{p_0}) \quad (5.14)$$

The negative value reflects the fact that the gas loses an amount of heat to the environment during the compression.

For reversible processes, the compression is given in terms of the initial state and the endstate, and with this in mind we can calculate p_0dV with the help from the ideal gas law:

$$p_0 dV = p_0 \int_{V_0}^{V_1} dV = p_0(V_1 - V_0) = p_0(\frac{NkT_1}{p_1} - \frac{NkT_0}{p_0}) = NkT_0(\frac{p_0}{p_1} - 1) \quad (5.15)$$

Adding together Equation (5.14) and Equation (5.15) one finds the total useful work that can be extracted from the compressed air:

$$W_{useful} = p_0 dV - T_0 dS = NkT_0(\frac{p_0}{p_1} - 1) + T_0 Nkln(\frac{p_1}{p_0}) \quad (5.16)$$

From the ideal gas law wa have NkT = pV, this gives the final expression for the total usefull work:

$$W_{useful} = p_1 V_{res}[ln(\frac{p_1}{p_0}) + \frac{p_0}{p_1} - 1] \quad (5.17)$$

We observe that the useful work depends linearly on the volume of the underground reservoar, so by doubling the reservoar volume one also doubles the useful work.

Assuming $V_{res} = 5 * 10^5 m^3$, p_0 = athmospheric pressure at sea level = $100kPa$, $p_1 = 1000kPa$, Equation (5.18) gives the following value:

$$W_{useful} = 10^6 Pa * 5 * 10^5 m^3 * [ln(\frac{10^6}{10^5}) + \frac{10^5}{10^6} - 1] \sim 7 * 10^{11} J = 700GJ. \quad (5.18)$$

We can then calculate how long this energy will last for a given power output:

$$storage\ time\ in\ hours = \frac{7 * 10^{11} J}{Power\ output * 3600s} \quad (5.19)$$

With power output = 50MW one finds that the storage time will be approximately 4 hours. To increase the storage time one could eighter increase the storage volume or increase the pressure. Alternatively one could lower the power output.

The energy above is the mechanical energy needed to compress the gass and it equals the mechanical work the gas does on the environment when it is discharged and expandes again.

We assumed that the compression was done isothermal, this implies that the reservoir, where the gas is stored, must be a heat bath and the compression must happend infinitely slow to allow the gas to continously transfer its heat to the reservoir trough a heat exchange. The second assumption was the assumption that air is an ideal gas. This is not too bad an approximation under room temperatures and atmospheric pressure. However, as the pressure increases the behaviour of the gas deviates more and more from an ideal gas and one needs a more complex equation of state to describe the gas. The last assumption was the assumption of a reversible process, this means that the thermodynamic varibales have definite values for each step in the process, and therefore, the work done will be the area under the well defined curve in a PV-diagram.[55] The assumption of reversibility says that the same amount of work done from the environments on the gas under compression can be delivered back to the environments when the gas is expanded again.

Despite the assumptions, the calculations above should give an indication of the order of magnitude a reservoir should be in to store an appreciable amount of energy.

In practice the air will reach high temperatures when compressed, and it actully needs to be cooled down again before pumped underground. When expanding again, the air must go through a turbine to produce electricity. It should also be heated up from an external gas source to increase the efficiency of the turbine. The turbine efficiency and the need for an external heat source gives the compression system a low efficiency. For every kWh of energy going in to the system, about one half kWh of electricity is produced.[56] This makes it less commercially viable for plants that cannot produce and store large amounts of energy at off peak periods when electricity price are low.

A requirement for the current CAES technology is the need for large underground storage facilities, as the calculation above indicates. This means that the plant should be in close proximity to well suited geological formations like abandoned mines, aquifiers and salt caverns that have large volume capacities. The calculation above indicates a magnitude of $10^5 m^3$ and above. An alternative to underground geological formations would be that the compressed air is stored in high pressure tanks at the surface. However, these tanks are not yet commercial viable due to their high cost. They would also have to be very large to reach the same energy storage potential as the underground systems.

There are research going on to increase the efficiency to around 70%, which would give the system about the same efficiency as pumped storage discussed earlier[56]. To reach this efficiency, there is a design called advanced adiabatic CAES. Here, the heat is removed from the air during compression, and stored in isolated tanks. The heat will then later be used to reheat the air as it is released from the underground reservoir. This avoids the use of external heat sources.

The thermal nature of CSP plants, where thermal energy is converted into electrical energy, indicates that the best suitable storage system should be able to utilize the thermal energy produced from the solar field. This can be done in the categories described in the following sections.

5.2 Thermochemical energy storage

An ideal thermochemical reaction for solar thermal energy storage is an endothermic reaction with a characteristic reaction temperature near the temperature produced by the solar concentrator. The reaction products must be easily separable and not undergo further reactions. Several types of reactions can be used in a thermochemical storage system, the main restriction is that the characteristic temperature of the reaction must be within reach for the solar concentrator that is being used.

One can divide the thermochemical systems into two systems; Systems that uses fuels cells in production of electricity, and systems that uses a conventional steam cycle to produce electricity. Below are one specific reaction presented from each of the categories:

5.2.1 Thermochemical storage combined with steam cycle

In this system we must have a reaction of the type

$AB + \Delta Q \rightleftharpoons A + B$

That is, the reactant in the endothermic reaction must be resynthesized in an exothermic reaction in which heat is produced. The heat produced will in an ideal thermodynamic reversible cycle be the same amount of heat that was needed for the endothermic reaction. This makes the storage system a closed loop with a fixed amount of reactants.

A thermochemical reaction which has recently been developed in combination with a Parabolic dish solar plant, is an ammonia based system where ammonia is dissosiated into Hydrogen and Nitrogen in an endothermic reactor which is placed at the focal point of the parabola[57].

Figure 5.1: Storage system based on thermochemical ammonia dissosiation [57]

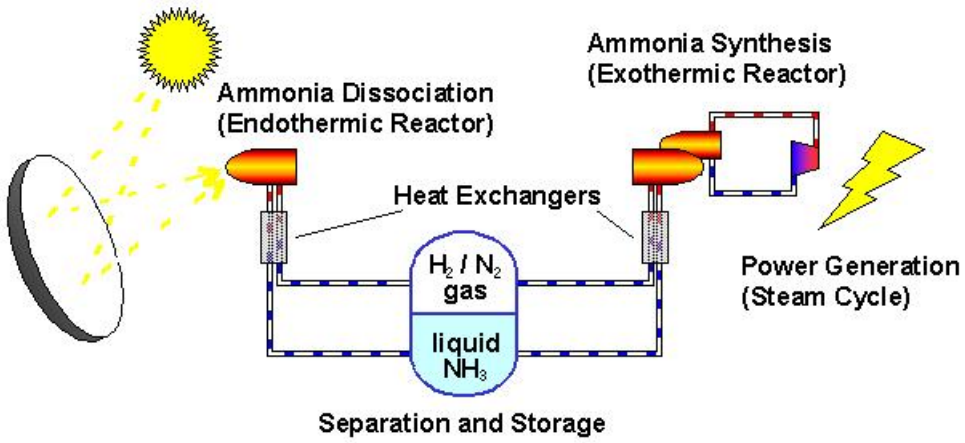

Both the exothermic and endothermic reactors uses standard catalyst materials to increase the reaction rates. The result is the two-way reaction

$$2NH_3 + \Delta Q \rightleftharpoons N_2 + 3H_2 \tag{5.20}$$

where $\Delta Q = 92,4$ kJ/mol of reactant mixture.

Parts of the dissosiated mixture of nitrogen and hydrogen are transfered to a storage system under high pressure to keep the mixture in a liquid form. Another part is transfered to an exothermic reactor which in practice will be placed close to the Power Plock of the plant. Here ammonia is reproduced and transfered back to the exothermic reactor. The heat produced in the reaction is tranfered through heat exchangers to a HTF fluid in a steam cycle.

Because the system is pressurized to the point that ammonia spontaneously condenses at the surrounding temperatures, and the Nitrogen/Hydrogen still is in a gaseous phase, it is possible to use the same storage system for both the ammonia and the Nitrogen/hydrogen mixture.[58] The system will also be a closed loop with a fixed amount of reactants.

5.2.2 Comments about the efficiency of the system

Once the reactant products are stored in liquid form in the storage system, there will be no losses since all the thermal energy now is stored as chemical energy at the temperatures of the surroundings.

However, there will be indirect losses due to the energy needed for powering the compressors that maintains the needed pressure. The heat exchangers that connects the exothermic reactor to the steam cycle will also have losses.

From thermodynamics we know that for a cycle to be reversible it must always be in thermodynamic equillibrium. Real chemical reactions can never be carried out in thermodynamic equillibrium (the reaction rates must then approach zero and nothing will happend) and they can therefore not be reversible. A system which is not in equillibrium will lose energy in form of heat until equillibrium can be reached. The endothermic part of the system must therefore always operate at temperatures above equillibrium and the exothermic part of system will opeate with temperatures below equillibrium. At night, isolation of the exothermic reactor becomes especially important since the temepraturs (especially in deserts) becomes very low.

There will also be initial losses between the solar collector and the exothermic reactor because of reradiation, and this loss increases as the reactor reaches its stagnation temperature. Also, if the characteristic temperature of the reaction is less than the temperature produced by the concentrated solar radiation, then the exess exergy is wasted (if not stored in the reactor), and this means a lower energy desity for the solar field. But this may not be a big problem as the solar system can be configured in such a way that the correct temperature can be reached, or that the reactor can take up more of the energy by feeding it with more reactants. Since the parabolic dishes have potential to reach much higher temperatures (over 2000°C) than the temperatures needed for this particular reaction ($450 - 500$°C), it means that the parabolic dishes can be made with cheaper materials with lower optical quality.

We can divide the efficiency of the total system into three parts: A thermal efficiency for the endothermic part of the thermochemical loop, η_{endo}, the work recovery efficiency, which is the chemical-to-thermal conversion efficiency for the exothermic part of the loop, η_{exo}. Lastly we will have a parasitic efficiency factor η_{par} which accounts for the energy needed to power the compressors.

$$\eta_{endo} = \frac{Exergy\ stored\ in\ reaction}{Exergy\ input}\ and\ \eta_{exo} = \frac{Exergy\ output}{Exergy\ stored\ in\ reaction} \tag{5.21}$$

From definiton, η_{endo} will be largely dependent on the characteristic temperature of the given reaction.The exergy stored in the reation is dependent on the amount of reactants in the reactor and the exergy input. The exergy input is dependent on the solar irradiation at the given location and the quality of the concentrator system. Lower needed temperature means cheaper materials with lower optical performance. There may also be possible to use the less expensive parabolic trough techonlogy for this particular system since the temperatures needed are within reach for the standard trough technology in use today.

We have for the total efficiency

$$\eta_{tot} = \eta_{endo} * \eta_{exo} * \eta_{par} = \frac{Exergyoutput}{Exergyinput} * \eta_{par} \tag{5.22}$$

where η_{par} is the efficiency of compressors (parasitic losses).

5.2.3 Thermochemical storage combined with fuel cell

Instead of a steam cycle for electricity production one could use fuel cells to produce the electricity. This would require the production of Hydrogen, if we wanted a hydrogen fuel cell. An alternative would be to produce the Hydrogen at the power plant and then transport the hydrogen out to the consumers through long distance pipelines.

In a possible future transportation system where fossil fuel is replaced with Hydrogen as a transportation fuel, it could be advantageous for the solar CSP plant to produce hydrogen from the termal energy received form the solar field. In practice this could be done in a specialized hydrogen producing power plant with no additional electricity production.

Another alternative would be a CSP plant where one part of the plant produced hydrogen and another part produced heat to run a steam cycle. Then, one also could produce electricity at night with an integrated thermal or thermochemical storage system. To be able to produce the hydrogen at night one would need a hydrogen producing reaction that could run on lower temperatures. To run high temperature reactions at night based on the stored solar energy would put high requirements on the thermal storage systems, but high temperatures to produce Hydrogen is not necessarily needed. It is possible to divide the reaction cycle into multiple steps. The energy requirements for each of the steps would add up to the total energy requirements to produce Hydrogen.

The splitting of water to produce Hydrogen can be done in several ways.

- **Electrolysis**
  This step reqires electricity to split water. Since the electricity first must be produced this procedure usually would give a low conversion efficiency.

- **Hydrocarbon based production**
  Fossil fuel, currently is the main source of hydrogen production. Hydrogen can be generated from natural gas with approximately 80% efficiency, or from other hydrocarbons to a varying degree of efficiency. Specifically, bulk hydrogen is usually produced by the steam reforming of methane or natural gas at high temperatures (700-1100°C), H_2O reacts with methane CH_4 to yield syngas.[19]

- **Thermochemical reactions**

  Here, one uses thermal energy to trigger endothermic reactions that can be used for Hydrogen production. There are three different approaches that can be used depending on the temperature that can be reached in the reactor.

1. Direct thermal dissosiation of water

   Any molecule can be separated into its constituents by direct thermal dissosiation. However, the direct thermal dissisiation of water requires temperatures above 2100K, and even at that temperature a small percentage of the molecules are being dissosiated[59]. A problem with this direct method, besides the needed high temperatures, is that the separation of hydrogen and oxygen here takes place in the same reactor chamber, and this can greatly reduce efficiency since the two atoms may recombine before the Hydrogen is taken out of the reactor.

2. Multiple step thermochemical cycle

   These cycles divide the total required amount of energy into many subreactions, each of them requires lower temperatures than with a direct approach. This helps reducing high temperature material requirements. In addition a catalyst that can be recycled is used to increase reaction rates at lower temperatures. A problem with multiple step cycles is that the overall efficiency tends to go down since each step loses some useful work to the environments. The most common multiple step method used today is the tree-step Sulfur-iodine cycle, which requires three steps and the highest temperature needed is 850 degrees, which can be obtained in combination with a nuclear power plant. [60]

3. Two-step thermochemical cycle

   These cycles require relatively high temperatures, but often temperatures that are within reach for a high concentrating solar thermal system, such as parabolic dishes or central power towers. The cycles which is of current interest by researchers are cycles based on Metal oxides. The cycle are divided into two steps , which takes place in two different reactors, or reactor chambers. The first step takes place in a reactor chamber directly exposed to the incoming solar power from the concentrating system. Here, oxygen atoms are separated from the metal oxide and directed outside before recombination. What is left is a reduced metal oxide that will be transported to the second chamber. In this chamber, H_2O from outside is introduced. The reduced metal oxide absorbs the Oxygen and Hydrogen is produced. This step is called the Hydrogen producing step, and the process is called hydrolysis. The Hydrogen producing step can potentially be proceeded without direct solar exposure.

The splitting of water to produce Hydrogen needs high temperatures. Most often temperatures above 1000 degrees celcius are required. To reach a high temperature one needs a high concentration ratio, and because of this, the parabolic trough technology is not well suited for hydrogen production. The high required concentration factors can instead be reached with the parabolic dish or the central tower. Often a combination of the two will be required.

The high temperature that can be reached with these two technologies allows a wide range of reactions to be used. Actually, over 200 different reaction cycles have been studied, and $12 - 14$ of them are under close research[60].

5.2.4 Thermodynamical considerations on a general two-step thermochemical cycle

In the following we will use a basic thermodynamic analysis (based on [61] and [62]) to determine the maximmum efficiency for the ideal two-step cycle.

The efficiency of an ideal, reversible chemical reaction with no entropy losses is given by the Carnot efficiency

$$\eta_c = 1 - \frac{T_0}{T_r} \tag{5.23}$$

where T_0 is the temperature of the environments and is assumed to be 300 K in this analysis. T_r is the temperature of the reactor.

Before the chemical reaction can start, the reactor must absorb the energy from the incoming irradiance emitted from the concentrator system. Therefore, the ideal efficiency will be the product of the carnot efficiency and the absorption efficiency[61]. The absorption efficiency is given by (We assume for simplicity the optical efficiency of the concentrator system equals 1, ($\eta_{optical} = 1$)

$$\eta_{abs} = \frac{P_{reactor}}{P_{solar}} = \frac{P_{solar} - P_{reradiation}}{P_{solar}} = 1 - \frac{P_{reradiation}}{P_{solar}} \tag{5.24}$$

where P_{solar} is the incoming power towards the reactor window, and $P_{reradiation}$ is the amount of power that is reradiated back to the environments from the reactor windows.

Assuming a black body receiver with no convection or conduction losses, the reradiation is given by the Stefan-Boltzmann radiation law. Assuming that the reactor window has a surface area that exceeds the "focal point area" and thus captures all the incoming radiation, P_solar is given by the product of the concentration ratio and the incident solar intensity per square meter at the earth's surface (I_s), we then get

$$\eta_{abs} == 1 - \frac{\sigma T^4}{C_g * I_s} \tag{5.25}$$

The reradiation from the reactor window $P_{reradiation}$, has the unit joule per seconds per square meter. To find the total reradiation losses, $Q_{reradiation}$, one must multiply with the window surface of the reactor. The same is true for the total incoming solar energy P_{solar}. So we have:

$$Q_{solar} = I_s * C * A_{window} \quad and \quad Q_{reradiation} = \sigma * T^4 * A_{window}. \tag{5.26}$$

Lets say we need a certain amount of solar energy for the reactor. Then, by increasing the concentration ratio one can reduce the needed window area to obtain the same amount of energy. This will at the same time reduce the reradiation losses. So we can then immediately conclude that it is possible to reduce the reradiation losses just by increasing the concentration ratio.

Now, since the incoming solar radiation is (almost) pure exergy we call the following efficiency the ideal exergy efficiency.

$$\eta_{idealexergy} = \eta_{abs} * \eta_c = (1 - \frac{\sigma {T_r}^4}{C_g * I_s})(1 - \frac{T_0}{T_r}) \tag{5.27}$$

The carnot efficiency alone gives the highest value when T_r is as high as possible. However, the absorption efficiency will become zero when T_r reaches the value such that the reradiation losses equals the incoming radiation. This critical temperature is called the stagnation temperature. The total exergy efficiency will therefore also be zero at this stagnation temperature. Therefore, the optimal temperature a receiver should have for the system to reach the highest efficiency must be below this stagnation temeprature. By inspection of Equation (5.27) we observe that the stagnation temperature will increase when the concentration ratio and the incident solar radiation increases, and the optimum temperature will therefore also increase.

A detailed investigation of the optimal temperature , T_{opt}, can be done by calculating the derivative of $\eta_{idealexergy}$ with respect to T_r and set it equal to zero[61]:

$$\frac{\partial \eta_{idealexergy}}{\partial T_r} = 0 \tag{5.28}$$

which results in the following 5. order polynomial

$$T_{opt}{}^5 - \frac{3}{4} T_0 T_{opt}{}^4 - \frac{T_0 I_s C_g}{4\sigma} = 0 \tag{5.29}$$

A plot of T_{opt} against C_g with various values of I is shown in Figure 5.2, together with a plot of $\eta_{idealexergy}$ against T_{opt}.

We see from the upper plot in Figure 5.2 that for the optimal temperature to exeed 2000 K one needs concentration ratios of over 20000, given an incident solar radiation of 1000 W/m^2. The efficiency that coresponds to T_{opt} = 2000K, for I = 1000 W/m^2 can be seen from the graph below, and it is close to 80%. The graphs of various I values coincides with each other at the graph below, indicating that the efficiency is more or less independent of the value of I, and more dependent on the concentration ratio, since the concentration ratio can make up for low values of I.

A more clear picture on how the efficiency vary with the actual temperature of the reactor can be seen with a plot of the actual temperature T_r versus the efficiency. (Figure 5.3) Various values of C is given as a parameter. I is assumed 1000 W/m^2 in each of the graphs.

Here, we can see clearly the decrease in efficiency when T exeeds T_{opt}, for various values of C, and reach zero when the temperature reach the stagnation temperature. The temperatures in the reactor will, for many two-step cycles, exeed 2000K. From the graph wee see that the concentration ratio should be above 2500 to give a reasonable maximum ideal exergy efficiency at that temperature. (Maximum $\eta_{idealexergy}$ for the temperature 2000K with a concentration ratio 2500 is, according to the graph, around $0,54$)

It is possible to construct collector systems with concentration ratios around 10000. This can be done by using a heliostatfield in combination with a central tower where another concentrator is placed. The solar beams can then be redirected down to a paraboloid which focuses the radiation towards the reactor chamber. The $\eta_{idealexergy}$ for a collector system with concentration ratio 10000 will be around $0,72$ with a reactor temperature at 2300K.

There are ways to increase the optimal temperature for a given maximum efficiency. The key lies in the stagnation temperature. If one can increase the stagnation temperature then the optimum temperature T_{opt} also can be incrased.

Figure 5.2: A Plot of the optimal temperature T against the concentration ratio C and the ideal exergy efficiency $\eta_{idealexergy}$ in the upper and lower graph, respectively

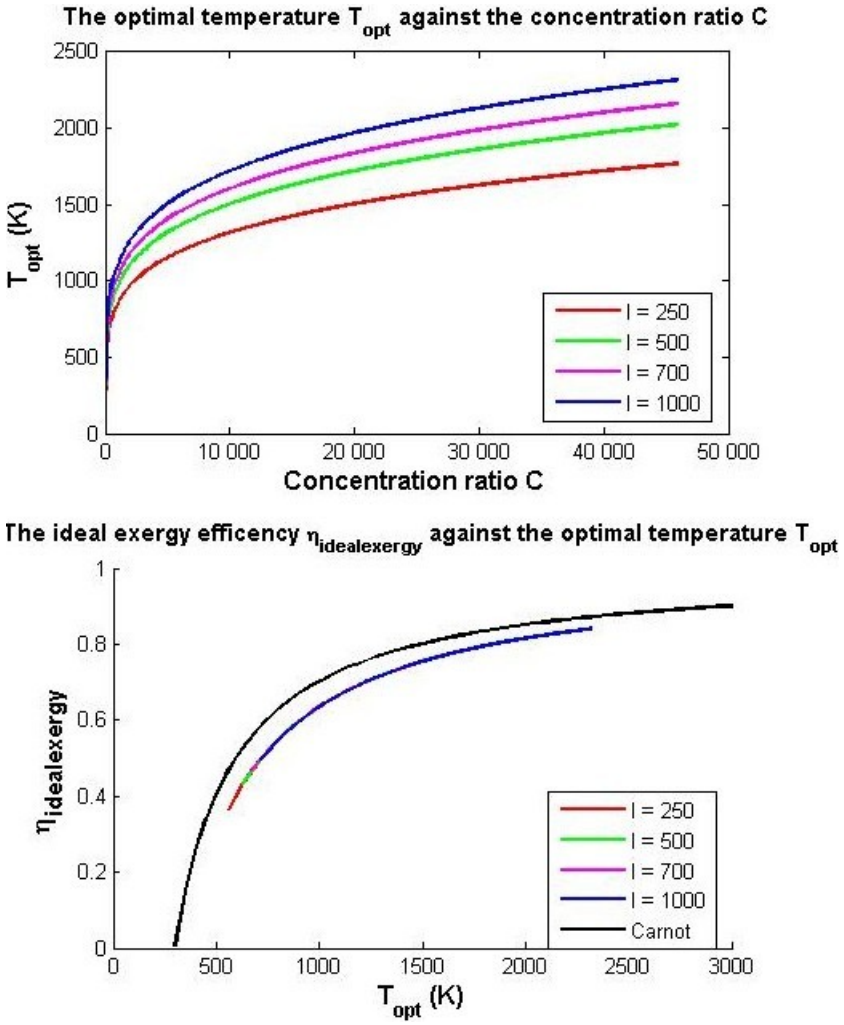

The stagnation temperature for the reactor is dependent on how large amount of the incoming radiation spectrum is absorbed and how large amount that is reradiated. We based our calculations on an ideal black body receiver which have a reradiation that follows the Stefan-Boltzmann law, with maximum reflectance and absorptance. It would be possible with selective surfaces to increase absorptance or reflectance for given wavelengths in the solar spectrum. This will effectively increase the stagnation temperature. A selective surface has different properties for different parts of the solar spectrum. The wavelength for which a Black body‘s radiation, with a given temperature T, peaks, can be found from Wien‘s displacement law:

$$T\lambda_{max} = 2,8978 * 10^{-3} Km \implies \lambda_{max} = \frac{2,8978 * 10^{-3} Km}{T} \tag{5.30}$$

For T = 2000 K, $\lambda_{max} = 1,45\mu$. The Solar radiation peaks at $\lambda_{max} = 0,5\mu$ (the Sun

Figure 5.3: A Plot of the actual temperature T_r of the reactor against the ideal exergy efficiency

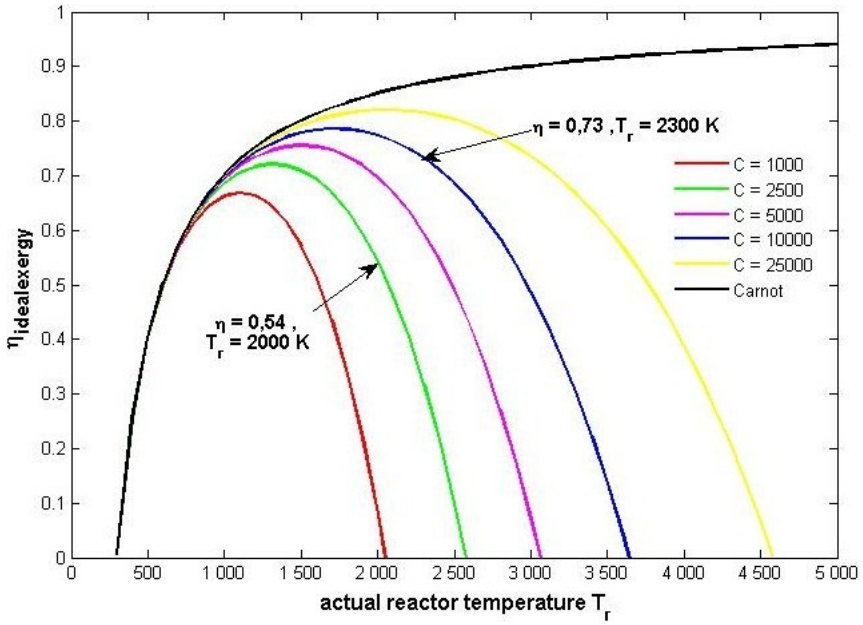

is a black body with T = 5780K) . Knowing this one can make reactor windows with high absorptance around wavelngths $0,5\mu$ and high reflectance around wavelengths $1,45\mu$.

5.2.5 A more realistic efficiency - including irreversible heat losses

What we found above was an expression for the ideal efficiency, when there was no irreversible heat losses in the reaction. What we will find now is a way to express the overall exergy efficiency for a chemical cycle, including irreversible heat losses in the reaction. We introduce the tree thermodynamical potentials G, H and S.

The total energy required to split water is a standard number that can be found in tables and is given in terms of the enthalpy change ΔH or the change in gibbs free energy ΔG , which is defined as

$$\Delta G = \Delta H - T\Delta S \tag{5.31}$$

and ΔH as

$$\Delta H = \Delta U + P\Delta V \tag{5.32}$$

where ΔS is the change in entropy for the reaction. ΔG can be understood as the amount of heat per mole of a chemical compund which can contribute to do useful work, for instance as electrical energy.

ΔH on the other hand, can be interpreted as to be the amount of heat released by a process when no work is being done on the environments, that is, all the energy is converted

into heat.

The total energy required to split water depends whether the water is in a liquid state or in a gaseous state. We have for the liquid state

$$\Delta H^\circ{}_{f,liquid} = -285,8kJ/mol \tag{5.33}$$

and for the gaseous state

$$\Delta H^\circ{}_{f,gaseous} = -241,9kJ/mol \tag{5.34}$$

The superscript $^\circ$ means that it is measured at standard conditions (298K and 1 atm)

We will in the following use $\Delta H^\circ{}_{f,liquid}$ as this usually gives a more correct picture of the real process, according to [63].

$\Delta H^\circ{}_f$ is known as the enthalpy of water formation and it is defined to be the change of enthalpy that accompanies the formation of 1 mole of a substance in its standard state from its constituent elements in their standard states.

By definition the Gibbs free energy of formation of water,$\Delta G^\circ{}_f$, is for the liquid state

$$\Delta G^\circ{}_{f,liquid} = -237,2kJ/mol \tag{5.35}$$

5.2.6 Ideal fuel cell efficiency

The efficiency of the ideal fuel cell where total entropy change equals zero can be found in the following way:

The production of one mole H_2O requires one mole of Hydrogen gas and a half mole of oxygen gas.

$$H_2 + \frac{1}{2}O_2 \rightarrow H_2O \tag{5.36}$$

In this process, the entropy decreases. The heat related to this entropy decrease is given by

$$T\Delta S = \Delta H^\circ{}_{f,liquid} - \Delta G^\circ{}_{f,liquid} = -285,8kJ/mol + 237,2kJ/mol = -48,7kJ/mol \tag{5.37}$$

The second law of thermodynamics tells us that the entropy can never decrease, so for the ideal case, this same amount of heat must be lost as heat from the fuel cell to the environments. So, the ideal fuel cell will therefore convert the $285,8$ kj/mol chemical energy into $285,8-48,7 = 237,2$ kJ/mol electrical energy, which is the gibbs free energy of formation. the ideal fuel cell efficiency is therefore

$$\eta_{FC} = \frac{\Delta G^\circ{}_{f,liquid}}{\Delta H^\circ{}_{f,liquid} = -285,8kJ/mol} = \frac{-237,2kj/mol}{-285,8kJ/mol} = 0,83 \tag{5.38}$$

The efficiency of the overall cycle will be the ratio of useful electric work per mol times the molar flow rate of hydrogen, over the initial solar power required for a given molar flow rate $\dot{n}$:

$$\eta_{exergy} = \frac{-\dot{n}\Delta G}{\Delta H_{tot}} kj/mol \tag{5.39}$$

where ΔH_{tot} is equal to the incoming solar power from the concentrator needed to produce n mole of hydrogen in the reactor. $\dot{n}\Delta G$, should be equal to the solar power from the concentrator required to produce n mol of Hydrogen, minus the power losses in the reactor and in the fuel cell for each mol of Hydrogen produced [62]:

$$\eta_{exergy} = \frac{P_{solar} - (P_{reradiation} + P_{reactorlosses} + P_{fcl})}{P_{solar}} = 1 - \frac{P_{reradiation} + P_{reactorlosses} + P_{fcl}}{P_{solar}} \tag{5.40}$$

The losses,P_{fcl} for the ideal fuel cell, was found above. The losses in the reactor, $P_{reactorlosses}$, is not known, but can be meaured for a given reactor design, and the reactants used.

This exergy efficiency differs from the ideal exergy efficiency we found first since we here have taken account for the irreversible losses in the reactor and the fuel cell. Because of this, this efficiency will be lower than the ideal exergy efficiency and are close to the value that can be obtained by real cycles.

An example of the value of this efficiency for a ZnO cycle with a concentration ratio of 10000 is 36%[62].

5.2.7 Examples of Thermochemical water splitting cycles

The cycles based on metal oxide catalysators combined with parabolic dish concentrators are undergoing intense studies and experiments today. The cycles have currently a low efficiency but the improvement potential are still big.

The general two step cycle using a metal oxide M_xO_y is

$$M_xO_y + \Delta H \rightarrow xM + \frac{1}{2}O_2 \tag{5.41}$$

$$xM + yH_2O \rightarrow M_xO_y + H_2 \tag{5.42}$$

The first step will always be endothermic and in the cycles discussed here, it will require a high temperature.

In the follwing, a reactor design, using an iron oxide, recently developed by Sandia National Laboratories is discussed[64].

The endothermic reactor is divided into two chambers, one chamber for the Oxygen separation, and one chamber for the Hydrogen separation.

The interior of the reactor contains rotating rings made up of a mixture of cobalt and iron oxide, where the iron oxide is the catalysator and therefore distributed over the surface of the rings. Each ring is about 1/3 meter in diameter and rotates between the two reactor chambers.

Sunlight from a heliostat is directed onto a parabolic dish which then focuses the light trough the reactor window, heating the interior to around 1500°C.

In the first chamber, the flakes of iron oxide on each ring releases oxygen molecules. The oxygen molecules is then separated and sent outside the reactor. The rotating disks then enters the second chamber. Here, at around 1100°C, CO_2 is added from the outside and the catalyst then absorbs oxygenatoms from this CO_2. The result is then Carbon monoxide (CO) which then is separated trough a membrane in the reactor. As the picture above shows, the iron oxide is regenerated and recycled back to the first chamber where new reactions take place.

Figure 5.4: Thermochemical cycle based on the Fe_3O_4 catalyst [64]

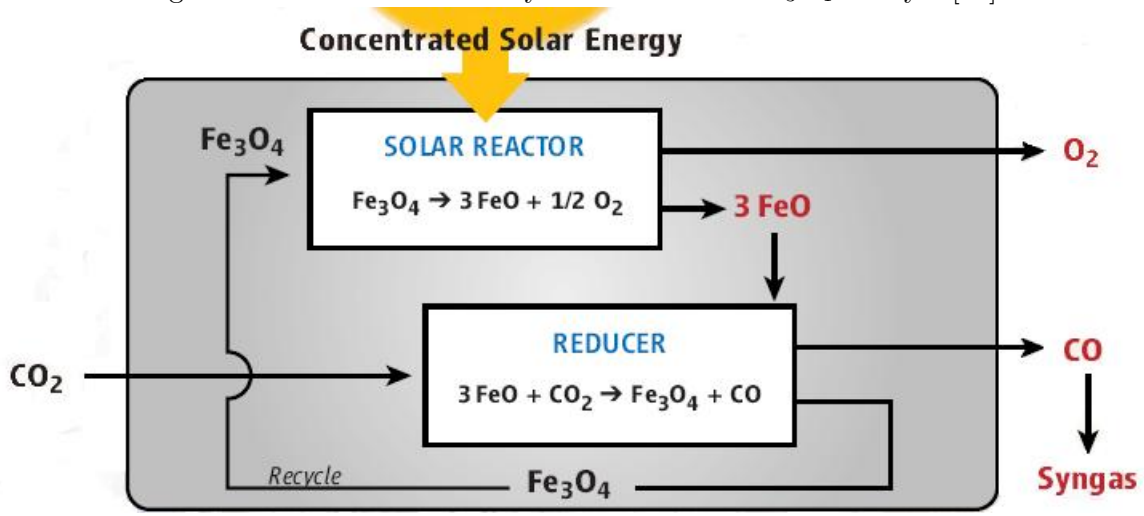

The same reactor design can also produce hydrogen. In this case, instead of CO_2, H_2O will be added in the second step. The catalyst picks up the oxygen atoms and the H_2 is separated:

$$Fe_3O_4 \rightarrow 3FeO + \frac{1}{2}O_2 \quad (1800K) \tag{5.43}$$

$$3FeO + H_2O \rightarrow Fe_3O_4 + H_2 \quad (1400K) \tag{5.44}$$

It might be advantageous to operate with higher temperatures for the first step if this step has the highest efficiency. Since the total energy can be stored in the reactant products, the second step then will require less direct solar energy. If the temperature gets high enough in the first step and the reactants can store the energy efficiently, the hydrogen producing second step may continue over night without solar input. For examble:

$$Fe_3O_4 \rightarrow 3FeO + \frac{1}{2}O_2 \quad (2500K) \tag{5.45}$$

$$3FeO + H_2O \rightarrow Fe_3O_4 + H_2 \quad (700K) \tag{5.46}$$

An increase in temperature in the first chamber would also help the iron oxide to give up a larger amount of its oxygen atoms.

Another cycle that is being developed at the Solar Technology Laboratory in Switzerland is a two-step cycle based on a zinc oxide catalyst:

$$ZnO \rightarrow Zn + \frac{1}{2}O_2 \quad (2100K) \tag{5.47}$$

$$Zn + H_2O \rightarrow ZnO + H_2 \quad (700K) \tag{5.48}$$

The first step is directly exposed to solar radiation. At 2100 K, the oxygen atoms separates from the zinc oxide and results in a mixture of Zink vapor and oxygen atoms. The zink

vapor is transported through a water cooled tube to the next chamber. This tube operates as a socalled quench. The quench rapidly cools down the zink vapor down to around 700K. This must be done to avoid recombination with the ozygen atoms before entering the second chamber. In the second step H_2O is added and the zinc powder absorbs the oxygen atoms. hydrogen is produced and the zinc oxide is reproduced, ready for another cycle.

Here, the first step is highly endothermic and needs a concentration ratio of over 5000. Because one uses a solid catalyst in form of the zinc oxide, with high heat capacity, the solar energy can be stored over night in the chemical bonds of the solid. Therefore,in principle, hydrogen production in the second step can proceed without interuption over night.

5.2.8 Key challenges to overcome for the two cycles discussed

The main loss in the reactor for the zinc oxide cycle is due to the cooling step. zinc vapor and oxygen molecules tends to recombine during the cooling after the first step.

To obtain the maximum amount of zink one must cool it down as rapid as possible, and by using a water cooled copper tube one can reach cooling rates around 1000K/s. With this method one have measured that around 18% of the initial zink vapor produced will make it through to the hydrogen producing step [65].

The heat loss related to the cooling is given by the molar flow rate times the enthalpy change of the reaction when cooled down from 2100K to 700K:

$$Q_{cooling} = \dot{n} * \Delta H|_{Zn(g)+0{,}5O_2 at 2300K \rightarrow Zn(s)+0{,}5O_2 at 700K} \tag{5.49}$$

given the molar flow rate the value can be found at standard conditions in standard chemical tables.

This problem with recombination is the biggest issue for the thermochemical reactors today and researchers are looking for new technology to improve this.

One of the solutions can be to develop a high temperature O_2 transport membrane which can be used within the reactor. The membrane patent is standard in many reactors but it is difficult to implement in the zinc cycle due to the presence of the high temperature zink vapor.

These losses and the losses related to the reradiation and losses in the fuel cell results today in an overall thermal to electric efficiency at just over 3% when the reactor is combined with a concentrator system. Engineers working on the systems today claims that the efficiency can be increased ten fold,and at least to over 20% in the following years to come[64].

Another challenge in this cycle is also due to the zink vapor in the first chamber. The zink vapor tends to reach the reactor windows and creates a shading effect for the incoming solar radiation which also decrease the efficiency.

[65] have made an estimate on how large a heliostat field (in combination with a central power tower) should be to be able to produce 100000kg hydrogen per day with 13 hours of storage. With the same solar intensity as in California ($\sim$ 2700kWh/year/m^2) a concentration rato of around 7000 is needed. With an assumption of 70% ZnO dissiciation in the first step and a100% conversion in the second step and an a annual sun to receiver/reactor efficiency of $44,9\%$, an heliostat field of 168000m^2 is needed.

5.3 Electrochemical energy storage

In this category we find the batteries. Storage using batteries are potentially capable of storing large quantities of energy, but they typcally have a relatively low power output. The battery research and development today are usually aimed towards small end-user applications, such as computers and, recenty, vehicles. Therefore large scale battery technology for grid applications are currently very expensive, and this is the biggest limitation for the deployment of the technology. There are current research in battery technologies specializing in large scale installations, for instance at MIT[22].

The largest capacity in use in the United States today is a Nickel-Cadmium battery tank installed in Fairbanks Alaska. Its capacity are 27 MW for 15 minutes which corresponds to 6,75 MWh. The capacity are used for stabilization of fluctuations on a transmission line.[66].

Another battery technology that are widely in use are Sodium/sulfur (Na/s) batteries. Here, Molten sulfur are used for the positve electrode and molten sodium for the negative. The battery have an efficiency of $\sim$ 90%. It is widely in use in Japan with a total of 270 MW installed, the largest single installation a 34 MW (245 MWh) unit used for wind farm stabilization[66].

Flow Batteries is also an interesting trend for grid storage application. The main difference between a conventional battery and a flow battery is that in a flow battery the electrolytes are stored in separated storage tanks outside the battery. The electrolytes can be circulated through the battery reactor, where a redox[1] reaction is producing the electricity. Since the electrolytes are stored in external tanks, the capacity of the system is very flexible and both the power capacity and the energy capacity can be varied independently. The system are also recycelable and it can provide energy over potentially thousands of charge/discharge cycles. Efficiencies for flow batteries are around 80%, a little lower than for the conventional batteries, due to parasitic losses for the pumping system.

Figure 5.5: Schematics of a flow battery [67]

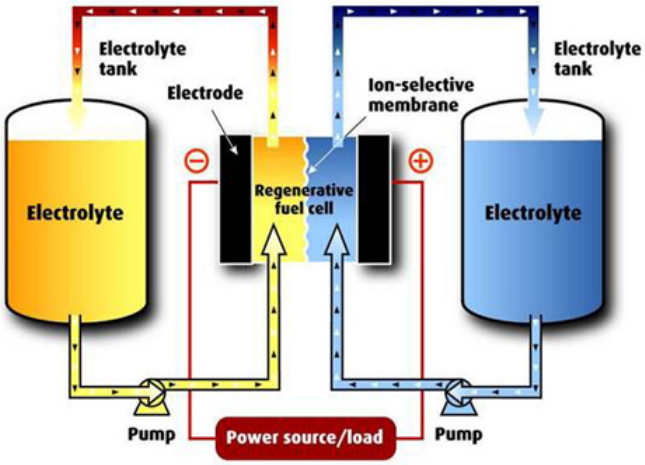

The most known flow battery technology are the Vanadium battery and zink bromine battery. The Vanadium battery can potentially last more than 12000 discharge/charge cycles[66].

[1] abbreviation for reduction-oxidation reaction. It is a chemical reaction where the atoms have their oxidation number changed.

Today, both the conventional batteries and flow batteries are very expensive per kWh. The Flow batteries based on Vanadium and zink bromine has total costs of several tousand euro per kW. However, it is assumed that the systems can approach a cost of 500 euro/kW or 100 euro/kWh[68]. This cost would be equvalent with a cost of 75 million euro for a storage capacity of 750 MWh , enough to produce 100MW of electric power for 6 hours, assuming a storage-to-electric efficiency of 80%. As we will see, even at this cost, there might be cheaper options available today for the concentrated solar power plants.

5.4 Thermal Energy Storage

The thermal storage option is maybe the most obvious way of storing energy for a solar thermal power plant. This is because the standard Parabolic trough plant and power towers in use today are transfering the solar radiation to a heat transfer fluid (HTF) before converting it to electricity, regardless of if there is a storage system or not. Since the heat transfer fluid already is present, one only needs to build in a storage facility in between the solar field and the power block, where the HTF can be stored, before sending it to the Rankine steam cycle for electricty production.

Ideally, the HTF and the storage fluid should be the same fluid in the same closed system. This would eliminate the need for heat exchangers which are a source of losses. The technology today, however, puts restrictions on what type of fluid which can be used as a HTF, so the material best fitted for storage may not be a material that can be used as HTF.

The HTF used at SEGS and which also is in use at all the recent built plants are various types of synthetic oil. At the one SEGS plant that did have thermal storage, this was also the storage fluid.

The central receiver plants Solar one and Solar two built in the end of the 80‘s and mid 90‘s , experimented with a storage system based on a mixture of Molten salts. and the recent built plants built in Spain and USA all have storage systems based on this mixture. The HTF in use at all of the plants is still synthetic oil.

For a material to be used both as HTF and a storage fluid, it should fullfill some requirements:

- allow for simple operation of solar field and storage system
- nontoxic and nonflammable
- easy to obtain/low cost
- high upper temperature with low vapor pressure
- low freezing point
- high energy storage density

None of the possible candidates fullfills all of the requirements today. The table below gives a list of the current HTF and storage medium in use and their properties [69].

Name	Synthetic oil	Hitech XL	Solar salt
Upper temperature	398	500	600
Freezing point(°C)	13	120	220
Heat capacity (J/kgK)(300°C)	2319	1447	1495
Density (kg/m^3)(300°C)	815	1992	1899
Energy density(kg/m^3K)	1,9	2,9	2,8
Cost ($/kg)	3,96	1,19	0,49
Other	flammable	chemical stable	chemical stable

The Synthetic oil is a Diphenyl biphenyl oxide and is called Therminol VP-1[70]. It has been in commercial use for many years and is still considered to be the best choice of HTF, but the maximum operation temperature of synthetic oil effectively puts an upper limit on the efficiency of the power block. Also, a direct thermal storage system using synthetic oil as storage medium is considered to be too expensive due to thick-walled high pressure tanks that would have to be used to store the hot oil. The need for these expensive tanks comes from the high vapor pressure for synthetic oil ($>$ 1 MPa at 400°C)[71]. Therefore, current commercial plants must rely on indirect systems, where three separate fluid cycles is operative: The oil cycle in the solar field, the storage fluid in the storage system and the steam in the rankine steam cycle. This design requires heat exchangers every time heat from one cycle is transferred to the other cycle, and every time some heat is lost, due to the heat differences across each heat exchangers. Therefore, one should search for fluids that can be used both as storage fluid and HTF.

Another approach would be to use water as HTF. If one could use water as HTF one would eliminate the heat exchangers between the solar field and power block ,and if also the water could be used as storage medium we would have a closed system with no need for heat exchangers. This apporoach is known as *Direct Steam Generation* (DSG) and has been investigated for many years[72]. The problem for this approach lies in the high vapor pressure for water, which means that it needs a high aplied pressure to maintain its liquid form at high temperatures. Also, the storage technologies designed for steam have a rather low capacity. Developement is leaning towards a latent heat storage system in form of phase change materials (PCM) in a combination with DSG.

5.4.1 Molten salt as storage medium and HTF

Molten salts have an advantage over synthetic oil in that it has a higher energy density. This means that in a given volume V, a larger amount of heat can be stored. Another advantage is that the molten salt can operate at considerably higher temperatures in the liquid state than the synthetic oil, under athmospheric pressure. Higher temperatures means higher efficiencies for the power block. However, this advantage cannot be fully exploited before the Molten salt can be used as a HTF in the solar field as well.
The main problem with molten salt is its high freezing temperature, and this is the main reason that it is not in use as a HTF. It requires cosiderable amount of heating to the pipes

to keep it from freezing[2]. The freezing can damage pumping systems and heat exchangers. The molten salt mixture in use in current thermal storage systems is Solar Salt, composed of 60% $NaNO_3$ and 40% KNO_3 and have a freezing point at 220°C and upper temperature 600°. Another mixture which can be used is Hitech XL, composed of 7% Sodium nitrate ($NaNO_3$), 45% potassium nitrate KNO_3 and 48% Calcium nitrate ($CA(NO_3)_2$). The 48% Calcium nitrate makes Hitech XL considerable more expensive than regular Solar salt[73]. Properties can be seen in table above.

The high freezing temperature for molten salts makes them not very suitable for HTF in medium temperature range power plants as parabolic troughs. They may be more feasible in central receiver systems where higher temperatures can be reached due to higher concentration ratios. Central receivers also have the advantage of a less complex piping system since the HTF only circulates between one single central receiver and the storage system.

For the parabolic troughs there may be more advantageous to search for chemical modifications of the current syntetic oil HTF. Also, Phthalate esters, which is a common substance in plastic, have been suggested. They are commercial available and have a relatively low cost, below $2/kg. They also have freezing point near zero degrees[74].

There are two different proven designs available for thermal storage of sensible heat[3], which is presented below.

5.4.2 Two-tank thermal storage system

- The indirect system

Here, molten salt is used as storage fluid, and synthetic oil as HTF in solar field.

The system consist of one cold storage tank, operating at $\sim$ 290°C, and one hot storage tank, operating at $\sim$ 390°C and a set of oil-to-salt heat exchangers with circulation pumps.

Figure 5.6: two-tank storage system [75]

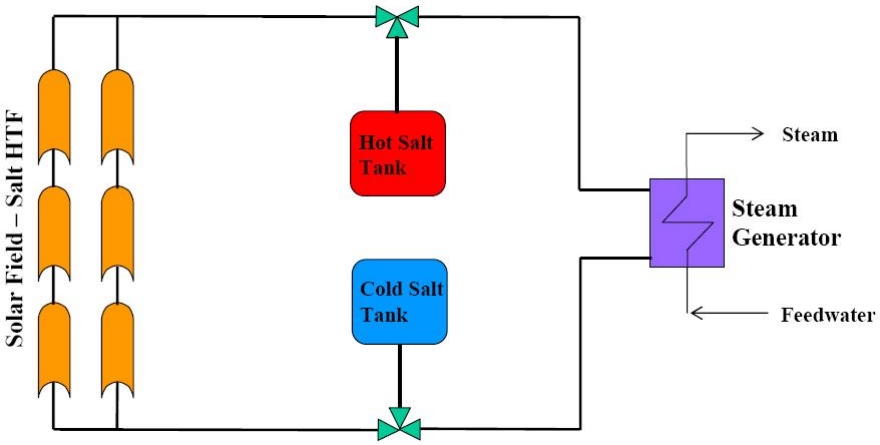

[2]The heat can be transported to pipes by a heat trace cables inside the heat collecting elements at the solar field.

[3]Sensible heat is energy that can be stored by a change in temperature, the other type of heat are latent heat, which is energy that can be released at constant temperature (by a phase change).

During storage charging, heat is transferred from the solar field HTF to the nitrate salt, coming from the cold tank, through an oil-to-salt heat exchanger. In this process, the HTF is cooled to 290°C and the salt from the cold tank is heated to 390°C, and then stored in the hot tank. During a storage discharge, fluid flow are reversed through the same heat exchanger. Under the discharge, salt from the hot tank transfers heat to the HTF which then transfers its heat to the Rankine steam cycle, and the salt returns to the cold tank.

The main issue related to the two-tank system is the cost of the storage fluid. Because large amounts is needed, it becomes relatively expensive. Also, two tanks are needed which makes it material intensive. Still, the method is the most efficient way to store large amounts of thermal energy, and it is the method which is in use at the recent built plants in Spain. However, there are other systems that might be cheaper.

- The Direct system

The direct system have been proven to work in combination with a central receiver system. In 1996, solar two in California installed a two-tank direct system with Solar salt both as HTF and Storage fluid. The reciever was constructed with hundreds of vertical tubes, and concentrated sunlight heated up the molten salt, as it flowed through the tubes, to around 565°C. [76] It was then stored in the hot tank. When power is needed, hot salt is pumped through heat exchangers which transfers heat to the Rankine steam cycle. After the heat transfer, salt is transferred to the cold tank, to be stored before it can be punped back to the receiver to be heated up again. Solar two was only an experimental project and was shut down in 1999.

Figure 5.7: Central tower with a direct two-tank storage system [76]

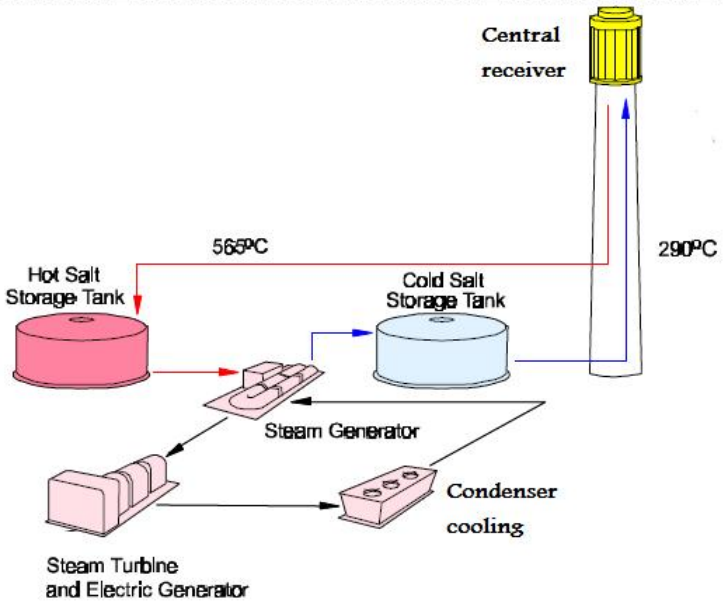

5.4.3 Single tank thermocline system

A thermocline tank is a single tank that stores both the cold and the hot storage fluid. In the tank, a thermal gradient separates the hot from the cold fluid. An economical advantage of the system is that a large fraction of the more expensive storage fluid can be replaced by a less expensive filler material, such as sand and rocks. The filler material together with the buoyant[4] forces helps to keep the thermal gradient stable. The thermocline is the region of the tank between the two temperature sources. In a test made by [75] in 2002 where the temperature difference was set to 60°C, the region occupied $1-2$ meter of the tank height. For bigger temperature differences the region will cover a larger region. This indcates that the thermocline system might be more advantageous for systems with smaller temperature differences.

Figure 5.8: Thermocline storage system [75]

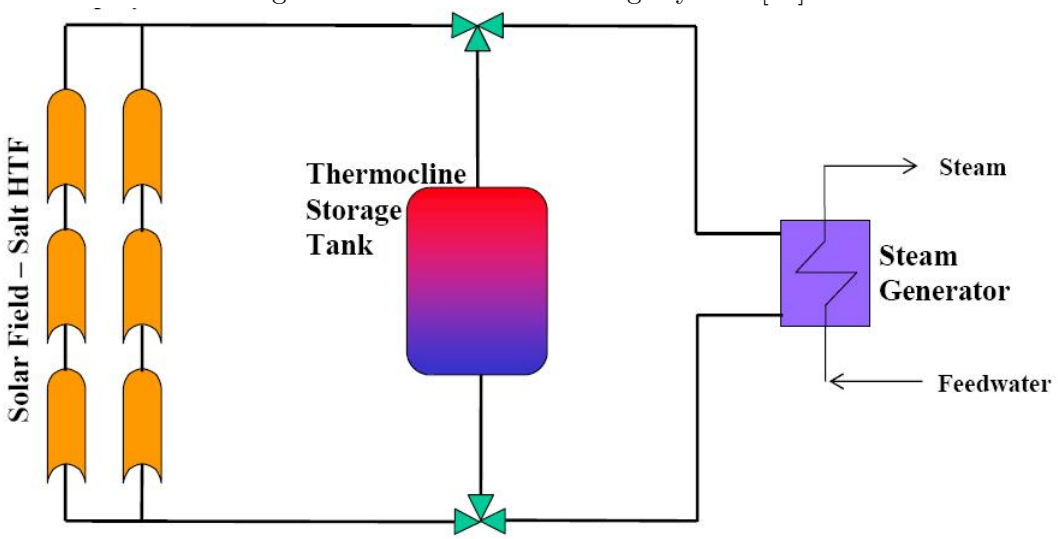

When the system is being charged, cold fluid is taken from the bottom, then heated up by the HTF through heat exchangers and then returns to the top of the tank. When the tank is discharged, hot fluid is taken form the top of the tank, and transfer its heat to the Rankine steam cycle through a heat exchanger, it then returns to the bottom of the tank.

- The direct system

The direct system was tested at solar one, built in 1986. Here, a synthetic oil called "caloria" was used both as HTF and storage fluid. The operating temperature for the fluid was between 218°C and 302°C. [71] Because of the low upper temperature, the power block efficiency was only 21% for the plant. Still, the thermocline system was proven to work and the thermocline temperature gradient was stable over longer periods.

[4]The buoyant force is an upward acting force that keeps materials floating when immersed in a fluid. Arcimedes principle states that: "Any object, wholly or partially immersed in a fluid, is buoyed up by a force equal to the weight of the fluid displaced by the object." Thus, if the density of the object is less than the density of the fluid, then the object will keep floating

- The indirect system

The indidrect thermocline system with Therminol VP−1 as HTF and Hitech XL as storage fluid has been tested by [71] for a parabolic trough system. The tests proved quartzite and silica sand to be a good filler material. The experiments indicated also that Hitech XL is not explosive in direct contact with the synthetic oil, so, an accidentally mixing of the two components should not create combustion. On the other hand, combining the oil with oxygen from the air is potentially dangerous. This puts high requirements on the piping system.

The thermocline system can be modelled with two first order differential equations, one for the fluid and one for the filling material. The energy balance for the system can be written, using Fouriers law and Newtons law of cooling, for the storage fluid, denoted with subscript f

$$(\rho C_p)_f \epsilon \frac{\partial T_f}{\partial t} = -\frac{(\dot{m} C_p)_f}{A} \frac{\partial T}{\partial y} + h_v (T_b - T_f) \tag{5.50}$$

and for the filler material (bed), denoted with subscript b

$$(\rho C_p)_b 1 - \epsilon \frac{\partial T_b}{\partial t} = h_v (T_f - T_b) \tag{5.51}$$

h_v is the volumetric heat transfer coefficient and $\epsilon = \frac{V_f}{V_f + V_b}$ is the volumetric void fraction of the filler material and describes how much fluid that is needed to fill the tank. A is the horizontal cross sectional area of the tank. $\dot{m}$ is the fluid flow rate and is assumed constant. It is assumed a one dimentional vertical fluid flow and that the temperature is constant on each horizontal layer.

The equations can be solved by the method of finite differences where the tank is divided into equal horizontal slices, and a initial vertical temperature distribution is specified. The local heat transfer coefficient for each of the slices can then be found and then, the local temperatures of the filler material and the fluid in each of the slices. Calculations can be done in time intervals of a few seconds and the slices can have a thickness in centimetres.

A numerical sumulation on a specific case have been done by [71] for a 16 meter tall and 34 meter in diameter thermocline tank with 688MWh$_t$ capacity. Quartzite and sand was used as filler material and Hitec XL as storage fluid. A void fraction of $0,24$ was assumed. The cold fluid was 298°C and the hot fluid was 390°C. The simulation yielded the temperature gradients illustrated in Figure 5.9 during charging (vertical axis is the height of the tank and horizontal axis is the temperature).

In figure 5.9, we observe that, initially, the first 8 meters of the tank has the lower temperature. When fully charged, the upper 10 meters have the highest temperature. The thermocline[5] region is a region of thickness around 6 meters. The maximum thermal capacity for the storage system will therefore be considerable lower for a thermocline tank than a two tank system in percentages, when compared to the thermal energy stored in the tank if the whole interior of the tank was at its upper temperature. As a result, the thermocline tank must be bigger to make up for the loss in capacity.

[5] The thermocline is the region in which the temperature changes more rapidly with depth than it does in the layers above or below

Figure 5.9: Temperatture gradients during charging of a thermocline tank [71]

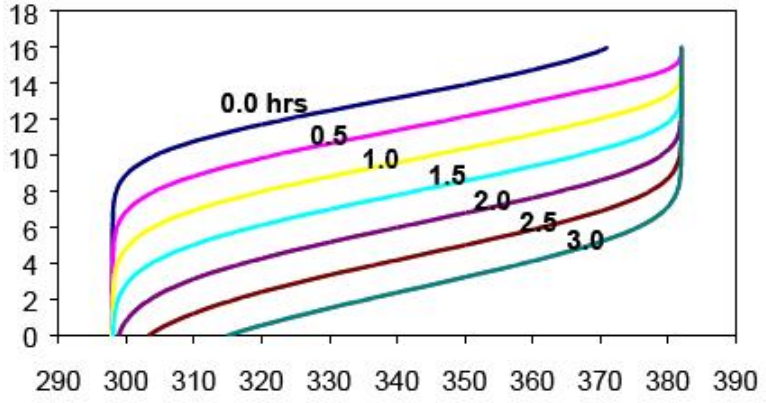

It is possible to give good approximations of the true thermal capacity of a system from the basic definition of heat capacity. The specific heat capacity is defined to be the amount of thermal energy ΔQ a material can store with a change in its temeperature, ΔT, per unit mass. The pressure is assumed to be constant during the temperature change, which is approximately true for the nitrate salt mixtures. The heat capacity can also be assumed constant within the temperature variations the storage system are operating with.

$$C_p = \frac{\Delta Q}{m\Delta T} \tag{5.52}$$

where, C_p (J/K) is the heat capacity of the material under constant pressure. It can be expressed with the specific heat capacity c_p (J/kgK):

$$C_p = \rho * V * c_p \tag{5.53}$$

where ρ is the density and V is the volume.

For simplification of notation we will in the following let $c_p = c$, and denote the specific heat capacity for the storage fluid with c_f and the specific heat capacity for the filler material with c_b.

First one calculates how much energy that could be stored if the entire interior of the tank was at its upper temperature. Then one must multiply with the maximum theoretical fraction of the tank that can be at its upper temperature(Cap_{max}). The temperature gradient for the thermocline system indicates that a fraction of $\sim 70\%$ of the maximum tank capacity can be used. For a two-tank system the fraction is around 90% , (a heel of salt at the bottom of the tank cannot utilize its thermal capacity)[71]. In general, Cap_{max} is a function of tank height in which the fraction increases with increasing height of the tank.

It would be interesting to calculate how large volume or how large mass of material is needed for a given required thermal capacity, for each of the four systems.

5.5 Estimation of tank volume and storage fluid

Lets assume a parabolic trough plant with a 100 MW turbine capacity. We would like to have a storage system that could supply peak load to the turbine for 6 hours. We assume the

thermal losses in the storage system to be a product of the losses related to the heat exchangers (η_{he}) and losses related to the storage tank itself $\eta_{storage}$, so, $\eta_{therm} = (\eta_{storage})\times(\eta_{he})$. In addition we have the power block efficiency η_{pb}. The void fraction for the filler material in the thermocline tank is assumed to be $\epsilon = 0{,}3$. $\eta_{storage}$ is assumed to be equal to $0,96$ for all cases. Each set of heat exchangers is assumed to have an efficiency of $0,98$. η_{pb} is assumed to be $0,3$ for the indirect ssytems, using the numbers from the Andasol plant, and $0,34$ for the direct systems, due to the higher operating temperature that can be used. T_{cold} equals 290°C for all systems and T_{hot} equals 390°C for the indirect systems and 450°C for the direct systems. ΔT = T_{hot}-T_{cold}.

We require the themal energy to be such that the storage system can supply peak load to the 100MW turbine for 6 hours. that is, 600MWh$_e$ of electrical energy is needed.

The thermal energy needed in the storage tanks depends then on the losses in between the turbine and the storage system. We have

$$\Delta Q_{needed} = \frac{MWh_e}{\eta_{pb}\eta_{therm}} \tag{5.54}$$

where MWh$_e$ is the required electrical energy.

Now, the stored thermal energy that would be in the tank if the whole interior was at its upper temperature is found from Equations (5.52) and (5.53)

$$\Delta Q_{max} = \rho V c \Delta T \tag{5.55}$$

However, the Cap_{max} factor must be multiplied in for the respective system to account for the interior which cannot be used and we obtain the following formula for the needed storage energy

$$\Delta Q_{needed} = \rho V c \Delta T Cap_{max} \tag{5.56}$$

Since all the quantites involved but the volume is assumed to remain constant, the volume of the needed material must be increased to compensate.

For the two-tank systems, V = V$_f$, the volume of the storage fluid, and we get the following fomula for the needed volume by combining Equations (5.56) and (5.54) and putting V$_f$ alone:

$$V_f = \frac{\Delta Q_{needed}}{\rho_f c_f \Delta T Cap_{max}} \tag{5.57}$$

For the thermocline systems, we have two materials involved so V = V$_f$ + V$_b$, V$_b$ beeing the volume of the filler material. Equation (5.56) in comination with Equation (5.54) becomes

$$\Delta Q_{needed} = (\rho_f V_f c_f + \rho_b V_b c_b) * \Delta T * Cap_{max} \tag{5.58}$$

V$_f$ for the thermocline system is related to the volume of the filling material V$_b$ through the volumetric void fraction of the filling material ϵ defined in Equation (**??**). Letting V$_f$ alone gives

$$V_f = \frac{V_b \epsilon}{1 - \epsilon} \tag{5.59}$$

by plugging this into Equation (5.58) and putting V$_b$ alone we arrive at the following formula for the volume of the filler material V$_b$

$$V_b = \frac{\Delta Q_{needed}}{\Delta T * Cap_{max}}[\frac{1-\epsilon}{\rho_f \epsilon c_f + \rho_b c_b (1-\epsilon)}] \tag{5.60}$$

We can now present the four cases :

- Case 1

  Indirect two-tank storage system

  Solar salt is used as storage fluid since this is a cheaper alternative and the high freezing point is not so critical in an indirect system as in an direct system. Heat capacity and density for the nitrate salts is found in the table above. Here we have a salt-to-oil heat exchanger and an oil-to-steam heat exchanger, (η_{he}) = 0,98*0,98 = 0,96. η_{pb} = 0,30 and $\eta_{thermal}$ = 0,96*0,96 =0,92.]

- Case 2

  Indirect thermocline system

  Solar salt is used as storage fluid and quartzite and silica sand as filler material. the heat capacity for quartzite is $c_b \sim$ 840 J/kgK and the density is ρ_b = 2650 kg/m^3, for simplicity we assume the same for silica sand (quartzite and silica sand are two crystalline forms of silica)[77]. The storage and heat exchanger efficiency is the same as in case 1 so $\eta_{thermal}$ = 0,92 η_{pb} = 0,30.]

- Case 3

  Direct two-tank system

  Hitech XL is used as storage fluid since this has a lower freezing point than solar salt. Here we have one set of heat exchangers so (η_{he}) = 0,98. $\eta_{thermal}$ = 0,98*0,96 =0,94 Since The Hitech XL have an operation temperature around 60°C more than syntetic oil, we assume η_{pb} have increased to 0,34.

- Case 4

  Direct thermocline system

  Hitech XL is used as storage fluid and quartzite and silica sand as filler material with its density and heat capacity given in case 2. η_{he} = 0,98. η_{pb} = 0,34]

We can summarize the results in a table, using the numbers for the different cases to calculate the needed thermal energy, needed volumes and masses of the storage materials. The volume of the storage fluid in the two-tank system is defined by Equation (5.57), and the total volume of the tanks are two times the Value of V_f. The volume of the storage fluid in the thermocline system is defined by Equation (5.59) , where the volume of the filler material V_b is given by Equation (5.60). The needed thermal capacity ΔQ_{needed} is given by Equation (5.54) for all systems.

	Indirect Storage		Direct Storage	
	Two-tank	Thermocline	Two-tank	Thermocline
Solar field HTF	Synthetic oil	Synthetic oil	Hitech XL	Hitech XL
ΔQ_{needed}(MWh)	2193	2193	1895	1895
T_{high} (°C)	390	390	450	450
ΔT (K)	100	100	160	160
Storage Fluid	Solar Salt	Solar Salt	Hitech XL	Hitech XL
Filler material	none	silicon/quartzite	none	silicon/quartzite
V_f (10^3 m^3)	30,9	13,8	16,4	7,4
m_f (10^6 kg)	57,8	26,1	32,7	14,8
V_b	none	32,3	none	17,3
m_b	none	85,0	none	45,9
Tank size(m^3)	30,9*2	46,1	16,4*2	24,7

If we let the number of storage hours for the system vary, a plot of the storage volume can be generated. In Figure 5.10 the needed storage fluid volume and tank volume is plotted against the storage capacity.

Figure 5.10: Volume of storage fluid is plottet aganst the storage capacity at the left plot and tank volume against storage capacity at the right plot

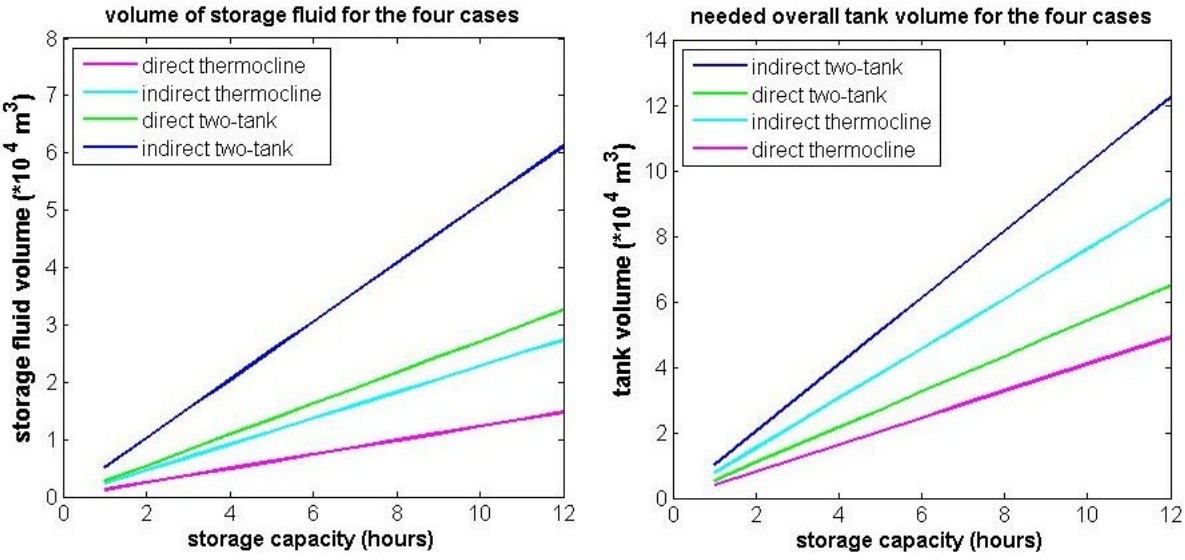

The graph to the left shows how the storage fluid volume increases with the needed thermal capacity. We observe that the direct two-tank system needs more fluid than the indirect thermocline system. However, in the graph to the right we observe that the indirect thermocline system needs a larger tank volume than the direct two tank system. This is because the filling material needed for the thermocline system requires a much larger volume than the storage fluid.

There are some uncertainities in the values used for η_{pb} and $\eta_{thermal}$. Higher values will lower the ΔQ_{needed}.The Cap_{max} value will also be higher when the height of the storage tanks increases. A higher Cap_{max} results in lower values for the needed volumes of filler material and storage fluid, V_b and V_f respectively. Another point to mention is the value of ΔT. ΔT will be somewhat lower due to losses in the storage tanks and across the heat exchangers, but this loss is assumed included in $\eta_{thernal}$. A lower $\eta_{thermal}$ will increase ΔQ_{needed} and this will increase the needed volume of storage materials.

From the table and plots we can conclude that the two-tank systems needs more storage fluid than the thermocline systems, around 120% more in both the indirect system and the direct system. However, the thermocline systems need a significant amount of filler material, resulting in that the thermocline system needs a $\sim 50\%$ larger single tank than each of the tanks in the two tank system. But the two tank system , will because of its two tanks come out with a $\sim 50\%$ overall larger tank volume than the thermocline systems.

Since the needed overall tank volume is less for the thermocline system and a large fraction of the storage fluid is replaced by a less expensive filler material we expect the thermocline system to be cheaper, both in the direct case and the indirect case.

5.5.1 Cost comparision of the four systems

The cost of the Storage systems is the sum of the cost of heat exchangers, the storage tanks and the storage materials. We can assume that the cost of the storage tanks and the storage materials is proportional to their volume. The tanks of the direct systems will be more expensive per m^3 than the tanks in the indirect systems since the higher upper temperature requires a more robust building material and a better isolation. Also, the filler material is significant cheaper than the storage fluid. According to [71], the filler material have a cost $C_{filler} = \$72/\text{tonne} = \$0,072/\text{kg}$. The tank cost for the indirect system is $C_1 = 155/m^3$. The cost of Solar salt and Hitech XL is $C_{solar} = \$0,49/\text{kg}$ and $C_{hitech} = \$1,19/\text{kg}$ respectively. The cost of the salt-to-oil heat exchangers needed in the indirect systems for the 688MWh system in [71] amounts to $\$5,5 * 10^6$. We will assume that the cost of the heat exchanger increases as a function of the storage capacity in hours: Since 6 hours of capacity needs $\sim$ 2000 MWh we can say that $\sim$ 2 hours needs $\sim$ 650MWh, so we have $C_{he} = h/3\$5,5 * 10^6$, where h is storage time in hours. We also assume that the cost of the tank in the direct systems is a factor $r = 1,30$ more expensive per m^3 than the tank cost C_1 in the indirect system.

- Case 1

  Total cost indirect two-tank system

$$C_{total} = C_{tank} + C_{salt} + C_{he} = C_1 * V_f * 2 + C_{solar} m_f + \frac{h}{3}\$5,5 * 10^6 \tag{5.61}$$

- Case 2

  Total cost indirect thermocline system

$$C_{total} = C_{tank} + C_{salt} + C_{filler} + C_{he} \tag{5.62}$$

$$= C_1(V_f + V_b) + C_{solar}m_f + C_{filler}m_b + \frac{h}{3}\$5,5 * 10^6 \tag{5.63}$$

- Case 3

  Total cost direct two-tank system

$$C_{total} = C_{tank} + C_{salt} = rC_1V_f \times 2 + C_{hitech} \times m_f \tag{5.64}$$

- Case 4

  Total cost direct thermocline system

$$C_{total} = C_{tank} + C_{salt} + C_{filler} = rC_1(V_f + V_b) + C_{hitech}m_f + C_{filler}m_b \tag{5.65}$$

Figure 5.11: Cost estimates plottet against storage capacity in hours

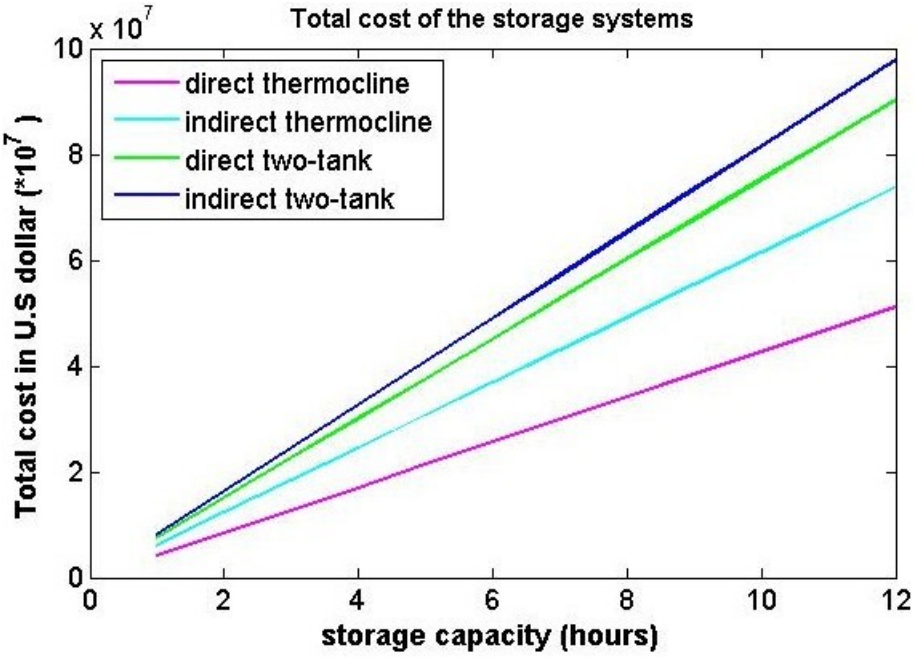

The plot in Figure 5.11 shows that the thermocline systems is considerable less expensive than the two-tank systems. The indirect two-tank system is slightly more expensive than the direct two-tank system. Most of the difference between theme are the cost of the oil-to.salt heat exchangers. The direct system would actually have been more expensive than the indirect system for a less expensive choice of the heat exchanger cost. Also, the choice of the factor r for the tank cost in the direct system is speculative, it may be higher but it may also be lower. a lower r-value would have resultet in a decrease in cost.It is important to be aware of these sensitivities in the parameter values.

For a 6 hour capacity, the direct thermocline have a $C_{total} \sim \$25$ million while the indirect two-tank system have a $C_{total} \sim \$50$ million.

However, the direct systems are not yet commercial available for the parabolic trough technology, and the indirect two-tank system has so far been the preferable storage system for the recent built plants.

The cost overview would have been somewhat different if we had replaced the parabolic trough plant with the central receiver plant in the analyis. This is because the central receiver have the possibility to use the less expensive solar salt in a direct system. Since solar salt can operate with temperatures up to 600°C this would have increased ΔT in our equations and as a result, less storage materials would be needed, and the tank volumes would also had gone down. This would have made the direct systems even more economical favourable than what we see from the graph with the parabolic trough system.

5.5.2 The storage system at the Andasol plant

The 50MW andasol plant in Spain have a indirect two-tank system with a $7,5$ hour storage capacity. The thermal capacity needed for this are 1050 MWh according to official numbers. The number are close to my calculations for a 100MW parabolic trough plant. My calculations showed that 2193 MWh was needed for a two-tank system to deliver peak load to a 100MW turbine for 6 hours.

How the thermal energy is distributed to the turbine throughout a day is described in the plot below:

Figure 5.12: Thermal energy distribution for the Andasol plant for a typical clear sky summer day[78].

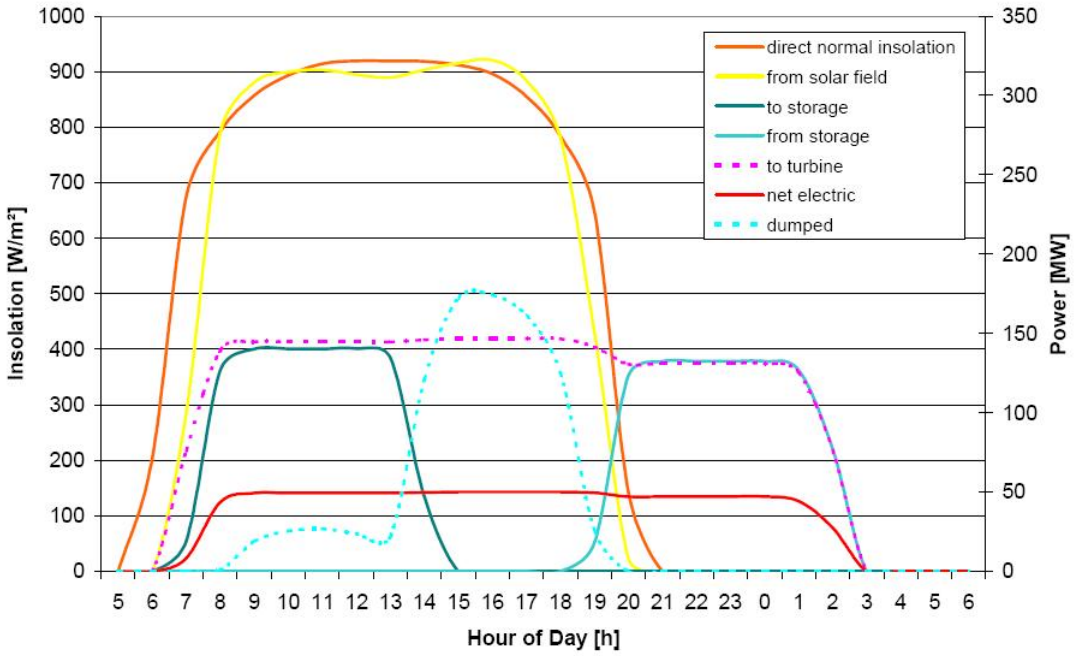

This plot describes a typical clear sky summer day for the Andasol plant. We see that the storage system is charged at the beginning of the day and then delivers its thermal energy

to the turbine for 7 hours after sunset. Observe also that the blue dotted line is an amount of solar thermal power that is beeing dumped. This reflects the fact that the solar field has been oversized to be able to store energy and deliver energy to the power block at the same time. When the storage system is fully charged the part of the solar field that was needed for the storage system is producing heat that exeeds the capacity for the turbine. A solution to this problem could be to oversize the turbine, but oversizing a turbine too much results in a decrease in turbine efficiency when the heat delivered to the turbine is much below its peak load capacity. Another solution would be to increase the storage capacity so that the charging period would last as long as the sun was shining. However, since the difference in number of sun hours in winter and in summer often is high, the storage system should be fitted to the winter season.

The Andasol plant has a solar field area of 510000 m^2. We can calculate how large the part of the solar field is that is used to charge the storage system. The plant is located in the Granada desert area south spain where the average annual insolation are 2136kWh/m^2/year. According to the figure we can assume a solar intensity at 900 W/m^2 during a clear summer day. To produce 50MW electric power with a solar-to-electric conversion efficiency at 15% would require a total solar field area of 370000m^2. Including some losses under charging we assume the total solar to storage efficiency to be 45%. So, 1050MWh storage would require 2333MWh from the solar collectors. Each square meter of collector can collect $900 * 7,5$Wh during the charging period. It would therefore require an area of $\sim$ 310000m^2 to charge the storage system in 7,5 hours. The total needed area would therefore be 680000m^2. Clearly, the actual solar field area of 510000 m^2 is not big enough. As a result of this the Andasol plant cannot run at full capacity during charging. Alternatively, the charging period must go over a longer period than $7,5$ hours. This can be achieved during summer months with more sunshine, but during winter months the days are shorter and the storage system will have less hours available for charging.

This calculation illustrates one problem with thermal energy storage for CSP. If the CSP power plant wants a stable capacity factor throughout the year, the solar field must be large enough to meet this capacity factor during winter when the solar energy received is at its minimum. However, when the solar field is built for the winter months with a high capacity factor, a considerable amount of energy must be dumped during summer since more energy is received per square meter and less area are required.

5.6 How can the LEC be decreased by including energy storage?

The introduction of energy storage at a solar thermal power plant will increase the annual amount of electricity produced by the plant. This will increase the socalled capacity factor of the plant.

5.6.1 The Capacity factor

The capcity factor of a power plant is defined to be the ratio of the actual electric power produced by the plant in a certain time interval over the electric power that the plant would have produced if it was running on its peak turbine capacity the entire time interval. It is

usually the annual capacity factor which is of interest, and here the time interval is over an entire year. We will in the following denote the annual capacicy factor with the symbol K.

$$K = \frac{kWh_{actual}}{kWh_{peak}} = \frac{kWh_{actual}}{kW_{peak} * h} \tag{5.66}$$

where h is the number of hours in one year (h = 8760)

5.6.2 The instant capacity factor

For solar thermal power plants designed to deliver base load power to the electricity grid, it is important to find the solar field area needed to reach a given capacity factor at the season with the lowest peak sun hours[6]. This will put an upper bound on the needed storage capacity and the needed solar field. For example, if the number of peak sun hours at a location is 6 in December, which usually is the month with the lowest number of peak sunhours, then, this is equvalent with that each square meter of collector surface will receive 6kWh during sunlight. From this number one can calculate the solar field area required to provide the storage system with the needed thermal energy. At summer, since the number of peak sun hours is higher, some of the thermal energy collected must be dumped, how much that must be dumped depends on the difference between the lowest peak sunhours in winter and the highest peak sun hours in the summer. It will also depend on the capacity factor at the lowest peak sun hours. If the sun shines for 10 hours with 900 W/m^2 delivered to the solar field during summer, the required storage capacity to reach a 80% capacity factor would be $\sim$ 9 hours. However, if during winter the sun shines only for 6 hours with 900 W/m^2, then the needed storage capacity would be 13 hours.

The levelized energy cost of a plant is given by Equation (5.67) in Chapter 4 but is repeated here:

$$LEC = \frac{FCR * C_{invest} + C_{O\&M} + C_{fuel}}{kWh_{actual}} \tag{5.67}$$

So, by definition of K, we see that by increasing K the Levelized energy could be reduced.

However, it is not a certain fact that the LEC will be reduced only by increasing the capacity factor. To increase the capacity factor for a solar thermal power plant one must increase the solar field area and also build a storage system. All this wil increase the initial investments C_{invest}. This is the explanation of why the LEC calculated in chapter 4 was higher for the Andasol plant compared to the two plants with no storage system.

For the simplified case that we average the energy received over an entire year, we can relate the capacity factor to the solar field area in the following way:

The overall solar-to-electric conversion efficiency η_{tot} is

$$\eta_{tot} = \frac{kWh_{actual}}{kWh_{thermal}} \tag{5.68}$$

where $kWh_{thermal}$ is the annual thermal energy collected in the solar field. kWh_{actual} is the annual electric energy produced.

[6]peak sunhours is here defined to be the number of hours with 1000W/m^2 that the total energy received per m^2 from sunrise to sunset represents

kWh_{actual} is given by

$$kWh_{actual} = A_{sf} * \eta_{tot} * I \tag{5.69}$$

where, A_{sf} is the solar field area and I is the annual incident solar radiation per square meter at the location of the plant.

By combining Equation (5.69) with the definition of the capacity factor K and letting A_{sf} alone we arrive at the following relation

$$A_{sf} = \frac{kWh_{peak} * K}{\eta_{tot} * I} \tag{5.70}$$

So, to double the capacity factor, one must also double the solar field area, assuming the other quantities in the equation is held constant.

A solar thermal plant without energy storage will have a maximum annual capacity factor around 25% (depends on the location). By introducing thermal storage one can in principle approach a 100% capacity factor, but this would require a quadrupling of the solar field area.

It becomes more and more important to reduce the cost of the solar field when the capacity factor increases. For Andasol to have a capacity factor approaching 100% it would require an solar field area of 1.3 km^2 (in summer conditions), today the solar field area of Andasol is 510000m^2. The total electric energy produced,kWh_{actual}, can be found in a table in Section 4.7. It is 156 GWh/y. We can then find the capacity factor from Equation (5.66). It is found to be K = $\frac{156*10^3 MWh}{50MW*8760}$ = 0,356.

Large two-tank storage systems requires large amounts of concrete and steel, and this must also be cosidered when analysing the levelized energy cost.

We see from Equation (5.70) that a high annual solar radiation and a high solar-to-electric efficiency is important to reduce the solar field area. The highest I available on earth is found around the equator belt and some places have annual irradiations around 2600kWh/m^2/year. η_{tot} are with current technology around 15% and this value may approach 20% by introducing some sort of direct storage system, to eliminate the heat exchangers and increase the steam temperature in the power block.

5.7 Storage methods in future

The ideal solar thermal power plant would have a closed cycle of one single fluid circulating between the solar field, storage system and the power block. Since the power block uses steam, the only answer for such a system is water. So far, this has not been achieved.

New types of storage systems would be required to be able to store large amounts of high temperature steam in an efficient and economical way. An alternative to this are development of a latent heat storage system based on phase change materials which can produce steam at constant temperature (during phase change). There has been research and development towards a first prototype powerplant with DSG and integrated PCM storage.[78] Various test loops with DSG have taken place at a test facility contructed in Spain in 1998 (The DISS (Direct Solar Steam) facility) but so far a first small DSG plant has not yet been achieved. This must be done before it can develop into large scale commercialization[79].

The potential advatages of DSG with PCM storage over the current indirect system with molten salt storage are two fold; 1 With a DSG system, the steam temperature approaches operation temperatures of 550°C., approaching a total solar-to-electric efficiency of 23%.

Today the solar-to-electric efficiency are $\sim$ 15% with steam temperature 390°C[79]. 2. Per unit volume, the PCM latent heat system offers at least 35% increase in storage capacity compared to the current molten salt system[80].

5.8 Storage systems with short discharge/charge periods

The storage systems presented here are systems that can be used to stabilize the electric grid for short periods of time. Their time of discharge and charging are short which makes them suitable when large amounts of power are needed over short periods.

5.8.1 The flywheel

The flywheel is a mechanical energy storage device which exploits the stored kinetic energy in a rotating disc.

Figure 5.13: A disc rotating with angular speed ω

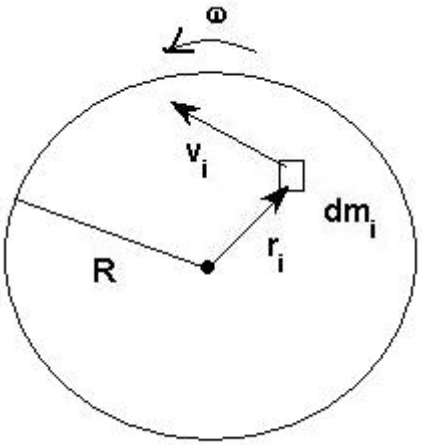

The kinetic energy stored in a rotating disc can be found by consider a disc with radius R and angular speed ω. The following equation express the kinetic energy in an infinitesimal mass element dm_i with position $\vec{r_i}$ relative the center and velocity $\vec{v_i}$ (see figure):

$$K_i = \frac{1}{2} dm_i {v_i}^2 = \frac{1}{2} dm_i \omega^2 {r_i}^2 \tag{5.71}$$

where ω is constant for all infinitesimal mass elements on the rotating disc.

To find the total kinetic energy we can integrate over all the mass elements m_i of the disc:

$$K_i = \frac{\omega^2}{2} \int {r_i}^2 dm_i = \frac{1}{2} I_c \omega^2 \tag{5.72}$$

where $\mathrm{I}_c = \int {r_i}^2 \, dm_i$ is the moment of inertia of the rotating disc with respect to the center c of the disc.(Axis of rotation is going through the center of the disc and is perpendicular to the disc.)

It can be shown that the moment of inertia is largest for a disc that have all its mass on the circumference at distance R from the center[81]. Therefore it is preferable to have a disc with most of its mass concentrated at the circumference. The moment of inertia is in this case given as $I_c = mR^2$ where m is the total mass of the disc.

The kinetic energy stored in the rotating flywheel is therefore

$$K = \frac{1}{2}m\omega^2 R^2 \tag{5.73}$$

There will exist a maximum upper limit for the ω for the flywheel. This is determined by the tensile strength of the material which is being used.[82] Beyond this maximum tensil strength the flywheel can potentially be fractured. For the ideal flywheel with all its mass concentrated at radius R, the tensil stress σ at the rim at angular speed ω is defined to be

$$\sigma = \rho R^2 \omega^2 \tag{5.74}$$

where ρ is the density of the flywheel. From this we find that the maximum angular speed ω_{max} is achieved when the tensile stress have reached the maximum tensile strength of the material $\sigma = \sigma_{max}$.

The maximum theoretical energy that can be stored in a specific flywheel will therefore be

$$K_{max} = \frac{1}{2}m\frac{\sigma_{max}}{\rho} \tag{5.75}$$

Composite metals based on carbon have a higher σ_{max} and a lower ρ than various types of metals and is therfore the preferable material for an ideal flywheel.

Carbon fibre can have a density $\rho = 1500$ kg/m^3 and a specific strength $\sigma_{max} = 2400{*}10^6$ N/m^2 [82].

Putting this into Equation (5.75) gives a theoretical maximum specific energy of 222 Wh/kg.

A flywheel of 500 kg could therefore store 111 kWh of kinetic energy. This ideal flywheel could inject a power of $\sim$ 20 MW for a discharge period of 20 seconds, or it could be released with a lower output for a longer discharge period, typically up to 15 minutes. Assuming it has a radius R = 1 meter it would have a $\omega = 1265$ Hz. That is, 1265 rounds per seconds or $\sim$ 76000 rpm (rounds per minute)

The flywheel can provide stabilization of fluctutations in the electric grid. Large systems consisting of many separate flywheels can be programmed to absorb energy from the grid or inject energy into the grid just by regulating its angular speed. Typical capacity of a flywheel on marked today are $\sim$ 25 kWh. Conventional flywheels are around 85% efficient due to friction in the mechanical bearings. It could alternatively be operated under magnetic fields to prevent friction, but this would require energy to operate as well.

Flywheels as a storage method for concentrated solar power (CSP) is due to their limited amount of energy that can be stored not preferable since discharge periods of up to 15 hours are required during nightime for a CSP plant. However, flywheels can be an important contributor to a future electric grid based on renewables to account for small fluctuations in the power source. This is useful for CSP power as well during short weather transients for periods of up to 15 minutes or so.

5.8.2 Superconducting magnetic energy storage

Superconducting magnetic energy storage (SMES) uses a closed loop of superconducting wire winded around a core to form a socalled coil.[83] The device stores electrical energy in the magnetic field that is being generated by the input direct current. In the ideal case, the direct current flows in the coil with no losses. The coil can be discharged by releasing the circulating current into the grid. SMES have typically very short discharge (seconds) and charging(minutes) periods.

The storage potential in the SMES can be found by using a result found in the Appendix C. In Appendix C it is found that if a current is flowing in a wire the flowing current will induce an emf in the wire. The current also generates a magnetic field , and the magnetic flux through the loop will be proportional to the current: $\phi = \mathrm{LI}$, where the constant of proportionality L is called the inductance. The value of the inductance is dependent on the shape of the wire (the coil in our case).

Furthermore, the work done on an unit charge against the emf ϵ of the circuit in one roundtrip is -ϵ. The amount of charge per unit time flowing down the wire is the current I, therefore the total work done per unit time is[84]

$$\frac{dW}{dt} = -\epsilon I \tag{5.76}$$

since $\epsilon = \frac{d\phi}{dt}$ and $\phi = \mathrm{LI}$ we obtain

$$\frac{dW}{dt} = -\epsilon I = LI\frac{dI}{dt} \tag{5.77}$$

The total work done (and therefore also the total energy stored since there are no losses from resistance) is found by integrating from 0 to I and Equation (5.77) becomes

$$W = \frac{1}{2}LI^2 \tag{5.78}$$

What this equation shows is that the energy stored is dependent on the geometry of the coil through L (the coil usually have a toroidal or a solenoidal shape), and the square of the current flowing in the coil.

The main drawback of SMES is that the system needs to operate under very low temperatures for the coil to remain superconducting at all times, the cooling system needed to achieve this are subject to losses. A non-superconducting coil could still store energy, but the storage time would be limited and losses higher[83]. Also, the SMES must be integrated with a converter station since the AC power from a power plant must be converted into DC before the energy can be stored in the coil. The converter is expensive and also subject to losses. (Typically $\sim 1\%$)

The advantages of the SMES is that it can store large amounts of power with a short charging cycle (minutes). All the power stored can be released within seconds which makes it very suitable for stabilizing fluctuations in the electric grid. Its advantages are also its weaknesses, it cannot provide firm power over a large period of time for instance for a CSP plant during nightime.

Chapter 6

Solar power and the electric grid

Concentrated solar power togheter with hydropower are unique among the renewables in that they relatively easy can implemement energy storage to balance natural occuring fluctuations in their source of energy. However, for CSP, it is both economical and material intensive to approach a capacity factor of 100%, and for Photovoltaic cells and wind energy, there exist no large scale storage methods. The lack of sufficient storage to reach the same level of reliable and continous power generation as fossil and nuclear power makes it necessary to balance the resulting fluctuations in the electric grid by changing the grid itself.

Today, each country have built their own electric grids to meet their own demands. The transfer of electricity between countries have been very limited since each country have their power sources within their own borders.

However, renewables needs regions with special conditions to maximize their output, and one single country may not have these ideal regions within their own borders. One country may have conditions that suits solar power well, while other countries have a larger wind potential. Also, one single country may be too small to balance the local variations in the power sources. Wind lulls may occure for short periods over a large area which cause a hault in the electricity production which can cause instability in the electric grid if a large fraction of the total electricity comes from these intermittent sources.

To achieve the same stability in the grid as we have today, but where a large fraction of the electric energy comes from renewables, there are two ways the electric grid should be changed.

1. Construction of a supergrid: Interconnect geographical distant regions by building long distance transmission lines with high capacity

2. Construction of a smart grid: develop a grid network management with more detailed functions of control

6.1 Roadmap 2050

The European union and the G8 defined in 2009 a goal to reduce greenhouse gas emission by at least 80% below 1990 levels by 2050

The Roadmap 2050[85] project is an initiative of the European Climate Foundation (ECF) and has been developed by a consortium of experts funded by the ECF, including several

european companies and academic organizations. They outlines plausible ways to achieve this target of 80% reduction.

In the following, most of the information is found from [85], if information is found another place it will be cited.

According to the roadmap 2050 technical analysis it is possible for Europe as a whole to reach this goal by only relying on energy sources within the European union. They analyses three different ways to achieve the goal based on the fraction of Renewable energy sources (RES) which will contribute to the total supply of electricity.

The different ways is denoted as the 40, 60 and the 80% RES(Renewable Energy Sources) pathways, each of them indicating how much of the needed electricity that will come from renewables. The remaining fraction in all threee pathways is divided equally between Carbon capture storage (CCS) coal and gas plants, and nuclear power. For example, for the 40% RES pathway, 40% comes from renewables, 30% comes from CCS coal and gas and 30% comes from nuclear power.

The power demand for the european union plus Norway and Switzerland is projected to be about 4900 TWh in 2050. Around 40% higher than today.

The distribution of total capacity between the sources which is suggested to be used in the model is given in the table below.

Figure 6.1: Required capacities for the mixture of power sources, given in GW installed in 2050 [85]

	Fossil fuels	Solar PV	Wind onshore	Wind offshore	Other[1]	Back-up plants
80% RES 10% CCS 10% nuclear	80	815	245	190	420	270
60% RES 20% CCS 20% nuclear	155	555	165	130	455	240
40% RES 30% CCS 30% nuclear	240	195	140	25	490	190
Baseline: 34% RES 49% coal/gas 17% nuclear	410	35	140	25	380	120

[1] includes nuclear, hydro, biomass, geothermal and solar CSP.

From the table it is clear that solar photovoltaic is considered to be a significant power source in europe in the 80% pathway. However, it must be noted that these numbers reflects the installed peak capacity. A calculation of actual energy produced from these installed capacities would give a different picture. If the installations had been running at their peak capacity over one year , that is an capacity factor K equal to one, the total electric energy produced from these capacities would be, in the 80% RES case, $\sim$ 17700 TWh, about 260% more than the assumed needed energy in 2050 (4900 TWh). The correct energy production can be found by accounting for their typical capacity factor(called load factor in roadmap 2050) In the table below I compare the installed capacity for 40% RES and 80% RES pathways

(40% RES)	Capacity (GW)	K_{min}-K_{max} (%)	$Prod_{min}$-$Prod_{max}$ (TWh)
Fossil	240	60-90	1261-1892
Solar PV	195	10-17	171-290
Wind onshore	140	25-35	307-429
Wind offshore	25	37-45	81- 99
Nuclear	190	90	1470
Other(-nuclear)	300	60-80	1655
Backup	190	5	83
total	1280		4945-5835

(80% RES)	Capacity (GW)	K_{min}-K_{max}(%)	$Prod_{min}$-$Prod_{max}$(TWh)
Fossil	80	60-90	420-631
Solar PV	815	10-17	714-1214
Wind onshore	245	25-35	537-751
Wind offshore	190	37-45	616- 749
Nuclear	62	90	490
Other(-nuclear)	358	63 (average)	2000
Backup	270	5	118
total	2020	(average)	4900-5950

The minimum and maximum numbers from the capacity factors are taken from the road map report[86]. The capacity factor for the energy sources under "Other", consists of nuclear(K = 90%), hydro(K = 35%), biomass(K = 80%), geothermal(K = 91%)) and CSP (K = 47%). For the 40% pathway, nuclear contributes with 30% of total energy supply. From this one finds that the installed capacity for nuclear power should be $\sim$ 190 GW in this case. For the 80% Pathway, nuclear power contributes with 10% which requires an installed capacity of 62 GW. For simplicity the rest of the capacity are divided evenly between the 4 other sources in "Other(-nuclear)".

We observe that for the most pssimistic numbers for the capacity factors the energy produced equals the assumed energy demand in Europe in 2050 (4900 TWh). This shows that the installed capacity fullfills the energy requirements for Europe even with the lowest capacity factors, both for the 80% RES pathway and the 40% RES pathway. If the highest capacity factors are achieved, it is possible to decrease the installed capacity in both the pathways. The most important observation here is the difference in installed capacity between the 40% pathway and the 80% pathway. The 80% RES pathway requires $\sim$ 60% more installed capacity than the 40% RES pathway to fullfill the energy requirements.

For the choice of power sources to become sustainable for europe in 2050 it is crucial that the electric grid have developed into a supergrid. Without the proper development of the grid, the intermittent power sources cannot give Europe the required electricity security. In all the pathways, big changes in the European transmission grids will be required to achieve this. For instance, Spain, who will be the largest contributor of concentrated solar power and photovoltaics to the supergrid will need an substantial increase in interconnection transmission capacity to France, which will be one of the largest contributors of nuclear power. Between 15 and 45 GW will be needed(depending on the choice between 40% RES and 80% RES). The current capacity is today less than 1 GW. (A map of the transmission capacities for the 40 and 80% RES pathways can be found in Appendix G.)

Another important issue is the needed backup capacity. In winter, when solar production is low and demand is high, backup capacity will be needed, and as a result 10 to 15% of the total generation capacity would be needed as a backup. These backup plants would have low capacity factors.(Around 5%)

A combination of transmission capacity between regions and backup capacity will be economical favourable. Back up capacity within each region can avoid the need for transmission lines which only will be used a few hours every year. Also, sufficient transmission capacity will avoid need for extended use of backup capacity withing each region by sharing resurces between the regions.

An interconnection by transmission lines between distant regions with different resource potentials makes it possible to exploit the observed negative correlations between the energy sources in the regions. The solar resource is at its highest in the summer, while it is observed that the wind resource is at its peak during winter. The same counter-cyclicality happends during day and night, where solar energy is available only at day time while wind energy produce more energy at night. By connecting regions with wind resources and solar resources togheter reduces the negative impact of variations in demand and supply in the grid, and this will also reduce the need for backup capacity and energy storage. An example on how the variation in demands on a daily and seasonal scale might look like is presented in the Figure 6.2. The vertical axis represents variations in percentages.

Figure 6.2: reduction of daily and seasonal fluctutations due to interconnections of regions [85]

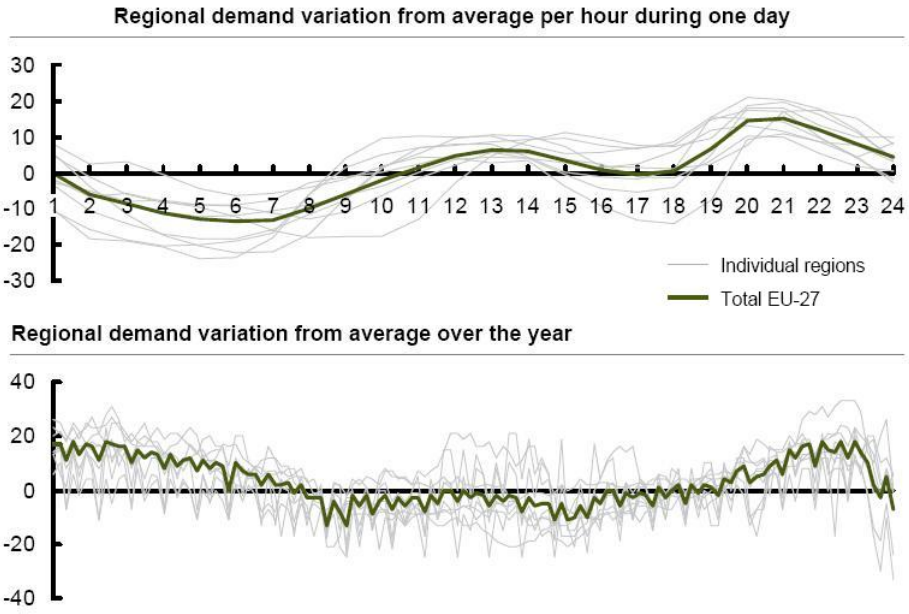

The construction of a socalled “smart grid” mentioned in point 2 at the beginning of this chapter includes various “intelligent” applications that can be implementet in to the grid. One of these applications are Demand Response (DR). This can be used to both temporarily lower demand when supply is insufficient, and to temporarily increase demand when supply is high. This way, demand response can help avoiding building,- and operational costs of

additional plants with low capacity factors. The consumers will have the chance to pay lower prices if the power generating capacity that would have been needed was from a power plant with high levelized energy cost, which usually is the case for plants with low capacity factors. Another advantage in an increase of demand when supply is high and vica versa would be less need for energy storage, since demand response instead makes the consumers adapt their consumption after the real time supply. It is shown in the road map report that a 20% demand response could contribute to a 24% reduction in needed transmission capacity in the 80% pathway. In the 40% pathway, however, the demand response have a insignificant impact on the transmission requirements.

Another interesting feature that can be added to a smart grid is time-based pricing which can be seen as a part of the demand response. Power companies today charge the same rate for every kWh of electricity, despite the fact that the cost of electrcity production may change significantly during a 24 hour period. Time based pricing may potentially change the consumer's pattern of thought regarding their electricity consumption. They may think more about when to use electricity and also how much they use. The smart meters performs two-way communications between consumer and producer and it becomes possible for the system to automatically turn end-use applications on or off, without inconvenience to the consumer.For instance, turning of an air condition system for 10 minutes won't affect the temperature in the house significantly[87].

The road map 2050 has also modelled a projection of needed grid investments during the time period from 2010 and 2050. The result is shown in Figure 6.3 . The model the calculation was based upon used an average transmission loss of 6% of the total energy that was transmitted. The vertical axis is scaled by thousand GW km. Also,a demand response of 20% is used which means that 20% of the daily energy demand is assumed to be able to be shiftet within a 24 hour period. The model assumes also that the grid development rate is driven by the builing rate of intermittent power sources (solar PV, offshore/onshore wind) since the stabilization of supply from these sources is the main purpose of the interconnections. For simplicity it is also assumed a linear build up of grid capacity between 1990 and 2010.

figure 6.3 shows that the build rate will be higher than the historical growth rate in all the pathways exept for the 40% RES pathway where the growth rate will be slightly less the in the years between 2040 and 2050. The rate shown is the average European rate. The expansion of the France/Spain interconnection mentioned earlier, will be siginficant higher than this average, while other regions will have a lower rate. The model is only a suggestion on how fast the grid should be expanded, and it requires that one start with the expansion today. If one delays the start of the investments one must eighter increase building rates at a later time, or the goal to be finished in 2050 must be delayed.

Figure 6.3: The needed growth rate for the construction of the int erconnections [85]

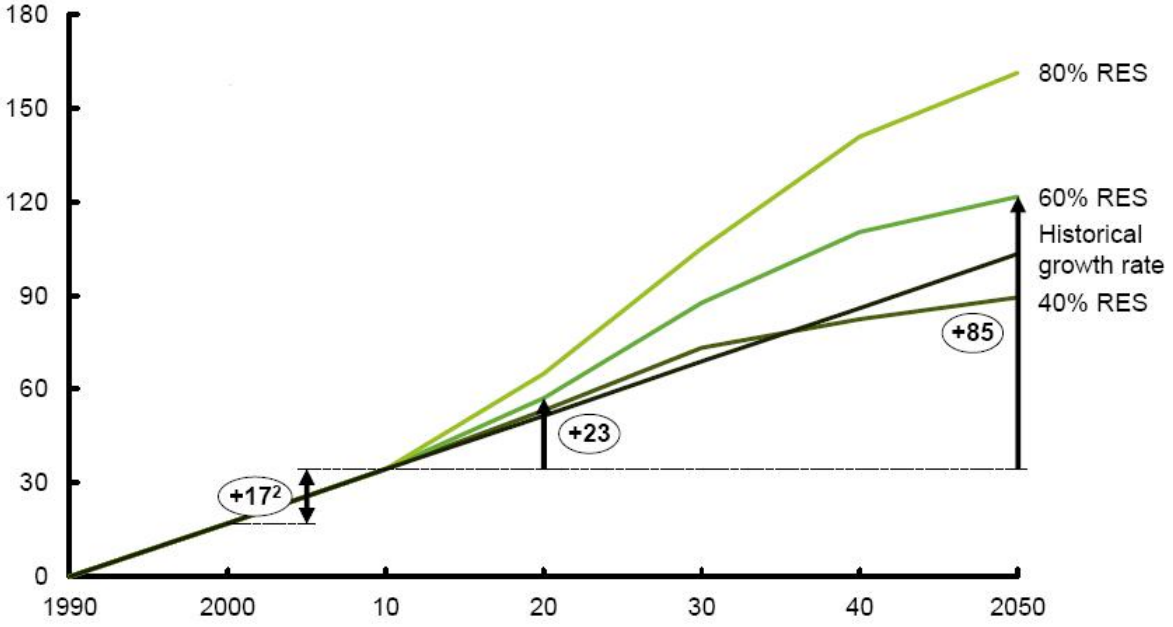

Whether or not the deployment rates for interconnection links and renewable power can be accomplished within the actual time horizon of 40 years are very dependent on political cooperation, pricing of carbon emission and the opposition of the civil society against deployment, especially regarding deployment of high voltage transmission lines in populated areas. These public objections against overhead lines may force decition makers to construct underground transmission cables instead of overhead lines and this will result in a significant increase in total cost.

The need for interconnections between separate AC grids and transmission of large amount of power over long distances must be taken into consideration when deciding what type of transmission technology which should be used for the interconnections. This will be discussed in the next chapter.

Chapter 7

Long distance power transfer

There are two main ways in which current can be transmitted: Alternating current (AC) or direct current (DC).

The major part of the high voltage transmission capacity in Europe are overhead AC lines. However, problems arise when connecting separate national electric grids to each other through AC power lines. Because AC oscillates at a certain frequency in a grid , the frequencies in two different grids often have small deviations which makes the two networks asynchronous. This can be solved by first converting the AC power to DC before transmitting it to the other network. When it arrives, the DC can be converted to AC again with synchroniced frequenzy and voltage.

The conversion from AC to DC and from DC to AC is accomplished in a converter station with the help of high voltage electronic semiconductor valves. The semiconductor valve is called "Thyristors" [88] which behaves similar to a diode, where the current is forced to move in only one direction. Each of the valves can be controlled with a control system software from computers. This makes it possible to accurately control the electricity flow (frequency control etc.)

Because of this control-feature it is possible to use High Voltage DC (HVDC) to interconnect asynchronous AC grids with each other[89].

Today, the European grid consists of several separate grids. Western Europe has one, the Nordic countries have one (Nordel), Great Britain have one and so on. All these grids deviate from each other in that there may be variations in frequency. (Although European countries operate with the same nominal frequency (50 Hz) there is always small deviations.) Further, between continents that uses 60 Hz(America) and continents that uses 50 Hz it would be impossible to connect directly through AC transmission lines.

There are also potential cost reductions when using HVDC instead of High Voltage AC (HVAC). This comes partly from the fact that AC transmission lines have a higher loss than DC transmission if the same amount of electric power is delivered. However, since HVDC needs converters at both ends, the losses from these may exceed the losses from HVAC transmission lines at short lengths. Thus, the initial overall losses of HVDC are higher, but total losses become less than for HVAC when transmission distance exceeds a certain distance. Also, the construction of the power lines is at a lower cost with HVDC than HVAC. This is because AC transmission needs a larger area to be deployed due to its three phase current, which needs three conductors. Therefore, the transmission path[1] in the terrain must be wider

[1]the technical term is "right of way" and it describes how wide the path must be for a transmission line to

which gives a harder impact on the environments. The cost of AC transmission lines must also include installation of shunt capacitators along the way (about every 100 km) because of the reactive power that is being produced. However, the main drawback of HVDC is their expensive converter stations which convert the DC into AC. Because of this, HVDC have a higher initial cost than AC and HVDC, as mentioned,can only be cost favourable over HVAC above a certain transmision length. We can describe the break even length for cost and losses with two equations. Let $C_{initial}$ be the additional initial cost which is required for HVDC compared to HVAC. Let $C_{HVDCline}$ be the cost of the HVDC transmission line per 100 km and $C_{HVACline}$ be the cost of the HVAC transmission line per 100 km. Let L be the length of the line in 100 km units. We must then have

$$C_{initial} + (C_{HVDCline} - C_{HVACline})L = 0 \tag{7.1}$$

The L value which fullfills this equation will be the cost break-even distance $L_{costbreakeven}$. For the loss break even distance, let $Loss_{initial}$ be the initial losses related to the converter stations in the HVDC system. Let $Loss_{HVDCline}$ be the loss per 100 km in the HVDC line and $Loss_{HVACline}$ the loss per 100 km in the HVAC line. We must then have

$$Loss_{initial} + (Loss_{HVDCline} - Loss_{HVACine})L = 0 \tag{7.2}$$

The L value which fullfills this equation will be the loss break-even distance $L_{lossbreakeven}$. The $L_{lossbreakeven}$ is generally different from the $L_{costbreakeven}$. $L_{lossbreakeven}$ depends on the voltage rating for the line and conductor specifications. The break-even length strongly depends on the type of transmission. For submarine cables the cost break-even distances is today typically around 100km. For overhead transmission lines it is around 450 km[90]. The cost and losses for HVAC and HVDC are illustrated in Figure 7.1.

Figure 7.1: Comparision of cost and losses between AC and DC power transmission [91]

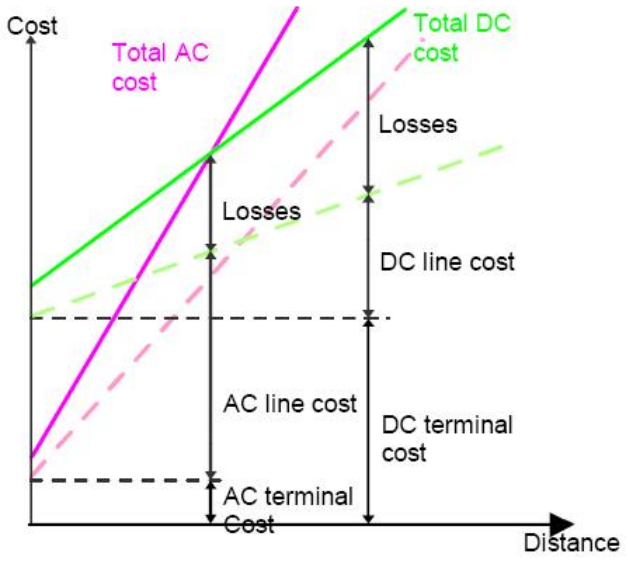

Historically, the biggest advantage of AC power was that it was capable of stepping up and down its voltage in an easy way by using a conventional transformer. These transformers

be deployed

cannot step up and down voltage with DC power, due to Faraday's induction law (see appendix C). Since there was no easy way of stepping up and down the voltage, the early DC generators had to be in close proximity to the consumers (within 1-2 kilometer.)[92] This was one of the reasons that AC power won the "war of currents"[2] at the end of the 19th century.
In the 1970's, the introduction of solid state semiconductor devices such as the thyristor made it possible to convert AC into DC and DC into AC in a reliable and efficient way, even at high power ratings (high voltage). This opened up the possibility for AC power generated at the power plant first to be stepped up in a transformer and then converted into DC power in the thyristors before transmitting the power over long distances. At the other end of the transmission link, the DC power can be converted to AC again before it is stepped down to the voltage level needed in the local power distribution. In 2003 a new type of thyristor called the LTT (Light Triggered thyristor) became available. This thyristor is triggered by a light pulse transmitted through an optical fiber. This gives the thyristors very short response time and improves the system's reliability and security features which is especially important when the HVDC is used as interconnection between asynchronous AC power grids.[90]

7.0.1 The NorNed transmission cable

Norway and the Netherlands installed in 2008 a submarine HVDC cable (the NorNed cable) for the purpose of power exchange between the Nordel grid and the Netherlands. With a length of 580 km it is the longest power transmission in the world through a submarine cable. In Norway, the 300 kV AC grid is connected to a substation where the AC is stepped up and converted into DC at a voltage-to-ground value of 450 kV. In the Netherlands, the Dutch 380 kV AC grid is connected to another substation where the incoming DC power is converted and stepped down[93]. The link is monopolar with two cables, which means that one of the terminals is grounded (connected to earth). One cable has a +450 kV potential difference to the ground while the other cable has a -450 kV potential difference to the ground. The power can be transmitted in both directions. See figure 7.2 for an illustration.

Figure 7.2: The NorNed HVDC submarine cable [93]

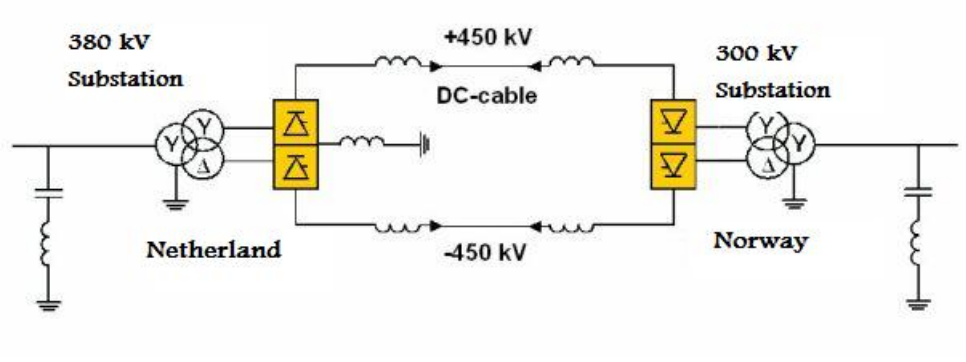

The NorNed transmission link could not have been realized by using a HVAC transmission. The reason is that AC cables generate an increasing variation of voltage with increasing distance, until the cable power capacity is fully taken up by the socalled reactive power. This

[2]The term refers to the market competition between AC and DC power in the 1880's, when Thomas Edison was the promoter of direct current while Nikola Tesla among others promoted alternating current to be used in a national grid.

happens because the cable has large capacitance and this limits the maximum transmission distance. (As mentioned above, normally, reactive compensation units like shunt capacitators are installed about every 100 km, and this cannot be done under water. Because of this, the practical distance has been 50km. Recently, a new cable type for submarine connections with lower shunt capacitance has increased the limit to about 100 km. With HVDC, there is no such limitation and therefore HVDC is the only viable technical alternative for distances above 100 km[90].

7.0.2 Transmission losses in DC transmission

For DC transmission the only significant loss is due to heat losses from the resistance in the conductors.

The voltage V over the transmission line can be interpreted as the work done per unit charge. The current I is defined to be the amount of charge flowing per unit time. From this we must have that the total power P delivered to the transmission line is

$$P = VI \tag{7.3}$$

The total resistance R of a wire can be given in terms of the specific resistance (resistivity) ρ at standard conditions (20°C) of the conductor material.(We denote the specific resistance at standard conditions as ρ°).

$$R = \rho^\circ \frac{L}{A} \tag{7.4}$$

where L is the length of the wire and A is the cross sectional area of the conductor. Thus, the total resistance is proportional to the length and inversely proportional to its cross section. The specific resistance of copper, which is the standard conductor material in submarine transmission cables, is $1,678 * 10^{-8}\Omega$m at standard conditions (20°C).[3]

The power loss due to the heat produced by the resistance can be approximated by Joule's heating law,

$$P_{heat} = RI^2 \tag{7.5}$$

This law applies only for a circuit that obeys Ohm's law, but it is a reasonable good approximation for direct current circuits, (approximately constant voltage and constant current over the transmission distance). Again, for a more accurate calculation, a temperature variation coefficient must be included)
As an example, the power loss in the NorNed HVDC cable can be calculated for the maximum capacity P = 700 MW. V is here 450kV, and the current I can be found from Equation (7.3)

$$I = \frac{P}{V} = \frac{700 * 10^6 W}{450 * 10^3 V} \sim 1550A \tag{7.6}$$

The length L of the cable is 580km and the crossectional area of the copper wire is according to [93] 800 mm^2 (actually the area varies for different parts of the cable but the main

[3]Since the specific resistance generally increases with temperature,the expression of the total R should be multiplied with a temperature dependent factor to give a more accurate calculation. The needed correction coefficients can be found in [94]

submarine part of the cable has this crossection) , from Equation (7.4) the total ressitance of the cable is

$$R = \rho \frac{L}{A} = 1,678 * 10^{-8} \Omega m * \frac{580 * 10^3 m}{0,0008 m^2} = 12,1\Omega \tag{7.7}$$

Finally, the heat loss is calculated from Equation (7.5)

$$P_{heat} = RI^2 = 12,1\Omega * 1550^2 = 29070205W \sim 29MW \tag{7.8}$$

In percent, the amount of the total power transmitted will therefore be:

$$\frac{29MW * 100}{700MW} \sim 4,1\% \tag{7.9}$$

According to [93] the measured loss for the NorNed cable at 600MW is $3,7\%$. The calculation above is off by around 10%. The reason for this deviation is partly that the resistance is dependent on the power load in the cable and partly that the temperature dependence is not included.

Other examples of losses from a HVDC transmission line is a ±300 kV, 1000 MW, HVDC Light link of distance 200 km. This has total loss in the order of $4,9\%$,at full load. found from [93]

The formulae (7.3 - 7.5) explain why it is important to have a high voltage at long distance transmission: If the voltage is stepped up the current must go down. And since the power loss increases with the square of the current, the power loss can be greatly reduced by stepping up the voltage.

Equations (7.3 - 7.5) also shows that transmission losses increases with the power load in the transmission line. For a more detailed analysis of the transmission losses it is therefore important to know the typical power load in the lines. A loss/cost-optimization of transmision capacity and power generation capacity must be made to find the most cost/loss efficient option.

This has been analysed in the roadmap 2050 report. A map of the needed transmission capacities with the transmission utilization factor[4] for the 80% RES pathway and 40% RES pathway, after optimization, are found in appendix G. The capacities are found with the assumption of a 20% demand response. (This is the same map that was referred to in Chapter 6)

[4]The transmission utilization factor is defined as the ratio: total annual flow/maximum theoretical annual flow

Chapter 8

Solar power from Africa to Europe

The Roadmap 2050 also discusses a 100% RES pathway, where all the electricity comes from renewable energy sources. It suggests that this can be done by importing 15% of the needed energy from the Sahara desert in North Africa. To add up to 100% they assume that enhanced geothermal power (Hot Dry Rock) is being developed in Europe and can contribute with 5% of the total energy supply.

The possibility of transmitting large amounts of power from Africa to Europe has been studied in detail by two DLR reports published in 2005[95] and 2006[1] and some of the results from these reports is used here.

The energy will be distributed to the region described in roadmap 2050 which is the 27 nations in the European Union (EU-27) plus Norway and Switzerland. The total energy demand in 2050 is assumed to be 4900TWh. The 15% that will come from North Africa amounts to 735 TWh.

8.1 Production of energy

The technology that will be used to produce the energy is concentrated solar power due to its possibility of energy storage. More specific, a mix of parabolic trough plants and central receivers will be used with thermal storage. The annual capacity factor is assumed to be 80% in both cases[1]. This capacity factor is chosen on the background of the roadmap 2050 report which assumes a capacity factor of 60% for the CCS coal and gas plants and 90% for the nuclear power plants. Since the solar power from Africa will replace these plants when going from a 80% RES pathway to a 100% RES pathway, it will require a capacity factor somewhere in between these two values.

We start the discussion by defining two cases:

- **Case 1**

  No technology improvements assumed. The overall efficiency of the systems today will therefore be assumed to be the standard also in 2050. That is an solar to electric efficiency of 15% for both technologies. The solar to storage to electric efficiency is assumed to be 14%. We assume that the solar to electric efficiency

[1]The annual Capacity factor must be clearly distinguished from the day to day capacity factor. There are differences between number of peak sun hours in summer and in winter in the North African countries. (The difference will be less the closer to equator you go)

equals the solar-to-storage-to-electric efficiency for simplicity. The storage system is the indirect two-tank system, based on the model from Chapter 5. For both cases it will be designed by assuming the annual energy is distributed evenly over the entire year.))

- **Case 2**

  Development of a direct system, where the HTF is used both in the solar field and in the storage system, is assumed in combination with a suitable storage system, this will result in a solar to electric efficiency of 20% for both technologies, and a solar to storage to electric efficiency of 0,19. Also here we assume for simplicity that the solar to electric efficiency equals the solar to storage to electric efficiency in calculations. The storage system will here be the direct thermocline system, and based on the calculations from Chapter 5, but with more optimistic numbers for the power block efficiency (η_{pb} is increased from $0,34$ to $0,38$).(In reality, the central receiver system has potential to reach a higher efficiency than the parabolic troughs do to a higher temperature that can be achieved in the power block. and if this is the case, it would be more economical favourable to put all the money on the technology with the best efficiency, although the relative costs of the different technologies also had to be considered)

In the end of the chapter we will introduce 3 different scenarios, where the transmission distance and annual irradiation differs, each scenario will be calculated for both cases.

8.2 Transmission of energy

The electricity will have to be transmitted over distances of $\sim$ 3000 to 5000 kilometres, depending on the location of the power plants and the european destination. Initially, there are three ways the energy potentially could be transmitted:

1: HVAC transmission lines As discussed, the HVAC is advantageous at transmission distances up to $\sim$ 450km for overhead lines. Also, HVAC systems are subject to big losses at large distances. For instance, For a 750kV transmission line the losses are 8% per 1000 km. Also, there are limitations on how much power that can be transmitted by an AC cable or line due to the reactive power that is being produced.

2: Hydrogen transportation. The transport of solar energy via hydrogen over a long distances would in principle be possible, but $\sim$ 75% of the electricity would be lost by the involved conversion, transport and storage processes. This alternative would therefore only be discussed if the Hydrogen was to be used as a transportation fuel. However, the scenarios discussed is instead leaning towards an electrification of the transport sector.

3 HVDC transmission lines The losses related to HVDC transmission comes almost only from ohmic resistance of the form RI^2, this results in losses from HVDC lines of about half the losses in a HVAC transmission line. Also, there are no technical limitations on the power capacity of a HVDC line since no reactive power is produced.

The comparisions of cost and losses for HVDC and HVAC for voltages that is required for a 5000MW transmission capacity is given in table below.

Based on the considerations above and the table we conclude that HVDC transmission will be the only reasonable option for the needed transmission distances and large amounts of power that must be transferred. HVDC will therefore be used for the interconnections.

Figure 8.1: Comparision of cost and losses for AC and DC power transmission [1]

Parameter	Unit	HVAC		HVDC	
Operation Voltage	**kV**	**750**	**1150**	**± 600**	**± 800**
overhead line losses	%/1000 km	8%	6%	5%	2.5%
sea cable losses	%/100 km	60%	50%	0.33%	0.25%
terminal losses	%/station	0.2%	0.2%	0.7%	0.6%
overhead line cost	M€/1000 km	400 - 750	1000	400 - 450	250 - 300
sea cable cost	M€/1000 km	3200	5900	2500	1800
terminal cost	M€/station	80	80	250 - 350	250 - 350

8.3 Solar resources and locations of power plants

The direct annual solar irradiation per square meter for North Africa and the southern parts of europe is illustrated below.

Figure 8.2: Direct annual solar irradiation for North Africa and souther parts of Europe. Saudi Arabia is to the right. Data produced by DLR in 2004

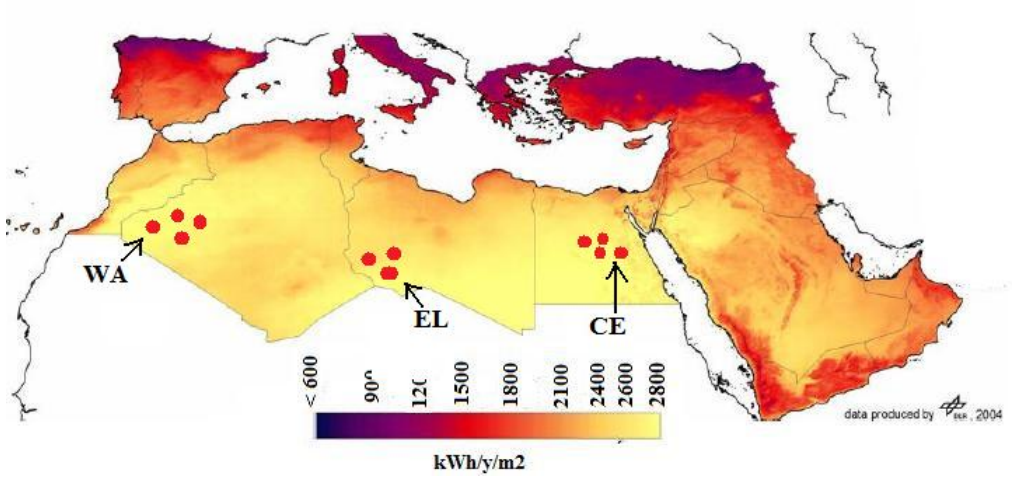

The irradiation map indicates the diffences in irradiation between Africa and southern Europe. The best sites in Spain has an annual irradiation of ~ 2100 kWh/y/m^2. In North Africa there exist locations with around 2800kWh/y/m^2, according to the DLR report. Therefore, 33% more electricity can be produced per square meter by plants located in these locations than if the same plants were located in Spain.

As mentioned above, the solar field will be designed by assuming the annual direct beam radiation is distributed evenly over the enire year. I do this since there are no accurate data available on how the insolation vary for specific seasons. An annual irradiation of 2800kWh/y/m^2 corresponds to 7671 Wh/m^2/day. We assume that this will be distributed over the day with 935 W/m^2 for 8,2 hours. To reach a 80% capacity factor based on this, a 11 hour storage capacity would be needed. The 2100 kWh/y/m^2 in Spain corresponds to 5753 Wh/m^2/day and 702 W/m^2 for 8,2 hours will be distributed over the day. In Chapter 9 I will discuss how this should be modified to account for seasonal and daily variations.

The red dots[2] on the map suggests where the locations of the power plants could be placed. The choice of locations is based on a choice of best possible solar irradiation. Also, slopes at an angle over $2,1^{circ}$ is avoided and locations of centre of demands are taken into consideration. [95] provides detailed analysis of available locations suitable for CSP. Based on suitable locations, solar to electric efficiency at 15% and a land use factor[3] of 30%, they have calculated technical potentials for CSP extraction.

The locations choosen are Western Algeria (WA), Southern Libya (SL)) and Central Egypt (CE).

8.4 End points of the transmission lines

The transmission destinations in Europe are assumed to be at the locations refered to as the "centre of gravity[4] " in the roadmap 2050. From these centers the local (national) AC grids distribute the imported electricity across the region, or it is transported through the European HVDC interconnections which is assumed built in 2050. The destinations are choosen to be Germany(Aachen) for the lines coming from Western Algeria, Italy (Milano) will be the destination for the lines coming from southern Libya and Poland (Warzawa) for the lines coming from central Egypt. These choices are in accordance with the choices made in the DLR report.

The table below shows the transmission lengths for each of the paths:

Figure 8.3: The transmission distance for the three different paths [1]

Western Algeria - Germany		**Southern Libya - Italy**		**Central Egypt - Poland**	
Country	**Length [km]**	**Country**	**Length [km]**	**Country**	**Length [km]**
Algeria	256	Libya	1326	Egypt	858
Morocco	835	Tunisia	701	Israel	59
Spain	932	Sardinia/Italy	313	Jordan	378
France	907	Corsica/France	216	Syria	495
Belgium	164	Italy	178	Turkey	1324
Germany	5			Bulgaria	448
				Romania	361
				Hungary	518
				Austria	72
				Slovakia	50
				Czech Republic	195
				Poland	355
Overhead line	3099	Overhead line	2735	Overhead line	5113
Submarine cable	18 (0.6 %)	Submarine cable	373 (12 %)	Submarine cable	30 (0.6 %)
Sum	**3117**	**Sum**	**3108**	**Sum**	**5143**

Knowing the transmission distance we can calculate the actual power that need to be produced by the plants in order to supply Europe with the needed power.

[2]The red dots does not reflect the size of the power plants relative to the scaling of the map

[3]The land use factor describes how many square meter of land that is needed for every square meter of solar collectors

[4]The centre of gravity is the geographical centre of a region. It is used as the point to and from which the regional demand and generation is connected and where all inter-regional flows start and terminate

We assumed the annual capacity factor of the plants to be 80%. This is equivalent to a peak load electricity production in a total of 7008 hours a year. 735TWh must therefore be delivered with a total power of 105GW.

8.5 Configuration of the interconnections

The power will be delivered through a number of bipolar transmission lines, each of them with two conductors. In case 1 we want to choose the highest possible transmission voltage that can be installed with today's technology.

The maximum transmission voltage that can be applied for the system is limited by several factors. A higher voltage requires a larger air clearance between the transmission line and the ground. Insulators must therefore be used. Also, new transformers that can tackle the high voltages must be developed. Up to now, the standard voltage has been 500 kV in DC systems, but recently a new transformer has been developed for a 800kV DC transmission in china[96]. Also, new improved insulators based on polymeric materials has been developed and this makes it possible to upgrade DC transmission voltages to 800kV[97]. We choose therefore the transmission voltage to be 800 kV in Case 1, which also is in accordance with the DLR model. According to [96] a suitable power rating with reasonable losses for a 800 kV HVDC transmission is between 5 and 6 GW. Based on this we choose the capacity for each transmission line to be 5 GW in case 1. This capacity will be divided between two conductors, each with capacity $2,5$GW. This is also in accordance with the DLR report.
It is quite possible that the voltages can be further increased in the future, therefore we use a voltage of 1MV in Case 2.

The bipolar system is illustrated below:

Figure 8.4: Bipolar HVDC interconnection between Africa and Europe [1]

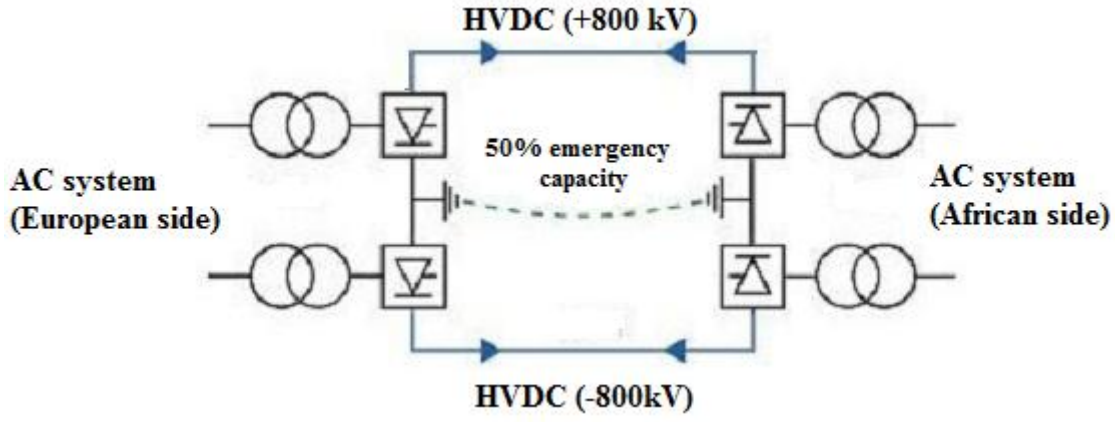

The ohmic heat loss for each conductor ,P_{heat}, is found in the same way as was done for the NorNed cable, taken reservations that the calculated loss is off by $\sim \pm 10\%$ from the actual value. The standard conductor material for long distance overhead transmission is aluminium. Aluminium has a resistivity $\rho^{\circ} \sim 2,65 * 10^{-8}$ Ωm at standard conditions, which is around 40% lower than for copper. However, aluminium has a lower weight and is cheaper than copper, which gives the opportunity to have a higher cross sectional area at the same

cost. Since the submarine fraction of the transmission distance is negligible, we can assume the whole transmission distance to be overhead lines to a good approximation for the total transmission loss.

The ohmic resistance in the conductors is given by

$$R = \rho^{\circ}\frac{L}{A} \tag{8.1}$$

where as before, L is the length of the conductor. The total cross-sectional area A for each conductor is here chosen to be 3200 mm^2 in accordance with the DLR model. (A larger cross-section results in a lower resistance, but the cost and weight will increase, compromises must therefore be made).

The preferred plant size for a parabolic trough power plant with thermal storage is according to [98] 250 MW. This plant size results in the most economical combination of power block size and solar fields. According to [99] it will be economically favourable to place plants in the same location and together in units. We assume therefore that four 250MW power plants, each with separated power blocks, are located at the same spot and therefore will be sharing the same operation and maintenance staff.[5]

The input data which is common for all three locations (WA, SL and CE) is given below.

Transmission system	
Voltage case 1	800 kV
Voltage case 2	1000 kV
Line configuration	bipolar HVDC
Conductors per line	2
Capacity per conductor	2,5 GW
Conductor material	Aluminium
Resistivity ρ	$2,7 * 10^{-8}$
Cross-sectional area A	3200 mm^2
Loss per converter station	0,7 %
Transmission loss per 1000 km case1	3,2
Transmission loss per 1000 km case2	2,1

Solar field	
Solar-to-electric efficiency (η_{tot}) case 1	0,14
η_{tot} case 2	0,19
Solar-to-storage-to-electric (η_{sse}) case 1	0,14
η_{sse}) case 2	0,19
Annual solar intensity I (kWh/y/m^2)	2800
Capacity factor	80 %
Power block capacity per unit	250 MW
Units per arrangement	4

[5]Installing multiple plants at a common site has potential to offer a reduction in LEC of 10 to 12%, due to greater quantities of bulk materials, common project development, construction and O&M staff.

Storage system	
Storage system case 1	indirect two tank system
Storage system case 2	direct thermocline system
Average radiation/m^2/day Africa	7,57kWh/m^2/day
Hours of storage per day	11
Storage-to-electric efficiency ($\eta_{thermal}$) case 1	0,28
$\eta_{thermal}$ case 2	0,35

For simplicity we choose in advance that 40 GW will be produced at transmission distance 5100 km in central Egypt(CE). This requires four red dots, each with 10 GW production capacity. Knowing the transmission loss per 1000 km we find the total loss ,including losses in converter stations (one on each side)[6] in case 1 to be $3,2\%/1000km*5,1+0,7*2 = 17,7\%$. Therefore, $7,1$ GW of the production is lost during transmission and $32,9$ GW is delivered to Europe. The power production that will be needed to deliver the remaining $67,1$ GW to Europe will be distributed over the two regions in Western Algeria (WA) and Southern Libya (SL). The total losses for the transmission distance 3100 km in WA and SL is $11,7\%$. The needed power production to deliver $67,1$ GW will therefore be 76 GW.

The results of the calculations for both the cases are given in the table below:

	Case 1			Case 2		
	WA	SL	CE	WA	SL	CE
Transmission distance(1000 km)	3100	3100	5100	3100	3100	5100
Transmission losses (%)	11,7	11,7	17,7	7,9	7,9	12,11
Power production (GW)	40	36	40	40	30	40
Transmission lines	8	6(+1x6GW)	8	8	6	8
Delivered power	35,2	31,8	32,9	36,9	27,7	35,3
Production per cite(red dot)	10	10(+1x6)	10	10	10	10
Number of cites	4	3(+1x6GW)	4	4	4	4

6(+1x6GW) under Southern Libya (SL) means that one 6 GW transmission line are required in addition to six 5 GW transmission lines.

The solar field area is found from the formula in Chapter 5: For the daily solar production, the solar field area A_{prod} is needed:

$$A_{prod} = \frac{kW_{peak}}{\eta_{se} P_s} \tag{8.2}$$

where, η_{se} is the solar-to-electric efficiency. P_s is the incoming solar power per square meter (kW/m^2). For the thermal energy storage, the solar field area $A_{storage}$ is needed:

$$A_{storage} = \frac{kW_{peak} * t}{\eta_{sse} I_s} \tag{8.3}$$

[6] Since the power must go through the converter station on the African side before it is transmitted, one should subtract this loss first to find the power into the transission line. This would give a transmission loss slightly less than I have calculated ($\sim 0,3\%$ less). Since my calculation of transmission loss initially have an uncertainity of $\sim \pm$ 10%, this deviation is neglected. Still, it is important to know the sources of the uncertainties

where η_{sse} is the solar-to-storage-to-electric efficiency. I_s is the daily solar energy per square meter (kWh/m^2). t is the number of storage hours and equals 11.

We assume for simplicity that $\eta_{se} = \eta_{sse}$ in the following calculations, that is $\eta_{se} = \eta_{sse}$ = 0,14 in case 1 and $\eta_{se} = \eta_{sse}$ = 0,19 in case 2.

The total needed area will be the sum $A_{prod} + A_{storage}$

The geographical area per 10 GW cite (red dot on the map) is calculated by assuming that each square meter of collector area needs 3 m^2 of geographical area. Also, each 1 GW arrangement is assumed to be separated from each other with an area-equvalent of 2 km^2.

The results are summarized in the table below:

	Case 1			Case 2		
	WA	SL	CE	WA	SL	CE
Annual energy from solar field per 250 MW unit (TWh)	12,5	12,5	12,5	9,2	9,2	9,2
Number of 250 MW units	160	144	160	160	120	160
Solar field area per unit plant (km^2)	4,47	4,47	4,47	3,29	3,29	3,29
Power produced pr GW delivered	1,13	1,13	1,22	1,07	1,07	1,14
Area per GW delivered	20,3	20,3	21,7	14,2	14,2	14,9
Geographical area per 10 GW cite	556	556	556	415	415	415
Geographical area per 10 GW delivered	629	629	671	446	446	467

We observe that the required geographical area per 10 GW cite is reduced to 415 km^2 in Case 2; this is only due to the increase in solar-to-electric efficiency from $0,14$ in case 1 to $0,19$ in case 2. As a comparision, the city of Bergen (large) has a geographical area of 445 km^2. The geographical area per 10 GW delivered is higher than the geographical area of the cites, since it requires more than 10 GW power produced at the site to deliver 10 GW at the destination.

For comparison, we may calculate how large the geographical area of a 10 GW wind park would be, assuming large wind turbines of $3MW$ capacity with rotor diameter 90 meter[100]. For maximum output the windmills should have a spacing of around 5 windmill diameters[4]. This means placing the windmills 450 meters apart. A 10 GW wind park requires 3333 3 MW windmills. This will result in a needed geographical area of $26km * 26km \sim 680$km^2. The windpark would typically have a capacity factor of maximum 40%, most often less, compared to the 80% capacity factor of the 10 GW solar site which means that twice as much solar electric energy would be produced in the area.

The thermal storage system for Case 1 will be identical with the indirect two-tank system modelled in Chapter 5, only with one slight difference, namely that the CAP$_{max}$ factor is increased to $0,95$ due to large scale. For Case 2 the direct thermocline system from Chapter 5 is used but with a more optimistic scenario. CAP$_{max}$ is assumed to have increased to $0,80$ due to large scale. We assume that solar salt can be used as the HTF which will result in a larger ΔT and as a result we assume the power block efficiency has increased to $0,38$. This, and a small increase in solar field efficiency ($0,50$ to $0,53$) will give a solar-to-electric efficiency of 20% which is the assumption in Case 2. The storage systems will have a capacity of 11 hours. Results are summarized in the table below.

	Case 1			Case 2		
	WA	SL	CE	WA	SL	CE
Storage capacity per unit (hours)	11	11	11	11	14	14
Thermal storage capacity per unit (GWh)	9,95	9,95	9,95	7,69	7,69	7,69
Thermal storage capacity per cite	398	398	398	308	308	308
Tank volume per unit($*10^4 m^3$)	26,6	26,6	26,6	8,8	8,8	8,8
Tank volume per cite ($*10^6 m^3$)	10,6	10,6	10,6	3,5	3,5	3,5
Salt volume per unit ($*10^4 m^3$)	13,3	13,3	13,3	2,6	2,6	2,6
Salt volume per cite ($*10^6$)	5,3	5,3	5,3	1,1	1,1	1,1

The decrease in needed thermal storage capacity in Case 2 reflects the assumed increase in powerblock efficiency. The tank volume per unit for the two-tank system in Case 1 is $26,68 * 10^4 m^3$. This is equvalent with two tanks with a diameter of 50 meter and height 58 meter. It is possible that it would be better to distribute the capacity on two storage systems, each with tanks half that size. In either case it is clear that the needed area for the storage systems is negligible compared to the needed area for the solar field. However, the needed amount of solar salt is not negligible, with an amount enough to fill 53 olympic size swimmingpools[7] per 250 MW units. Having said that, the constituents of solar salt are quite common. Potassium nitrate which stands for 50% of the solar salt is a main ingredient in fertilizers and in 2008 the global production was 36 million metric tonnes.[101]. The totalt amount of salt that would be needed (116 GW capacity) amounts to 117 million tonnes (solar salt has density 1899 kg/m^3) ,half of this would be Potassium nitrate. So the amount needed would be about twice the production today. Since the building process of the plants wlll have to go over many years this does not need to be a problem.

We will now assume three different scenarios:

- **Scenario 1**
  All the plants are located in southern Europe with an average transmission distance of 1500 km. The annual direct solar radiation is here assumed to be I = 2100 $kWh/y/m^2$.

- **Scenario 2**
  All the plants are located in Africa with an average transmission distance of 3100 km and I = 2800 $kWh/y/m^2$.

- **Scenario 2**
  All the plants are located in Africa with an average transmission distance of 5100 km and I = 2800 $kWh/y/m^2$.

For all the three scenarios we apply the two cases defined earlier, case 1 with no assumed technology improvements and case 2 with optimum technology improvements. We then make plots that shows different quantities against the percentage of the total energy need in Europe covered by the power plants.

Scenario 1 is the red curves in all the plots, Scenario 2 has yellow curves and scenario 3 har green curves.

Figure 8.5: The number of transmission lines needed to deliver a given percentage of European power consumption in 2050. Case 1 is the upper graph for each of the scenarios

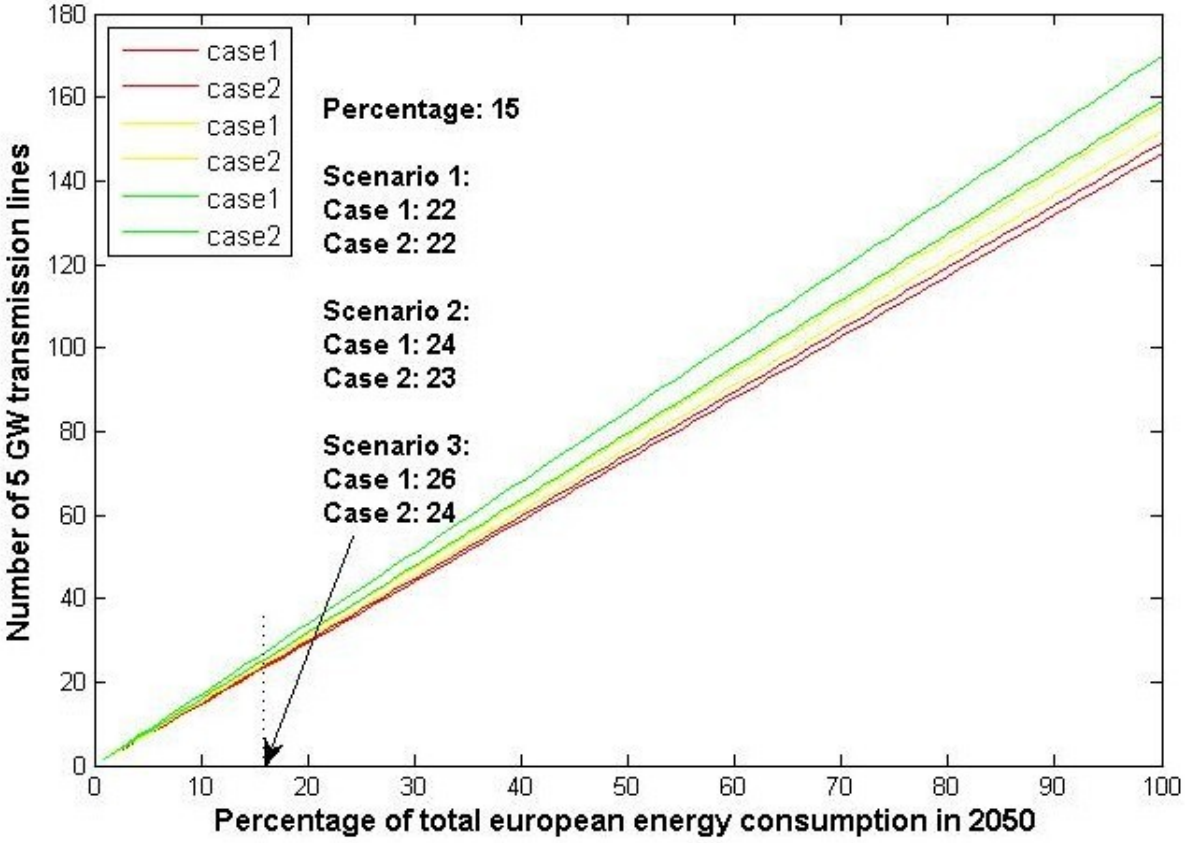

For example the number of transmission lines needed to deliver a given percentage of European power consumption in 2050 (each transmission line with 5 GW capacity)

Figure 8.5 shows that Scenario 1 (green) will require less transmission lines than the two other scenarios where the solar power comes from Africa. The reason for this is that the longer the distance, the more is lost on its way and the more must be produced at the production site to deliver the given amount of energy at the destination. Therefore, the needed transmission capacity increases with transmission distance. It is possible that the capacity of each transmission line could be increased in Case 2, where the transmission voltage is 1000kV. This could decrease the number of transmission lines. However, as the capacity of the transmission line increases, a larger percentage of the total power transmitted is lost. To prevent this increase in loss, a larger cross sectional area of the conductors is required. This will increase the weight of the transmission line and also increase the cost. Nevertheless, it is preferable to have as few transmission lines as possible since each of them are very expensive and give large impacts of the environments near its transmissin path in the terrain. It might also be restrictions on the pathway the transmision line can take, due to populated areas etc. So, if it is possible to increase capacity for each transmission line in near future, this may be the best choice.

The plot above showed that the number of transmission lines is lowest at the shortest trans-

[7] One Olympic size swimmingpool has dimensions 50mx25mx2m = 2500 m^3

mission distances. However, since the direct solar irradiation is significant lower in southern Europe than in Africa it will require a larger solar field to produce a given amount of energy. So, despite the fact that the needed power to be produced is lower in southern Europe, it might still be more economical to produce more power in Africa at longer transmission lengths. This can be seen in Figure 8.6.

Figure 8.6: The solar field area needed to deliver a given percentage of European power consumption in 2050. Scenario 1-3 corresponds to red, yellow and green graphs, respectively.

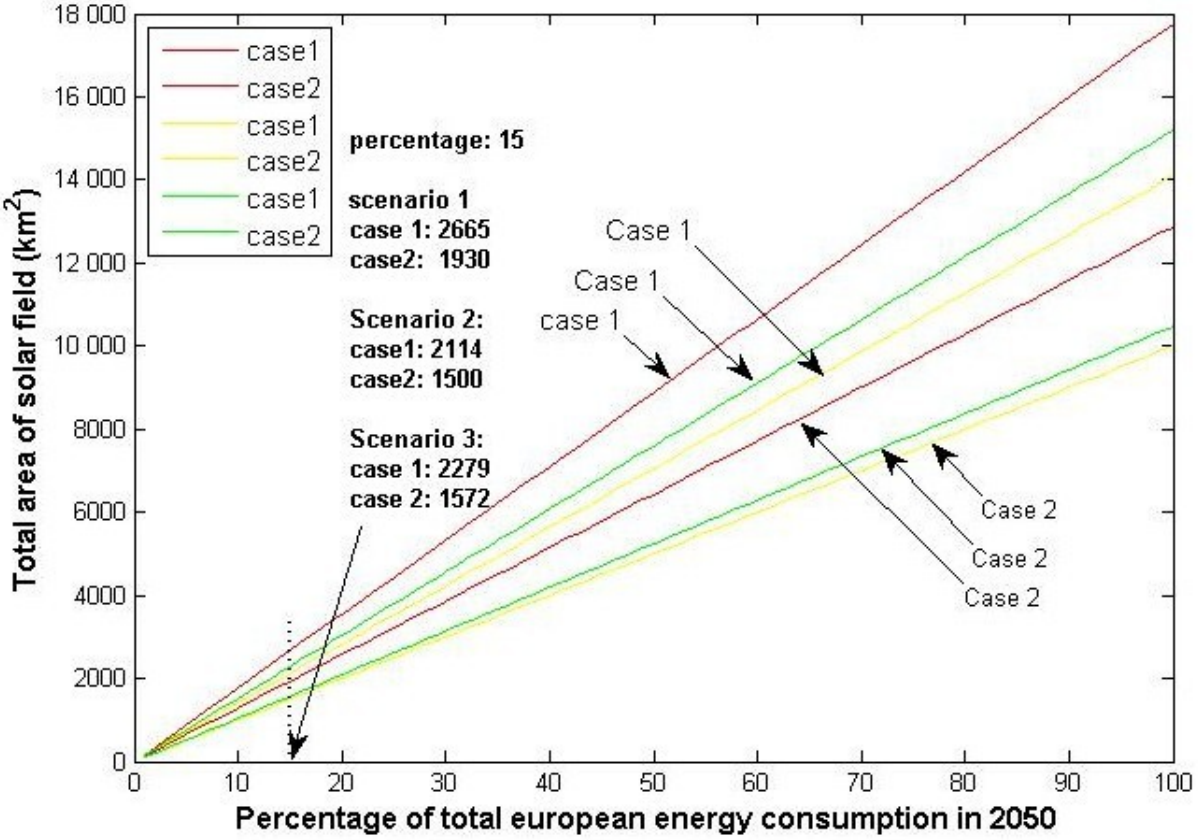

We observe that for both cases, scenario 2 requires considerable less solar field area than scenario 1, also slightly less than scenario 3. When the percentage is 15 of total european need, scenario 1 would need a 390 km^2 larger area than scenario 3 for case 1. As observed in the earlier graph, scenario 1 would need four transmission lines less than scenario 3, and the transmission lines would be 3600 km shorter in length. According to the DLR report, the overhead line cost for a 800 kV bipolar HVDC system amounts to around 300 million euro per 1000 km. The terminals costs around 300 million euro each. We need two of them per transmission line. Therefore, the transmission lines for scenario 3 would cost $4 * 5,1 * 300 + 300 * 8 + 22 * 3,6 * 300 \sim 32$ billion euro more than in scenario 1. To calculate the cost of the 390 km^2 extra solar field area in scenario 1 we can use the cost of the Andasol plant found in Chapter 4. The Andasol plant was found to cost \$780 = 630 euro per square meter. The 390 km^2 of solar field would therefore cost $630 * 390 * 10^6 = 246$ billion euro. From this we understand that it is economically favourable to build the power plants at places where solar radiation is highest and the needed solar field area is the lowest, even when the transmission

distances are considerable higher.

We observe also from the plot how great an impact a change in solar-to-electric efficiency has on the solar field area. Case 2 for Scenario 1 will actually require less solar field area than case 1 for scenario 2 and 3, despite the fact that the solar irradiation is much higher in these scenarios. This can be explained by that a change in efficiency from 14% in case 1 to 19% in case 2 is an increase of $\sim 36\%$. While the difference in solar radiation (2100kWh/y/m^2 in scenario 1 and 2800kWh/y/m^2 in scenario 2 and 3) is $\sim 33\%$.

As a curiousity we can find from the plot the required solar field area to deliver 100% of the needed energy for scenario 3 (green graphs).

Case 1 would require a solar field area of 15200 km^2, and case 2 would require an area of 10500 km^2 . Note that this is the physical area of the solar collectors in the solar field. The geographical area would be about three times as big. That is, case 1 would require a geographical area of 46000 km^2, about the size of Finnmark fylke in Norway which has an an area of $\sim$ 49000 km^2.

The needed tank volume for the storage system to accompany the solar field area for the different scenarios is shown in Figure 8.7.

Figure 8.7: The total tank volume needed for a 11 hour thermal storage capacity for the CSP plants required to deliver a given percentage of European power consumption in 2050. Scenarios 1-3 corresponds to red, yellow and green graphs, respectively.

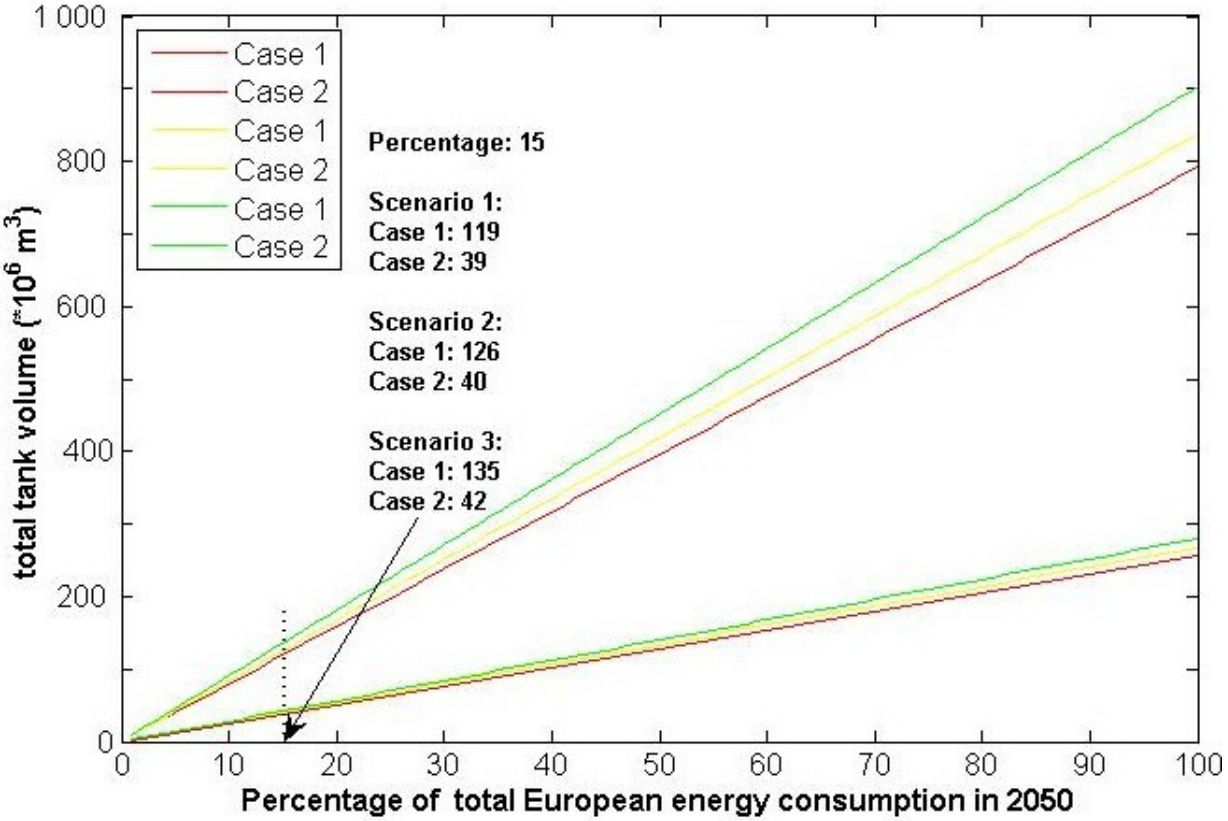

Figure 8.7 shows that Scenario 1 needs less total tank volume than Scenario 2 and 3 for both cases. This is logical since the needed total tank volume is dependent on the needed power production, and increases when this increases. The numbers from this plot can be more

comprehensive if we convert them to power plants units. Each unit power plant is of 250 MW size. For Cases 1, the total needed power production in Scenario 1 required to deliver 15% of european energy in 2050 is $111,8$ GW, for Scenario 2 it is $118,3$ GW and for scenario 3 it is $127,5$ GW. This is eqivalent with 447, 473 and 510 250 MW power plants respectively. So, to find the tank volume per 250 MW power plant, we just divide the total tank volume on the number of 250 MW power plants. The number should be the same for all the scenarios, and it is $\sim 26,6 * 10^4 \mathrm{m}^3$. That is, every 250 MW power plant will need a tank volume of $\sim$ 266000 m^3 in case 1, which is identical with the number found in the tables for the specific cites presented earlier.

The tank volume needed in Case 2 is considerable smaller than in Case 1 and therefore seems to be preferable. However, the storage system which is assumed in Case 2 have not yet been applied in commercial large scale power plants, and in future power plants it might be more likely that a storage system in combination with direct steam generation will be used

Chapter 9

Modifications on the model

The analysis in the preceeding section was based on the annual direct beam energy received per square meter of collector surface. The annual capacity factor K was assumed to be 80%. The annual energy received were distributed evenly over the year. Therefore, what we have found is how large the solar field should be to deliver a given amount of energy annually with this annual capacity factor and annual energy per square meter.
The problem with this approach is that the energy is not evenly distributed throughout the year. Regions located to the north of equator will have winter months with considerable less solar radiation than the summer months.The difference between summer and winter becomes less closer to equator, but the difference is still appreciable in Algeria, Libya and Egypt which are located at at around 25° latitude. The length of day (time between sunrise and sunset) in these countries varies between $\sim$ 10 hours in winter and $\sim$ 14 hours in summer[102]. The intensity also vary between the seasons with highest intensities in summer and lowest intensities in winter. This comes from the fact that the sun is lower in the sky at solar noon[1] during low peak winter than in the high peak summer.

Therefore, the mean value used will give a too small solar field area during winter to be able to reach the assumed capacity factor. In summer, the required area to reach the needed capacity factor will be smaller than this average value found in the analysis, therefore excess heat will be produced by the solar field which makes it possible to approach a 100% capacity factor during summer.

If one would like to have a capacity factor of 80% during the lowest irradiations in winter we must first find the amount of energy received during the day in this period. A quantity that is often used for solar installations are the low peak sun hours. The low peak sun hour is defined to be the average amount of direct beam energy striking a surface during a day at the period with the lowest daily solar irradiation. It describes how many hours with 1000W/m^2 the total energy between sunrise and sunset represents. Since the annual irradiation per square meter is 2800kWh/m^2 at our specific cites in Africa, the average daily irradiation is $\frac{2800kWh/m^2}{365} \sim$ 7,7 kWh/day/m^2. This corresponds to $7,7$ peak sunhours on average per day. The low peak sun hours will be a number below this and the high peak sun hour will be a number above.

Lets denote the low peak sunhours with sunhour$_{low}$ and the high peak sun hours with Sunhour$_{high}$. sunhour$_{low}$ < sunhour$_{high}$

The needed solar field area to reach a given number of full load storage hours, denoted by

[1] solar noon is the time of day when the sun is at its highest in the sky

t, during the lowest irradiation period (in December) will be

$$A_{december} = \frac{kW_{peak} * t}{\eta_{sse} * 1000W/m^2 * sunhour_{low}} \tag{9.1}$$

This area will be dedicated for charging the storage system.

In summer, the required solar field area will be smaller due to more solar radiation per square meter. The area needed will be

$$A_{june} = \frac{kW_{peak} * t}{\eta_{sse} * 1000W/m^2 * sunhour_{high}} \tag{9.2}$$

The excess solar field area during the high peak sun hour (in june) will be

$$A_{excess} = A_{december} - A_{june} = \frac{kW_{peak} * t}{\eta sse * 1000W/m^2}[\frac{1}{sunhour_{low}} - \frac{1}{sunhour_{high}}] \tag{9.3}$$

We have now only accounted for the solar field area required for charging the storage system. The solar field area required for production of electricity during sunlight must also be added. This will also define the needed number of storage hours, t, defined earlier. This is a litte more complicated since the production of power is dependent on the instantaneous power received from the sun. The intensity of the sun will be lower in the beginning of the day and in the end of the day since the sun then is lower in the sky and the airmass the sunbeams must travel through is high.

Lets say the value where the intensity is high enough to give maximum power output during winter to be the average intensity between sunrise and sunset. We denote this average incoming power during sunlight with I_{avg}. Based on this, the needed solar field area for direct production of peak load power during sunshine wil in december be:

$$A_{prodlow} = \frac{kW_{peak}}{I_{avg} * \eta_{tot}} \tag{9.4}$$

Since we are using the average here, it is clear that there will be periods with lower intensity early in the day and in the end of the day,and a period wth intensity above the average in the middle of the day. Therefore, the solar field will produce less power before and more power after this average have been passed.

The difference are illustrated in Figure 9.1

I_{avg} is defined mathematically to be

$$I_{avg} = \frac{1}{sunset - sunrise} \int_{sunrise}^{sunset} I(t)\, dt \tag{9.5}$$

where sunset - sunrise defines the number of hours with daylight.

In the $2 * t_{below}$ hours the intensity is below this average, it is possible for the solar field area dedicated for charging the storage system to contribute to the power production. In the t_{above} hours the intensity is above the average, the solar field dedicated for power production can contribute to the storage system. In practice this will work smoothly since there are no real separation between the fraction that contributes to charging of storage system and the fraction that contributes to electric power production. The $2 * t_{below}$ and t_above can be

Figure 9.1: Difference in intensity between the lowest period in december and the highest period in june. I_{avg} is the average intensity striking a surface in the lowest period in december, t_{below} is the number of hours where the intensity is below this average right after sunrise and right before sunset. t_{above} is the number of hours the intensity is above the average in december.

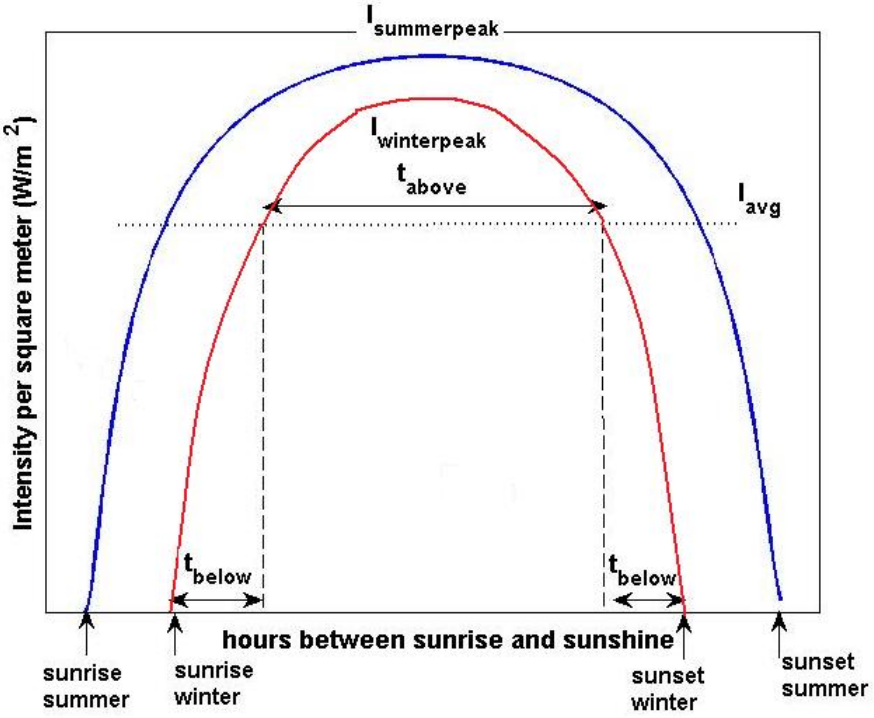

modified by changing the intensity that defined $A_{prodlow}$, I_{avg}, such that the power production is at peak load during the whole day and the storage system is fully charged during the course of the day. Further, we observe that the total energy received in the summer are higher than in winter. The area between the two graphs represents this excess energy. The capacity factor will increase due to the higher number of hours that are above the average winter intensity. The needed number of storage hours to reach the designed capacity factor will be lower due to more hours of sunshine. Therefore, the capacity factor might exceed 100% in the peak period, depending on the capacity factor the solar field is designed for during winter, and how large the diffference between the low peak and high peak are. If it exceeds 100%, there will be some dumping of thermal energy collected in the solar field. An alternative to dumping would be an oversized turbine to use the excess heat to produce electricity for local cooling needs which is of particular interest in the hot climate in Africa during summer. However, oversizing the power turbine too much will reduce the turbine efficiency when it operates below design capacity, compromises must therefore be made. It would also be possible to have a turbine available in reserve to take care of the excess heat during summer.
See Appendix E for more details on how to determine the solar radiation.

We can do an example calculation to see how the needed solar field area could increase relative our average-based calculation in Chapter 8, to have a minimum capacity factor of 80% during the period with lowest radiation. Lets say that $sunhour_{low}$ is 5,5 hours in december. Furthermore, we assume that I_{avg} equals 800 W/m^2, and the number of hours that the

intensity is above this average is $t_{above} = 6$ hours during this low peak period. To reach a 80% capacity factor will therefore require 13 hour of storage. (instead of 11 which we assumed in our model) We find then, for a 250 MW peak load turbine that

$A_{prodlow} \sim 2{,}1$ km^2 and $A_{december} \sim 4{,}2$ km^2, which gives a total of 6,3 km^2 . The solar field area based on the annual radiation averaged evenly over the year was found to be $\sim 4{,}5$ km^2, so with these example numbers the needed solar field must be increased with 40% to reach a 80% capacity factor during december.

Since Spain is located farther north, the difference in daylength between summer and winter are higher here (9 hour daylength in December and 15 hour daylength in June). Because of this a larger fraction of the energy must come from storage than in the north african countries.

9.1 Exploiting negative correleations between wind and solar power

Having said all this, it is not necessarily a problem that more solar power is being produced in the summer than in the winter. If the before mentioned negative correleation between solar power and wind power can be exploited it is possible that the European energy security can be maintained by producing more wind power within Europe during winter. It would also be possible to combine windpower and solar power production in Northern Africa to even out the differences between winter and summer. This way the transmission lines could reach a higher utilization factor in winter months without having to oversize the solar field to fit winter conditions. This approach would possible also be more economical as the LEC for wind currently are lower than the LEC for solar.

Chapter 10

Conclusion

This thesis has given an overview of the challenges related to storage and transfer of solar energy, with a case study on long distance power transfer, we can conclude with the following:

In the years between 1991 and 2006, no commercial concentrated solar power (CSP) plant was constructed. However, due to new renewable-friendly incentives in Spain and the USA, investors have again opened up their eyes for CSP. Three new parabolic trough power plants have already been built and more are in the construction phase. It will be important for the future development of the CSP industry and technology that this trend continues, as high deployment rates and an increase in plant size are effective paths towards cost reductions.

CSP is the only technology relying on an intermittent power source that have technology available for the implementation of economical feasible large scale energy storage systems. This makes it possible for CSP in favourable locations with a stable high incident solar radiation (insolation) to provide base load power with high capacity factor throughout the year. However, the only commercialized storage system for CSP today is an indirect two-tank system with molten salt as storage fluid and synthetic oil as heat transfer fluid (HTF). This system is material intensive and has a high cost. Also, the relatively low temperature of the synthetic oil puts an upper limit for the power block efficiency. One should therefore look for an alternative system. Currently there are two alternatives to the indirect two tank system; The first is the single tank thermocline system which uses less storage volume and at a lower cost. The thermocline system has been proven to work in test facilities, but not yet been commercialized. The second alternative is a plant with direct steam generation (DSG), integrated with a steam storage system or a storage system based on phase change materials. The DSG system with integrated storage is still under development and a fully working test plant has not yet been constructed.

Up to now, it has been the parabolic trough plant which has been the CSP technology of choice. It is possible that the construction of large scale central receivers will give efficiency improvements due to the higher temperature that can be reached. The less complex piping system combined with the high achievable temperatures make it possible to use the state of the art two-tank storage system with a direct approach, where the molten salt can be used both as a HTF and as a storage fluid without the risk that the molten salt freezes during night time. This can improve the overall efficiency by avoiding the oil-to-salt heat exchangers and increasing the steam temperature in the power block.

We have also noticed that with the high concentration ratios that can be achieved for parabolic dishes and central receivers, production of Hydrogen is possible through two-step thermochemical cycles. Of particular interest are the metal oxide based cycles which potentially can let the hydrogen producing step proceed without direct solar exposure.

In a case study, it has been demonstrated that it is in principle possible for Europe to maintain its energy security in a 100% RES (Renewable energy sources) pathway, where nuclear power and CCS coal and gas plants are replaced by CSP plants in Northern Africa. The electricity can be transmitted to Europe through HVDC transmission lines. It might be problematic to find available transmission paths for the relative high number of transmission lines which is required. Populated areas and difficult terrain wil put restrictions on where the transmission paths can be laid. The CSP plants in North Africa could deliver power to Europe with an $\sim$ 80% annual capacity factor. A stable capacity factor throughout the year could be achieved, but this would require a further oversizing of the solar field and an increase in storage capacity to account for shorter daylengths and less insolation during winter months. In this case it would be produced excess heat during summer which could be used to provide electricity for local cooling needs which is of particular interest in the hot summerclimate in North Africa.

To maintain the energy security for an electric grid where a large fraction of the power is based on intermittent power sources, big changes in the grid are required. It is crucial that the European grid is being developed into a supergrid where geographical distant regions is connected together through HVDC interconnections with high capacity. Also here it will be issues related to deployment of transmission lines through populated areas, more expensive underground cables will here be an alternative for the overhead lines. The development of the supergrid will also be important if a large fraction of the energy supply comes from base load CSP plants in North Africa.

Appendix A

Photovoltaic power

[1] The photovoltaic (PV) cells are made of semiconductors, and the most common material in use today are silicon. An atom of silicon has 14 electrons, arranged in three different energy shells. The outer shell is the important one. In silicon, this shell is only half full, having four electrons, called the valence electrons. To fill it up with the four missing electrons, each silicon atom interacts with four of its neighbour silicon atoms, and this process is whats forms the crystalline structure of silicon. Because of this structure, the electrons can't move freely around, and thus pure silicon is not a good conductor. However, there is one method to improve the conductivity, called "doping".

A solar cell consists of several different components placed in layers on top of each other. The two parts where the photovoltaic effect takes place are called the p-type and the n-type semiconductor. In the production of these two layers, silicon vapor is doped with impurities of other atoms.

A.1 p-type semiconductor

To form the p-type semiconductor, the semiconductor is doped with atoms with fewer valence electrons than the atoms in the semiconductor material. To make p-type silicon, for instance, one dopes it with Boron which has only three valence electrons. As a concequence of this, there will, in the p-type silicon, exist crystalline structures that contain atoms with one electron less than the neighbouring atoms, resulting in holes for electrons outside to fill. So, instead of having free electrons, p-type silicon has free holes, and in that sense they carry a positive charge. Thus, we have a p-type semiconductor, where the "p" stands for positive.

A.1.1 n-type semiconductor

The electron economy is the other way around for the n-type semiconductor. Here the semiconductor material is doped with atoms having one more valence electron. In the case of silicon, phosphorous, with its five valence electrons, is the dopant of choice. The consequence of the doping is that there will exist crystal structures with one electron in excess. This extra electron will now be very loosely bounded to the crystalline structure, only held in place by a positive proton in the phosphorous nucleus. When the solar cell is hit by radiation, the photons can, dependent on their energy, knock this electron loose from its bond so that the

[1] the discussion in this appendix is based on the references [103],[104] and [105]

electron can move freely within the crystal and therefore contribute to an electrical current when an electric field is applied. The free electrons have negative charge and therefore this is called an n-type semiconductor.

The holes in the p-type semiconductor will move in the direction of the electric field and the electrons in the n-type semiconductor will move against the field. This is utilized when the two types are brought together in a p-n junction.

A.1.2 The p-n junction solar cell

For the free electrons to produce electricity, they must be separated from the material before recombination and directed into an electric circuit. To separate the electrical charges, the solar cell must have an electric field. The needed field can be produced by putting together the p-type semiconductor and the n-type semiconductor. When the two semiconductors are in contact, the free electrons on the n-side are rushing over to fill the free holes on the p-side. This results in a charge difference between the two semiconductors, with a netto positive charge on the n-side and a negative charge on the p-side, and an electric field is formed at the interface, the p-n junction. The p-n junction behaves like a diode and the netto movement of charges from one side to the other is known as the "dark current", dark because the current is there, even when no radiation from sun is present. The field at the junction is known as the built-in field and it forces the electrons to move towards the negative surface. This prevents them for recombining with the ionized atoms and instead making them available for the electrical circuit. At the same time, the holes move in the opposite direction, towards the positive surface, where they are waiting for new electrons to be released by the incoming photons.

Appendix B

Radiation theory

B.0.3 Planck's law

A Black Body is an object that absorbs all electromagnetic radiation incident on it. In practice, a black body can be approximated by a cavity where the incoming radiation is in thermal equillibrium with the radiation emitted fromt he cavity walls. An object is in thermal equillibrium with its surroundings when the rate of absorption equals the rate of emission, the temperature will then be constant. This constant temperature is called the stagnation temperature of the object.

Black bodies absorb and emit thermal radiation in a characteristic spectrum called the Black body radiation spectrum. This spectrum is described by Planck's law

$$I(\nu, T) = \frac{2\pi h\nu^3}{c^2} \frac{1}{exp[\frac{h\nu}{kT}] - 1} \tag{B.1}$$

I is the intensity of the radiation per unit area per unit frequency, ν is the frequency, T is the absolute temperature of the black body surface, c is the speed of light, h is Planck's constant and k is Boltzmann's constant.

The distribution was found by Max Planck in 1900. By assuming that the emitted radiation energy was a discrete variable with values $E_n = nh\nu$, Planck found a ditribution that agreed with observation. [106] Before his discovery, classical physics could not explain observations related to the spectral distribution. The disagreement between theory and observations was called the ultraviolet cathastrophe.[1]

B.0.4 The Stefan-Boltzmann law

The Stefan-Boltzmann law says that the total intensity radiated per unit area from a black body is entirely dependent on the absolute temperature, to the forth power of the black body surface temperature[2].

Stefan-Boltzmann's law can be found by integrating the intensity I from Plancks law over all frequencies:

[1] It refers to the significant disagreement between experimental measurements of I and the predictions from classical physics at short wavelengths. Planck's quantization of the energy solved the disagreement and at the same time laid the fundament of further development into what was later called quantum mechanics

[2] The law was first found empirically by Josef Stefan in 1879 and then derived from classical thermodynamics by Ludvig Boltzmann four years later

$$P = \int_0^\infty I(\nu, T)\, d\nu = \sigma T^4 \tag{B.2}$$

where, σ is Stefan-Boltzmann's constant.

Objects that do not behave like black bodies emit less power by a factor ϵ, known as the emissivity. Thus, for non-blackb odies we have

$$P = \epsilon\sigma * T^4 \tag{B.3}$$

where 0 ¡ ϵ ¡ 1

B.0.5 Planck's law as a function of wavelength

Plancks law can also be expressed in terms of the wavelength λ through the relation

$$\lambda = \frac{c}{\nu} \Longrightarrow d\nu = -\frac{c}{\lambda^2} d\lambda \tag{B.4}$$

P then becomes

$$P = \int_0^\infty I(\nu, T)\, d\nu = \int_0^\infty I(\lambda, T) * -\frac{c}{\lambda^2}\, d\lambda = \int_0^\infty \frac{2\pi c^2 h}{\lambda^5} * \frac{1}{exp[\frac{hc}{kT\lambda}] - 1}\, d\lambda = \int_0^\infty \hat{I}(\lambda, T)\, d\lambda \tag{B.5}$$

where

$$\hat{I}(\lambda, T) = \frac{2\pi c^2 h}{\lambda^5} * \frac{1}{exp[\frac{hc}{kT\lambda}] - 1} \tag{B.6}$$

represents the intensity per unit area per unit wavelength. The minus sign dissappeared in the integral above since the limits was reversed under the substitution. The total intensity over the entire surface can be found by integrating P over the entire surface of the black body.

In Figure B.1, $\hat{I}(\lambda, T)$ is plotted for T = 5780 K , which is the black body temperature for the sun. That is, the temperature of a black body that emits with the same intensity as the sun. The intensity distribution is also plotted for T = 300 K for comparision in the plot below.

The maximum values for the graphs show for which wavelengths the intensity peaks, and as the temperature increases the intensity peaks move to shorter and shorter wavelengths. This observation can be generalized for all temperatures, Wien's displacement law.

Figure B.1: The blackbody radiation spectrum for two temperatures as a function of wavelength

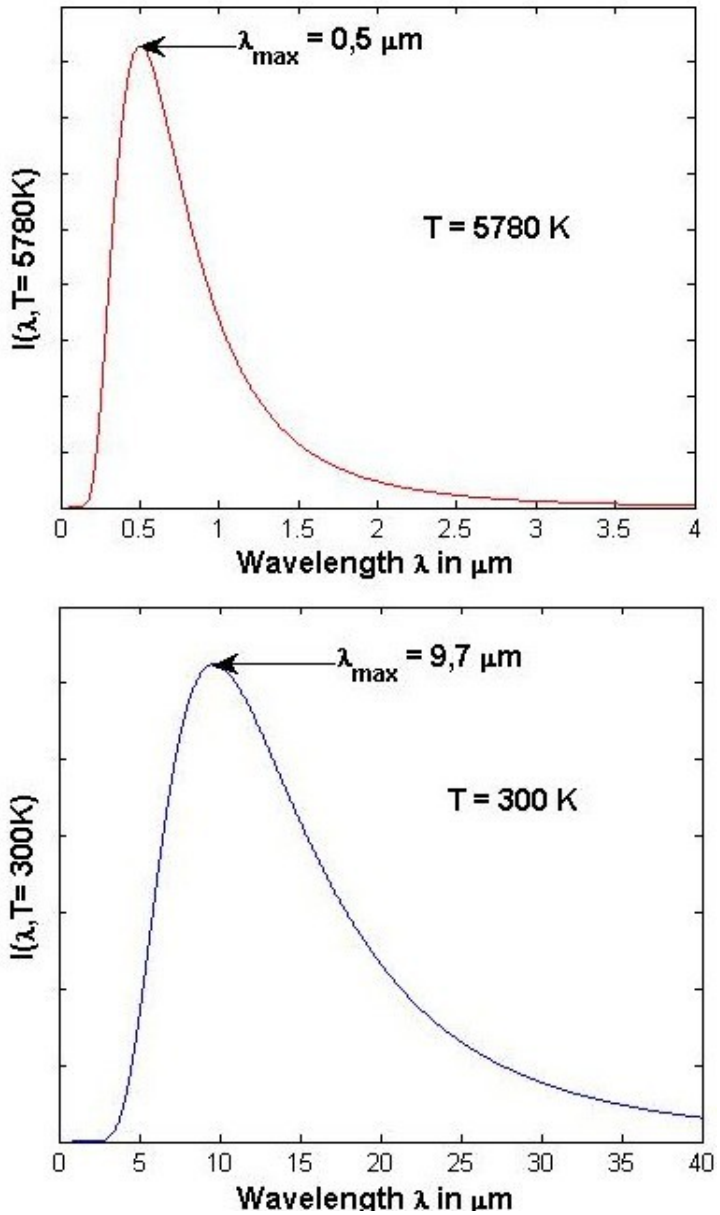

B.0.6 Wiens displacement law

Wien's displacement law gives a relation between temperature and the wavelength that gives the maximum radiation intensity from a black body. The law states that the intensity is at its maximum at a wavelength which is inversely proportional to the absolute temperature of the black body. The law can be found with the help from Plancks law.

Taking the derivative of Planck's radiation distribution $\hat{I}(\lambda, T)$ given by Equation (B.6) and setting it to zero:

$$\frac{d}{d\lambda}(\hat{I}(\lambda, T)) = 0 \tag{B.7}$$

followed by factorizing out common factors from the resulting expression, leaves us with the following expression

$$\frac{hc}{kT\lambda}\frac{exp[\frac{hc}{kT\lambda}]}{exp[\frac{hc}{kT\lambda}]-1} - 5 = 0 \tag{B.8}$$

By making the substitution x = $\frac{hc}{kT\lambda}$ Equation (B.8) becomes

$$\frac{xe^x}{e^x - 1} - 5 = 0 \tag{B.9}$$

This can be solved numerically and the solution is x = $4,9651$
The substitution above can then be solved for Tλ and we find

$$T\lambda_{max} = \frac{hc}{kx} = 2,898 * 10^{-3} Km \tag{B.10}$$

This is Wien's displacement law which states quantitatively how the maximum intensities are displaced towards shorter wavelengths when the temperature of a black body increase,

A illustration of the intensity distributions for T = 5780 and T = 300 is given in Figure B.2.

The graphs in Figure B.1 illustrate Wien's displacement law for black body temperatures representative for earth and sun. The intensities for the T = 5780 distribution are concentrated around shorter wavelengths. but the graph for T = 300 is displaced towards wavelengths in the infrared spectrum. We observe that the distribution for T = 5780 K decreases fast for longer wavelengths (around 3μm). We also observe that the distribution for T = 300 K, start increasing for wavelengths above 3μm. The fact that the graphs do not overlap significantly makes it possible to develop receivers/collectors with selective surfaces which have high absorption for wavelengths below the cutoff wavelength (in this case at around 3μm) and high reflectivity for the wavelengths above. This can effictively increase the stagnation temperature which will make a collector system more efficient.

To see how the maximum intensities in the plot in Figure B.1 really scales for different temperature we exploit the fact that $T\lambda_{max}$ is a constant. With the use of the substitution x defined above, $\hat{I}$ can be written

$$\hat{I} = \frac{2\pi c^2 h}{\lambda^5}[e^x - 1]^{-1} \tag{B.11}$$

we have $\lambda = \frac{hc}{kTx}$ so Equation (B.11) becomes

$$\hat{I} = \frac{2\pi k^5}{c^3 h^4} T^5 x^5 [e^x - 1]^{-1} = \beta T^5 f(x) \tag{B.12}$$

where $\beta = \frac{2\pi k^5}{c^3 h^4}$ = const and f(x) = $x^5[e^x - 1]^{-1}$ Since x is constant for $T\lambda_{max}$, f(x) is also a constant and we can conclude that The maximum intensities for two different temperatures will scale as T^5. The maximum intensity for T = 5780 K will therefore be a factor $\frac{5780^2}{300^2}$ $2.6548 * 10^6$ higher than the maximum intensity for T = 300 K

We may divide the black body spectrum into three parts; the ultraviolet, visible and the infrared spectrum. We can then calculate the fraction of the total intensity for each of the three parts. The fraction we are looking for is

$$Fraction = \frac{\int_{\lambda_1}^{\lambda_2} \hat{I}(\lambda, T)\, d\lambda}{\int_0^{\infty} \hat{I}(\lambda, T)\, d\lambda} \tag{B.13}$$

where $[\lambda_1, \lambda_2]$ is the range for each part. The range and the resulting fraction for the black body temperature for the sun (T = 5780 K) is summarized in the table below

Spectrum	Range (nm)	Fraction (%)
Ultraviolet	0 - 380	10,8
Visible	380 - 760	47,7
Infrared	760- ∞	41,5

In Figure B.3 , the black body spectrum from the sun are divided into the parts given above

Figure B.2: Black body radiation spectrum for the sun (T = 5780) divided into Ultraviolet(UV), Visible and Infrared(IR)

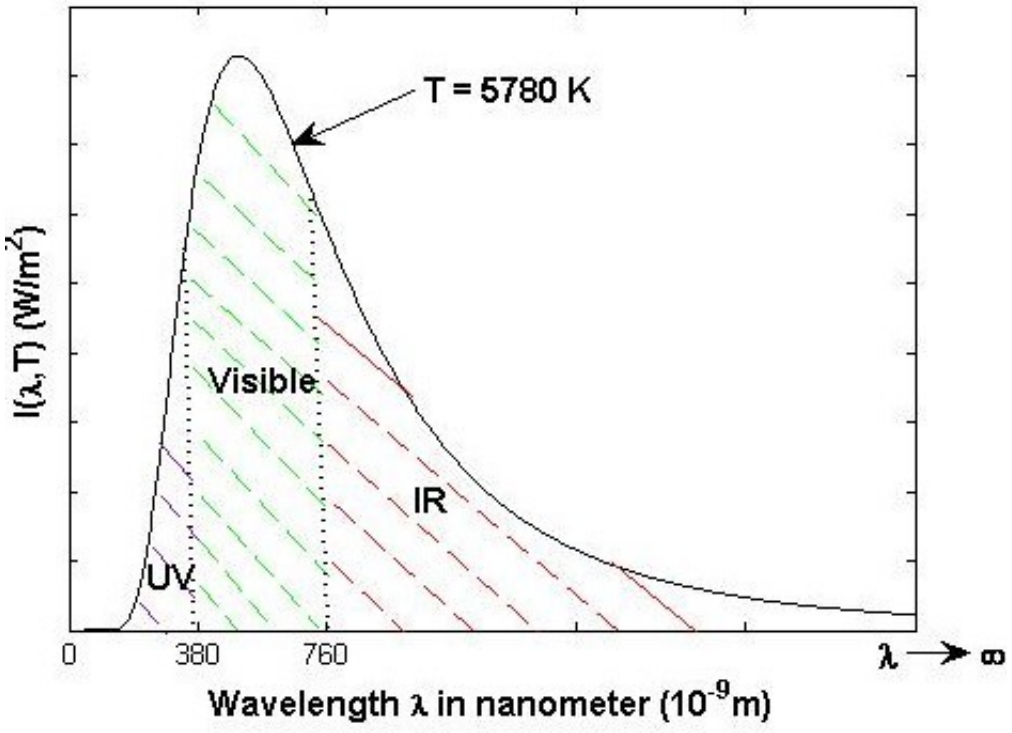

Information in this appendix was mostly found from [12]

Appendix C

Faradays law

In 1831 Faraday in a series of experiments, one involving moving a magnet across a wire, and one involving changing the strength of the magnetic field with both magnet and wire at rest, found that a changing magnetic field induces an electric field.

Before stating his law we must define some important concepts

C.0.7 Electromotive force

The emf is the electromotive force that drive current around a loop. It is defined as the line integral of the force (per unit charge) around the circuit.

$$\epsilon = \oint \vec{f} \cdot d\vec{l} \tag{C.1}$$

It can be shown in general that whenever (and for whatever reason) the magnetic flux through a loop changes, an emf ϵ = - $\frac{d\phi}{dt}$ will appear in the oop, where ϕ is the flux of the magnetic field $\vec{B}$ going through the loop:

$$\phi = \int \vec{B} \cdot d\vec{a}\, dx. \tag{C.2}$$

where $d\vec{a}$ is an infinitesimal area element of the loop. This is known as the universal flux rule.

In the experiments Faraday conducted, it was an induced electric field that generated the emf, therefore we must have:

$$\epsilon = \oint \vec{E} \cdot d\vec{l} = -\frac{d\phi}{dt} \tag{C.3}$$

when inserting Equation (C.2) into Equation (C.4) we obtain

$$\epsilon = \oint \vec{E} \cdot d\vec{l} = -\int \frac{d\vec{B}}{dt} \cdot d\vec{a} \tag{C.4}$$

this is Faradays law in integral form

Assuming now that we have two loops of wires at rest separated from each other. By running

a steady current I_1 around loop 1 a magnetic field $\vec{B_1}$ is produced (By ampere's law). Some of the magnetic field lines will pass through loop 2, giving rise to a flux ϕ_2 of $\vec{B_1}$ through loop 2. According to Biot-Savart law, the B-field caused by the current I will be proportional to the current. Therefore, the flux ϕ_2 must also be proportional to the current I_1: $\phi_2 = MI_1$, where the constant of proportionality is called the mutual inductance of the two loops.

Now, if we change the current I_1 in loop 1, ϕ_2 will change. Faraday's law then says that this changing flux will induce an emf in loop 2:

$$\epsilon = -\frac{d\phi}{dt} = -M\frac{dI_1}{dt} \tag{C.5}$$

This emf generates a current in loop 2. So, despite the fact that the wires are not connected to each other, a current will flow in loop 2 everytime the current is changed in loop 1.
The changing current in loop 1 will also induce an emf in the source loop itself. The field and therefore also the flux, will again be proportional to the current generated by the emf: $\phi =$ LI, where the constant of proportionality L is the self inductance of the loop. L is measured in Henry (H) 1 H = 1 Vs/A.
From this basic physics it is possible to explain the basic principles of how a transformer works.

C.0.8 The ideal AC transformer

The basic transformer is constructed by winding two wires (coils) around an iron core. The wire where the alternating current is introduced is called the primary coil, the other, outgoing wire is called the secondary coil. the alternating current through the primary coil will induce a changing magnetic field in the iron core. According to Faradays law, the changing flux from the magentic field will induce an electric field in the secondary coil, and this electric field generates an emf.

It is possible to have a transformator with air between the coils, but the Iron core can produce a much stranger magnetic field, and helps concentrate the flux so that the same flux passes through ech winding.

By assuming that the same flux passes through every winding of both coils we can find a relation between the voltage and the number of windings. We assume that the primary coil has N_p windings and the secondary coil has N_s windings. From Faraday's law we get

$$\epsilon_p = -N_p\frac{d\phi}{dt} \; and \; \epsilon_s = -N_s\frac{d\phi}{dt} \tag{C.6}$$

where ϕ is the magnetic flux through one winding of the coil. We can from these two equations find the ratio of the emfs:

$$\frac{\epsilon_s}{\epsilon_p} = \frac{N_s}{N_p} \tag{C.7}$$

since the voltage V = - $\int \vec{E} \cdot d\vec{l}$, and the induced electric field is what causes the emf, ϵ can be interpreted as the work done per unit charge and is therefore equal to the voltage across the circuits, therefore

$$\frac{V_s}{V_p} = \frac{N_s}{N_p} \tag{C.8}$$

Figure C.1: A transformer which takes an input AC voltage of amplitude V_p in the primary coil, and delivers an output voltage of amplitude V_s in the secondary coil. [107]

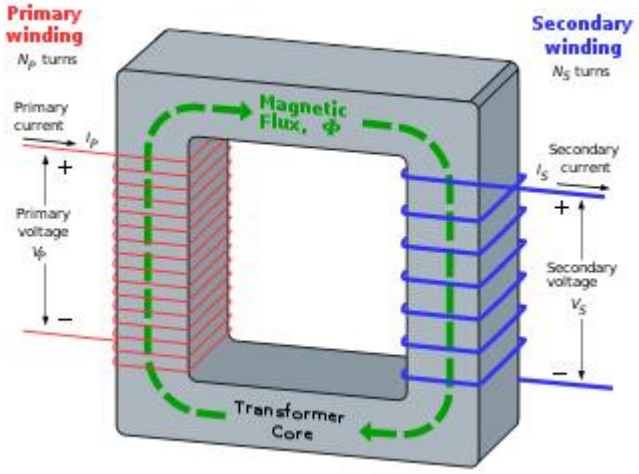

The voltage can be stepped up if $N_s > N_p$ and stepped down if $N_s < N_p$.

An ideal transformer will not loose any energy and therefore all the incoming energy is transferred from the primary coil to the magnetic field and into the secondary coil. The incoming power in the primary coil must therefore equal the outgoing power in the secondary coil.

$P_p = V_p I_p = V_s I_s = P_s$

If the voltage is stepped up in the secondary coil, the current must go down to not violate concervation of energy, and this is what actually happends in the transformer. Since the current go down by stepping up the voltage, the ohmic transmission losses in the transmission line decreases as the square of the current. This is why it is so important to step up the voltage before transmitting power over long distances.[1]

Basically, the power company generators produce electricity by rotating 3 coils or windings through a magnetic field within the generator. These coils or windings are spaced 120 degrees apart. As they rotate through the magnetic field they generate power which is then sent out on three 3 lines (three-phase power). Three-Phase transformers must have 3 coils or windings connected in order to match the incoming power and therefore transform the power company voltage to the level of voltage needed for long distance transmission.

[1]The derivations in this appendix is taken from [84]

Appendix D

Concentration ratio

Since the sun is not an idealized point source, the sunrays hitting earth are not parallell. For this reason, the sun rays hitting an idealized paraboloid will not be reflected onto a singular point (the focal point), but rather produce a circular image centered at the focal point. The diameter d of this circle can be given in terms of the rim angle ψ_{rim}, the focal length f and the angular diameter θ_s of the sun seen from earth:[62]

$$d = \frac{f\theta_s}{cos\psi_{rim}(1 + cos\psi_{rim}} \tag{D.1}$$

The rim angle is defined to be the angle the rim of the concentrator are making with the focal point (the focal line for the parabolic trough, as seen in picture below)

Figure D.1: For a linear concentrator, the rim angle ψ_{rim} are defined to be the angle rim of the concentrator are making with the focal line[108]

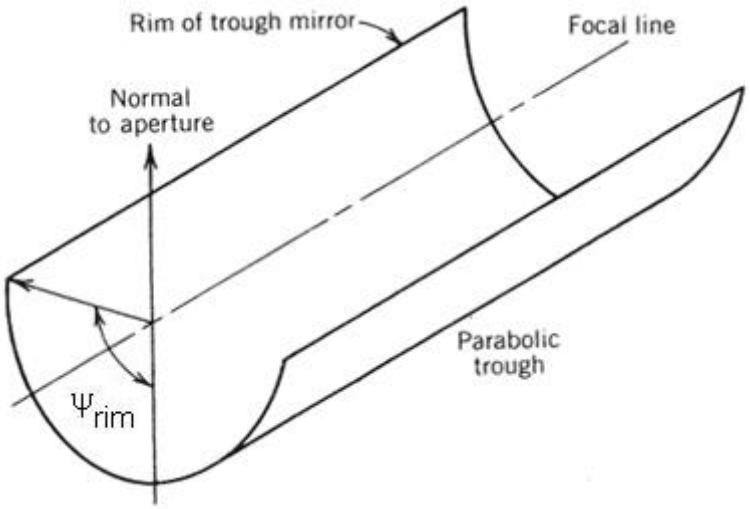

The angular diameter of the sun seen from earth can be approximated by the actual diameter (radius times two) of the sun divided by the distance between earth and sun, R.

Figure D.2:

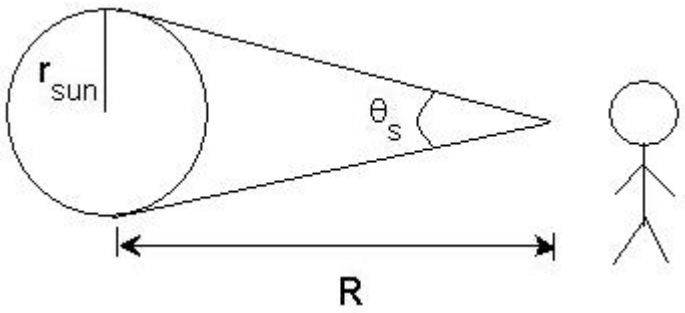

From the picture we find that

$$tan(\frac{\theta_i}{2}) = \frac{r_{sun}}{R} \tag{D.2}$$

the angular diameter is therefore (for R ¿¿ r_{sun})

$$\theta_s = 2 * tan^{-1}(\frac{r_{sun}}{R}) \sim \frac{r_{sun}}{R} \tag{D.3}$$

Plugging in values for the mean sun-earth distance R and the radius of the sun (center-photosphere distance) we find that $\theta_s \sim$ 0,0093 rad $\sim$ 0,50°.

with a rimangle 45° and focal length of 25 meter the diamter of the circular image can be found from Equation (D.1): d $\sim$ 0,2 meter.

the receiver surface must therefore have at least this size to capture all the incoming radiation.

D.0.9 The concentration ratio

The angular diamter of the sun will also put an upper limit on the thoretical possible concentration ratio.

The concentration ratio is defined in two different ways

the optical concentration ratio C_{opt} is defined to be the averaged radiation flux I_r on the receiver integrated over the receiver area A_r, divided by the insolation incident on the mirror area of the concentrator:[108]

$$C_{opt} = \frac{\frac{1}{A_r}\int I_r \, dA_r}{I_a} \tag{D.4}$$

The geometric concentration ratio C_g are defined to be the concentrator area A_c divided by the receiver area A_r:

$$C_g = \frac{A_c}{A_r} \tag{D.5}$$

Sine many receivers are larger than the concentrated solar image, the geometric concentration are often preferred since it better can account for heat losses in the receiver. If the

irradiance is uniform over the entire receiver area, the optical and geometric concentration ratios are equal.

We will now find the upper limit for the concentration ratio for an ideal paraboloid.

The maximum theoretical concentration ratio for an ideal paraboloid is achieved when

We consider a paraboloid at distance R away from sun. The concentrator has area A_c and the receiver has area A_r [109]

Figure D.3:

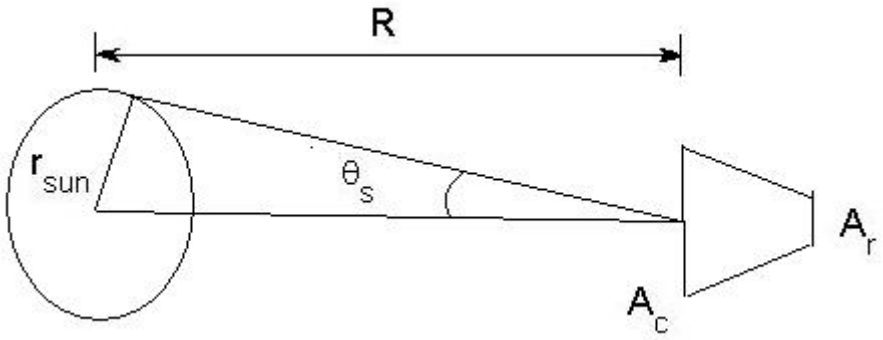

For the ideal case the energy Q_{s-r} from the sun on the receiver is the fraction of radiation emitted by the sun hitting the concentrator area. Assuming sun is a black body we have

$$Q_{s-r} = \frac{4\pi {r_{sun}}^2}{4\pi R^2} A_c \sigma {T_s}^4 = \frac{r_{sun}}{R^2} A_c \sigma {T_s}^4 \tag{D.6}$$

An ideal black body receiver radiates energy according to Stefan-Boltzmann: $A_r \sigma {T_r}^4$, where T_r is the receiver temperature. This energy will be the maximum energy that can be reradiated back to the sun so we denote it by Q_{r-s}. When T_s and T_r are equal, we must have

$$Q_{s-r} = Q_{r-s} \Longrightarrow \frac{r_{sun}}{R^2} A_c \sigma {T_s}^4 = A_r \sigma {T_r}^4 \tag{D.7}$$

The result is[1]

$$\frac{A_c}{A_r} = \frac{R^2}{{r_{sun}}^2} = \frac{1}{sin^2(\frac{\theta_s}{2})} = C_{max} \tag{D.8}$$

Putting in the angular diamter of the sun we find $C_{max} \sim 46000$

For linear concentrators it can be shown that the maximum concentration ratioa are

$$C_{lin} = \frac{1}{sin(\frac{\theta_s}{2})} \sim 212 \tag{D.9}$$

From this we see that the linear concentrators such as the parabolic troughs have significant lower maximum concentration ratio than the paraboloids (Parabolic dishes).

[1]This result can also be derived form basic optical principles, see for example [110]

Since this theoretical maximum only applied for one single concentrator unit, It is possible to exceed the theoretical maximum with systems where more than one concentrators are working together.

Appendix E

Deterministic and stochastic dependencies on solar radiation

The determination of I_{avg}, t_{below}, t_{above}, $sunhour_{low}$ and $sunhour_{high}$ defined in Chapter 9 consist of a deterministic factor (given by the lattitude, date etc) and one Stochastic (non-deterministic) factor.

The deterministic factor can be fully determined by calculating the radiation striking a horizontal surface relative earth at the top of the atmosphere. It is possible to determine this radiation at any instant of time at any location to a very high degree of accuracy. The way it is done is to express the direction of the sunrays through a set of different angles which vary with time and location.

The daily extraterrestial solar radiation striking a surface parallell to the earth is given by

$$E_h = \frac{86400 \times S}{\pi}(\omega sin\phi sin\delta + cos\delta cos\phi sin\omega) \tag{E.1}$$

Where the angles are defined as

- ϕ: the lattitude, defined as positive on the northern hemisphere
- δ: the declination: the angle between the line drawn from the center of the earth to the sun and the earth's equatorial plane is called the declination angle
- ω: the hour angle is the angular distance between the meridian of the observer and the meridian whose plane contains the sun. The hour angle is zero at solar noon since the meridian plane of the observer contains the sun. The hour angle increases by 15 degrees every hour.

More details about the angles can be found in [12] or in [108]

A plot of Equation (E.1) is given in Figure E.1.

We see that the variations between the seasons are lowest at equator (0°). Algeria, Libya and Egypt is located around 25° latitude , close to the tropic of cancer where the sun is directly overhead at solar noon in june. Spain is located at around 40° (see Figure E.2) latitude

Figure E.1: The variation in daily radiation as a function of the angle the sun is making with a horizontal surface relative earth [108]

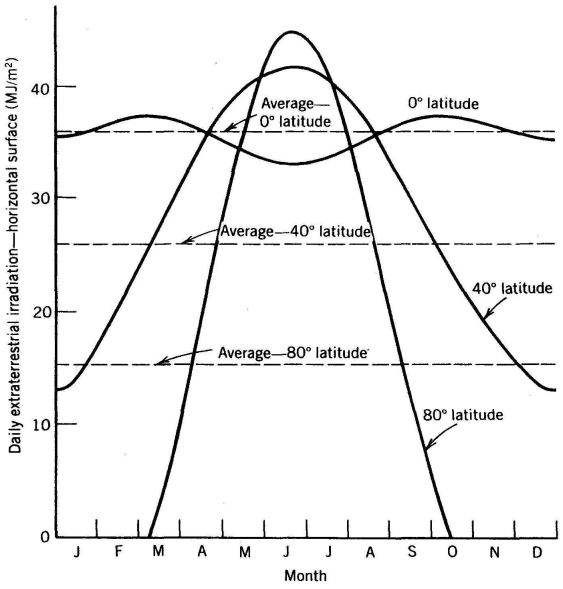

and we see how strongly the radiation vary with the seasons.[1]

Figure E.2: Map of the world with latitudes

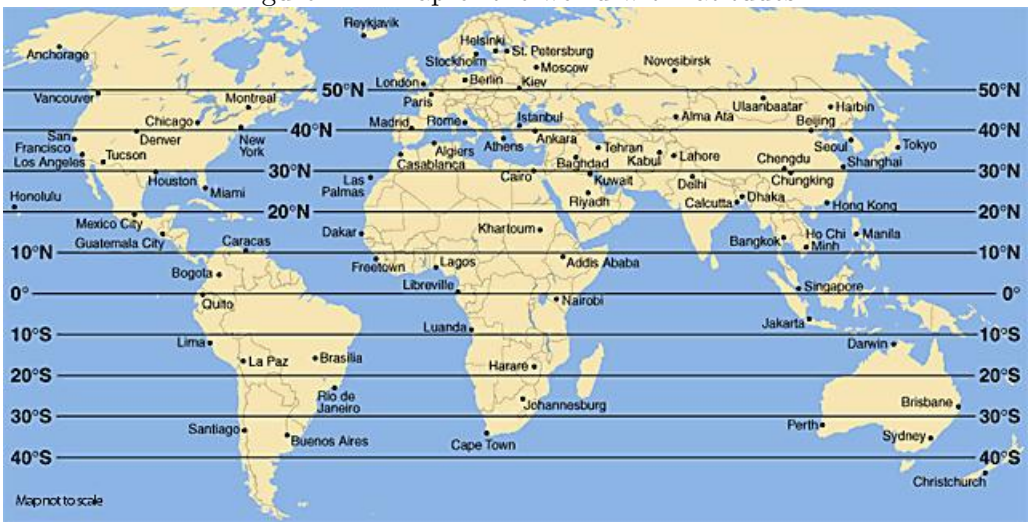

The Stochastic factor is dependent on the local weather and athmospheric variations, especially the degree of cloudiness. Clouds will significantly decrease the amount of direct beam radiation and increase the amount of diffuse radiation which is of no use for the concentrators.

[1]Note that the figure shows the radiation hitting a horisontal surface relative earth. Since the collectors in the solar field can track the sun, the varations in latitude will be less than what is seen here. However, the angle the sun is making with the vertical also describes how much air mass the sunrays must go through, and the airmass is independent on whether the surface is perpendicular to the sun rays or not.

The degree of cloudiness is given by the clearness index C , (it is usually denoted by K but I have used this letter for the capacity factor). The Clearness index is usually given as an average over a time interval, often a month. It is defined as the ratio of the observed insolation H at a location and the maximum theoretical insolation, H_0, at the same location, that is the insolation that would be observed if the sky was clear the whole time interval:

$$C = \frac{H}{H_0} \tag{E.2}$$

The North African countries have an annual clearness index that vary between $0,55$ and $0,91$[24].

Since the parabolic troughs track the sun by rotating along only one axis (north-south axis on the northern hemisphere) they cannot be directed directly towards the sun at all times during the day, therefore, the direct beam radiation per square meter of concentrator is given as

$$I_{direct} = I_n cos\theta_i \tag{E.3}$$

where I_n = is the direct beam radiation at normal incidence and θ_i is the angle the sun rays makes with the normal of the concentrator surface. θ_i for systems tracking the sun in a north south axis is small during summer but have greater varations in winter. [108]

As mentioned earlier, the intensity of this direct beam radiation also vary throughout each day as a funcion of the air mass. This variation with the air mass can be described by the empirical equation [111]

$$I_n = S * Albedo^{AM^{0.678}} \tag{E.4}$$

Multiplying it with the clearness index C and combining with Equation (E.5) gives

$$I_{direct} = S * (1 - albedo)^{AM^{0.678}} * C * cos\theta_i \tag{E.5}$$

where S = 1367W/m^2 is the solar constant, Albedo = 0,3 is the reflectance at the top of the atmosphere and AM is the air mass. The air mass can be given as a function of the solar azimuth angle θ_z by the empirical formula:[108]

$$AM = \frac{1}{cos\theta_z + 0.50572(96,07995 - \theta_z)^{-1.6364}} \tag{E.6}$$

Assuming for the ideal case that $\theta_i \sim 0$, and C = 1 , we can plot the irradiation as a function of the solar azimuth angle using Equations (E.5) and (E.6).

Figure E.3: Direct beam radiation towards the concentrator surface as a function of the solar azimuth, assuming $\theta_i = 0$ and C = 1. Negative azimuth angles is here the angles the sun is making with the vertical before midday

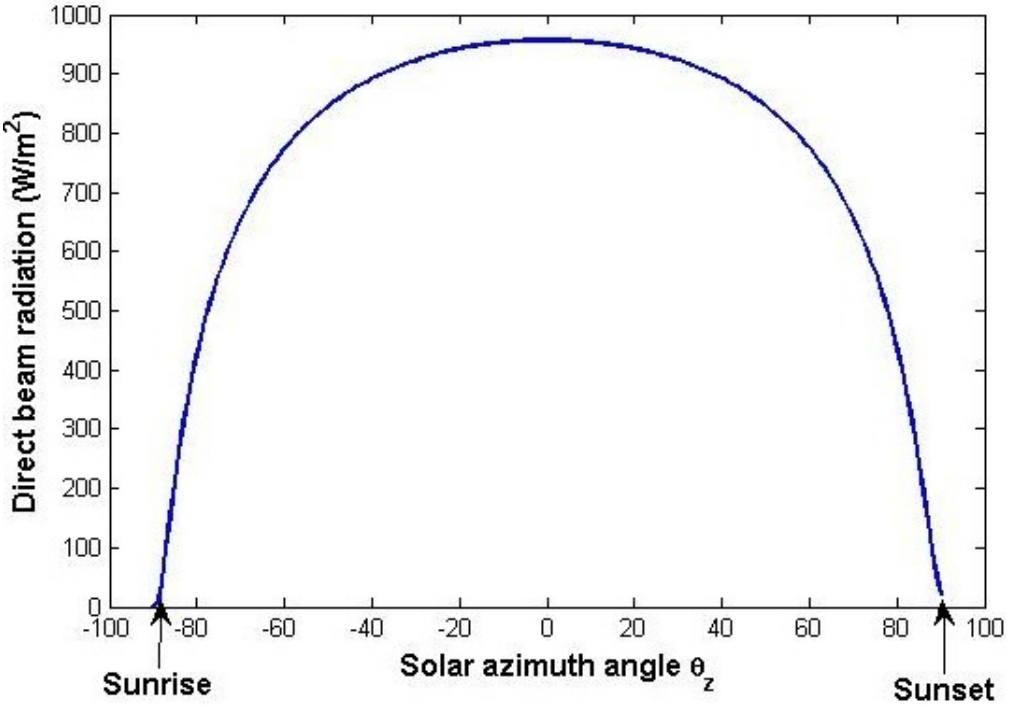

The solar azimuth angle is given in degrees. We observe that the direct beam radiation is relatively stable between the interval -60° ¡ θ_z ¡ 60°. The peak is at airmass 1 (AM1 (when $\theta_z = 0$)) and here the intensity is $\sim$ 950 W/m^2.

Note that this plot is only representative for the period when the sun is directly overhead at solar noon (This happends in june at 23,5° latitude and never happends at latitudes north for 23,5°). For regions located north of 23,5° the peak will be lower. Since the north African countries are very close to the 23,5° latitude, the plot is a good representation in summer for these countries (assuming clearness index C = 1)

Appendix F

Pictures of the recent built plants in Spain and the U.S

Figure F.1: The Andasol 1 plant in front and the Andasol 2 plant up to the left. The andasol 3 plant will be constructed in the region to the right in the picture.togheter they will have a solar field area of around 1,5 km^2 The storage system and the powerblock is located in the middle of each solar field. Notice how small the storage system and the power block are in comparision with the solar field. [112]

Figure F.2: A closer picture of the indirect two-tank storage system at Andasol. The system have a thermal capacity of 1050 MWh, enough for 7,5 hours of full load power production (50MW) [113]

Figure F.3: A closer look at the parabolic troughs which collects the solar energy and focus it on the receiver tube filled with Heat Transfer fluid at the focal line. The location are Nevada solar one in Nevada, U.S [114]

Appendix G

Transmission requirements for the 40% RES and 80% RES pathways

Figure G.1: Needed transmission capacities for the 80% RES pathway. numbers in parantesis represents the existing capacity. A 20% demand response is assumed

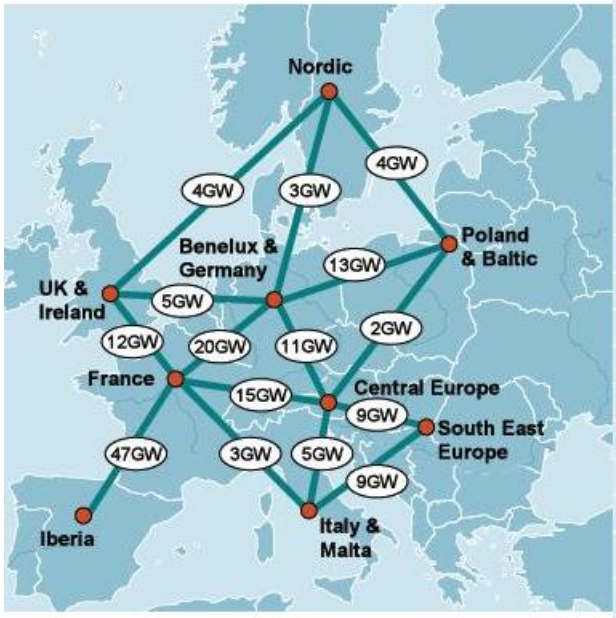

Interconnection	Capacity additional (existing) [GW]	Annual utilization [%]
UK&Ireland-France	10 (2)	78
UK&Ireland-Nordic	4 (0)	90
UK&Ireland-Benelux&Germany	5 (0)	81
France-Iberia	46 (1)	74
France-Benelux&Germany	14 (6)	77
France-Central-Europe	12 (3)	89
France-Italy&Malta	0 (3)	92
Nordic-Benelux&Germany	0 (3)	85
Nordic-Poland&Baltic	3 (1)	72
Benelux&Germany-Central-EU	7 (4)	68
Benelux&Germany-Poland&Baltic	12 (1)	82
Central-Europe-Poland&Baltic	0 (2)	72
Central-South East EU	7 (2)	76
Central-Europe-Italy&Malta	0 (5)	69
South East EU-Italy&Malta	8 (1)	74
Total	**127 (34)**	

According to [115] a 20% demand response result in a $\sim$ 24% reduction in transmission requirements. Still, with the optimization, we observe the substantial increase in transmission capacity between Spain and France which will be required in a 80% RES pathway. The annual utilization describes how much of the time during the year the transmission lines transfer power at full capacity. More details can be found in [115].

Figure G.2: Needed transmission capacities for the 40% RES pathway. numbers in parantesis represents the existing capacity. Also here a 20% demand response is assumed.

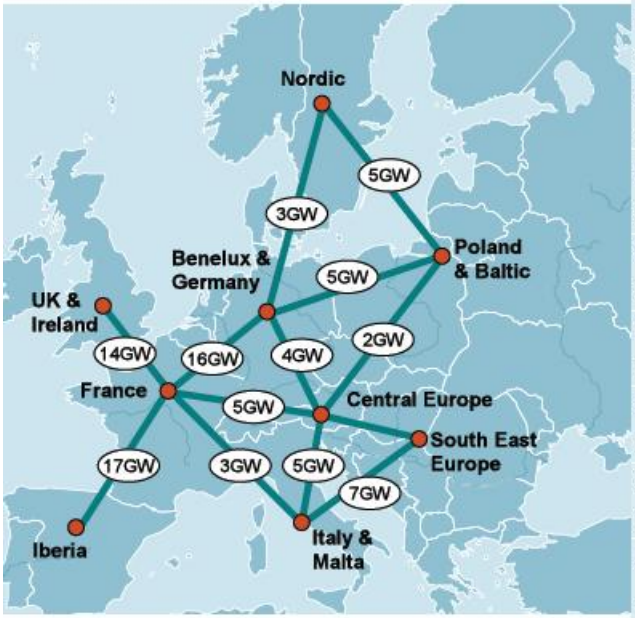

Interconnection	Capacity additional (existing) [GW]	Annual utilization [%]
UK&Ireland-France	12 (2)	85
UK&Ireland-Nordic	0 (0)	0
UK&Ireland-Benelux&Germany	0 (0)	0
France-Iberia	16 (1)	82
France-Benelux&Germany	10 (5)	91
France-Central-Europe	2 (3)	98
France-Italy&Malta	0 (3)	91
Nordic-Benelux&Germany	0 (3)	66
Nordic-Poland&Baltic	4 (1)	72
Benelux&Germany-Central-EU	0 (4)	46
Benelux&Germany Poland&Baltic	4 (1)	82
Central-Europe-Poland &Baltic	0 (2)	80
Central South East EU	0 (2)	54
Central Europe Italy	0 (5)	32
South East EU-Italy	6 (1)	80
Total	**55 (34)**	

The 20% demand response have negligible impact on transmission requirements for the 40% pathway. We obeserve that the 40% RES pathway requires 72 GW less capacity than the 80% RES pathway, reflecting that in a 40% RES pathway, less power is produced by the intermittent sources and more power are produced withing each region.

Bibliography

[1] German Aerospace Center (DLR). Trans-mediterranean interconnection for concentrating solar power, 2006.

[2] The Intergovernmental Panel on Climate Change. A report of working group i of the intergovernmental panel on climate change, 2007. http://www.ipcc.ch.

[3] M. King Hubbert. The world's evolving energy system, 1981. American Journal of Physics 49 november 1981.

[4] David Mackay. sustainable energy - without the hot air, 2008. http://www.withouthotair.com.

[5] Massachusetts Institute of Technology, 2008. http://web.mit.edu/newsoffice/2008/china-energy-1006.html.

[6] International energy agency, 2008.

[7] Roger A. Hinrichs and Merlin Kleinbach. Energy - its use and the environment, 2006. Brooks Cole; 4 edition ISBN-13: 978-0495010852.

[8] Gordon J. Aubrecht. Energy - physical, environmental, and social impact, 2006. Benjamin Cummings; 3 edition ISBN-13: 978-0130932228.

[9] The Intergovernmental Panel on Climate Change. Ipcc third assessment report, 2001. http://www.ipcc.ch.

[10] Duffy P. and Santer B. Solar variability does not explain late-20th-century warming., 2009. Phys today.

[11] Kevin E. Trenberth. An imperative for climate change planning: tracking earths global energy, 2009. Curr.Opin.Environ.sustainability 1 19.

[12] Finn Ingebretsen ivin Holter and Hugo Parr. Fysikk og energiressurser, 1998. Universitetsforlaget ISBN: 9788200229278.

[13] Active Cavity Radiometer Irradiance Monitor. http://www.acrim.com.

[14] Dennis L. Hartmann. Global physical climatology, 1994. Academic Press; 1 edition ISBN-13: 978-0123285300.

[15] S. Valley. Handbook of geophysics and space environments, 1965. McGraw-Hill.

[16] SoDa (Solar radiation data. Services for professionals in solar energy and radiation, 2006. http://www.soda-is.com/eng/map/.

[17] EPIA. European photovoltaic industry association, 2008. http://www.epia.org/policy/national-policies/germany/german-pv-market.html.

[18] EIA. U.S Energy information administration, 2008. http://www.eia.doe.gov/pub/international/iealf/table18.xls.

[19] common resource. reference to picture, unknown. http://en.wikipedia.org/wiki/Solar_-cell.

[20] S.M. Sze. Physics of semiconductor devices, 1981. Wiley and Sons Inc. ISBN: 0471 05661-8.

[21] Jenny Nelson. The physics of solar cells, 2003. Imperial college press ISBN: 1-86094-340-3.

[22] Nancy Stauffer MIT. Building solar cells from ribbons, 2007. http://web.mit.edu/mitei/research/spotlights/building-solar.html.

[23] renewableenergyworld.com. Spire produces most efficient large area cpv cell, 2010. http://www.renewableenergyworld.com.

[24] STANFORD UNIVERSITY Global Climate Energy Project (GCEP). An assessment of solar energy conversion technologies and research opportunities, 2006. http://gcep.stanford.edu/pdfs/assessments/solar_assessment.pdf.

[25] renewableenergyworld.com. German researchers crack 20 percent thin film solar cell efficiency ceiling, 2010. http://www.scientificamerican.com.

[26] Cleantech. Kyocera sets new solar cell efficiency record, 2010. http://cleantechnica.com/2010/02/14/kyocera-sets-new-solar-cell-efficiency-record.

[27] Ren21. Renewable energy policy network for the 21st century, 2009. http://www.ren21.net/pdf/RE_GSR_2009_update.pdf.

[28] European Commision. reference to picture, unknown. http://ec.europa.eu/research/energy/eu/research/csp/index_en.htm.

[29] Stirling Energy Systems. Stirling energy systems, 2010. http://www.stirlingenergy.com/technology.htm.

[30] The California Energy commission. Imperial valley solar project, 2010. http://www.energy.ca.gov/sitingcases/solartwo/index.html.

[31] NREL/Solarpaces. Concentrating solar power projects, 2010. http://www.nrel.gov/csp/solarpaces/power_tower.cfm.

[32] Solarpaces. Solar parabolic trough system description, 1998. http://www.solarpaces.org/CSP_Technology/docs/solar_trough.pdf.

[33] Energy Efficiency, Renewable Energy, and DOE. Solar energy technologies program, 2010. http://www1.eere.energy.gov/solar/linear_concentrators.html.

[34] Sargent, Lundy Sunlab, and NREL. Assessment of parabolic trough and power tower solar technology cost and performance forecasts, 2003. http://www.nrel.gov/solar/parabolic_trough.html.

[35] Solar Millenium. The parabolic trough power plants andasol 1 to 3, 2008. http://www.solarmillennium.de/upload/Download/Technologie/eng/Andasol1-3engl.pdf.

[36] GE energy. Ge's h system, 2008. http://www.ge-energy.com/prod_serv/products/gas_-turbines_cc/en/h_system/index.htm.

[37] U.S Department Of Energy. Doe solar energy technolgies program fy 2008 annual report, 2008. http://www1.eere.energy.gov/solar/pdfs/fy08_annual_report_43987.pdf.

[38] Dr. David W. Kearney. Parabolic trough collector overview, 2007. http://www.nrel.gov/csp/troughnet/pdfs/2007/kearney_collector_technology.pdf.

[39] C. Kennedy K. Terwilliger and M. Milbourne. Development and testing of solar reflectors, 2004. http://www.nrel.gov/docs/fy05osti/36582.pdf.

[40] Toby Procter CSP today newspaper. Parabolic trough reflectors: Does glass still have the cutting edge?, 2010. http://social.csptoday.com/industry-insight/parabolic-trough-reflectors-does-glass-still-have-cutting-edge.

[41] German Aerospace Center and Solarpaces. Optical characterisation of reflector material for concentrating solar power technology, 2009. http://elib.dlr.de/61684/1/SolarPaces2009_Mirror-Characterisation.pdf.

[42] Reflectech. Reflectech, 2010. http://www.reflectechsolar.com.

[43] Guardian Industries. Guardian industries, 2010. http://www.guardian.com/en/na/gp_-014929.html.

[44] Hank Price Eckhard Lupfert David Kearney Eduardo Zarza Gilbert Cohen Randy Gee Rod Mahoney. Advances in parabolic trough solar power technology, 2002. http://nd.edu/ me463d18/Files/Derek/Sources/parabolic_trough.pdf.

[45] Skyfuel Inc. skyfuel inc, 2010. http://www.skyfuel.com/.

[46] SolarPACES. Concentrating solar power projects, 2010. http://www.nrel.gov/csp/solarpaces/.

[47] American Society of Mechanical Engineers. Development steps for parabolic trough solar power technologies with maximum impact on cost reduction, 2007. http://www.pre.ethz.ch/publications/journals/full/j138.pdf.

[48] Andreas Hberle et.al. The solarmundo line focussing fresnel collector. optical and thermal performance and cost calculations., 2003. http://www.solarpaces.org/CSP_Technology/docs/solarpaces_fresnel_9_2002.pdf.

[49] California Energy commision. Comparative costs of california central station electricity generation technologies, 2007. http://www.energy.ca.gov/2007publications/CEC-200-2007-011/CEC-200-2007-011-SD.PDF.

[50] National Renewable Energy Laboratory. Baseline cost of energy, 2008. http://www.nrel.gov/wind/coe.html.

[51] Nuclear Energy Agency and International Energy Agency. Projected costs of generating electricity, 2005. http://www.iea.org/publications/free_new_Desc.asp?PUBS_ID1472.

[52] Reiner Gaertner. Germany embraces the sun, 2007. http://www.wired.com/science/discoveries/news/2001/07/45056.

[53] Greenpeace Solar paces and ESTIA. Concentrated solar thermal power - now, 2005. www.greenpeace.org.

[54] Electric storage association (ESA). Technologies and applications, 2009. http://www.electricitystorage.org.

[55] W. Greiner et. al. Thermodynamics and statistical mechanics, 2004. Springer ISBN 978-0-387-94299-5.

[56] Michael Schirber. How compressed air could power the future, 2008. http://www.livescience.com/technology/080604-pf-caes.html.

[57] The Australian National University Solar Thermal group. Closed loop thermochemical energy storage system using ammonia, 2008. http://solar-thermal.anu.edu.au/.

[58] K. Lovegrove. Thermodynamic limits on the performance of a solar thermochemical energy storage system, 1993. INTERNATIONAL JOURNAL OF ENERGY RESEARCH, VOL. 17,817-829 (1993).

[59] S.Z. Baykara. Hydrogen production by direct solar thermal decomposition of water, possibilities for improvement of process efficiency, 2004. International Journal of Hydrogen Energy 29 (2004) 1451 1458.

[60] U.S. Department of Energy. High-temperature water splitting, 2008. http://www1.eere.energy.gov/hydrogenandfuelcells/production/water_splitting.html.

[61] A. Steinfeld. Solar thermochemical production of hydrogena review, 2005. http://www.pre.ethz.ch/publications/journals/full/j111.pdf.

[62] A. Steinfeld. Solar hydrogen production via a two-step water-splitting thermochemical cycle based on zn=zno redox reactions, 2002. http://pre.ethz.ch/publications/journals/full/j78.pdf.

[63] A-T-Raissi et.al. Hydrogen production via solar thermochemical water splitting, 2004. NASA/CR2009-215441.

[64] Science magazine. Sunlight in your tank, 2009. www.sciencemag.com.

[65] W. Weimer et.al. Development of a solar-thermal zno/zn water-splitting thermochemical cycle, 2009. http://www.nrel.gov/hydrogen/pdfs/development_solar-thermal_-zno.pdf.

[66] Petra De Boer et.al. Technologies, 2009. http://www.electricitystorage.org.

[67] netPowertech. Technologies, 2007. http://www.netpowertech.com.

[68] Petra De Boer et.al. Flow batteries, 2009. http://www.leonardo-energy.org/webfm_-send/164.

[69] D.M. Blake et. al. New heat transfer and storage fluids for parabolic trough solar thermal electric plants, 2002. http://www.jkearney.com/ dwk/TES_Papers/Blake_Advanced_-HTF.pdf.

[70] Therminol. Thermonol heat transfer fluid, 2010. http://www.therminol.com/pages/.

[71] James E. Pacheco et.al. Development of a molten-salt thermocline thermal storage system for parabolic trough plants, 2002. http://www.p2pays.org/ref/22/21032.pdf.

[72] Zarza et.al. Direct steam generation in parabolic troughs: Final results and conclusions of the diss project, 2010. DLR and Cieamat institute.

[73] Markus Eck and Klaus Hennecke. Heat transfer fluids for future parabolic trough solar thermal power plants, 2008. German Aerospace Centre (DLR) Institute of Technical Thermodynamics.

[74] L. Moens and D.M. Blake. Advanced heat ransfer and thermal storage fluids, 2004. http://www.nrel.gov/docs/fy05osti/37083.pdf.

[75] A. Brosseau et.al. Testing thermocline filler materials and moltensalt heat transfer fluids for thermal energy storage systems used in parabolic trough solar power plants, 2004. http://www.nrel.gov/csp/troughnet/pdfs/brosseau_sand2004_3207_final.pdf.

[76] Bruce Kelly. Two tank direct thermal storage system solar two and solar tres central receiver power plants, 1999. www.nrel.gov/csp/troughnet/pdfs/kelly_solar_two_experience.pdf.

[77] Azom the A to Z of materials. Silica silicon dioxide, 2009. http://www.azom.com.

[78] M. Medrano et.al. State of the art on high-temperature thermal energy storage for power generation, 2004. Renewable and Sustainable Energy Reviews 14 (2010) 5672.

[79] E. Zarza et.al. The diss project: Direct steam generation in parabolic troughs operation and maintenance experience, 2001. Proceedings of Solar Forum 2001 Solar Energy: The Power to Choose April 21-25, 2001, Washington, DC.

[80] Solar Energy Research lnstitute. Phase-change thermal energy storage, 1989. http://www.nrel.gov/csp/troughnet/pdfs/3516.pdf.

[81] Lovhoiden et.al. Generell fysikk for universiteter og hgskoler. bd. 1 mekanikk, 2001. Universitetsforlaget ISBN: 82-15-00006-1.

[82] Dr Alan Ruddell. Investigation on storage technologies for intermittent renewable energies, 2003. http://www.itpower.co.uk/investire/pdfs/flywheelrep.pdf.

[83] John D. Boyes. Technologies for energy storage - flywheels and super conducting magnetic energy storage, 2003. Sandia National Laboratories.

[84] David J. Griffiths. Introduction to electrodynamics, 2008. Person Benjamin cummings ISBN 0-13-919960-8.

[85] European Climate Foundation (ECF). Roadmap 2005 - a practical guide to a prosperous low carbon europe, 2010. http://www.roadmap2050.eu/.

[86] European Climate Foundation (ECF). Volume 1 - technical and economic analysis, appendix a - generation, 2009. http://www.roadmap2050.eu/downloads.

[87] Jeremy Leggett. The solar century, 2009. Profile books Ltd. ISBN: 9781846688737.

[88] ABB. Hvdc thyristor valves, 2008. http://www.abb.com/industries/db0003db004333/284fe98f752a0588c1

[89] Siemens. High voltage direct current transmission - proven technology for power exchange, 2008. http://www.siemens.com/pool/en/whats_new/features/power/hvdc_-proven_technology.pdf.

[90] Chan-Ki Kim Vijay K. Sood et. al. Hvdc transmission - power conversion applications in power systems, 2009. John Wiley and Sons ISBN 978-0-470-82295-1.

[91] R. Rudervall et.al. High voltage direct current (hvdc)transmission systems technology review paper, 2008. ABB group.

[92] Wikipedia. War of currents, 2009. http://en.wikipedia.org/wiki/War_of_Currents.

[93] J.E. Skog et.al. The norned hvdc cable link power transmission highway between norway and the netherlands, 2006. www.abb.com.

[94] N. Negra et.al. Loss evaluation of hvac and hvdc transmission solutions for large offshore wind farms, 2008. Electric Power Systems Research 76 (2006) can be found at www.sciencedirect.com.

[95] German Aerospace Center (DLR). Concentrating solar power for the mediterranean region, 2005. http://www.dlr.de/tt/med-csp.

[96] ABB Power Technologies AB. Ultra high voltage dc systems, 2008. www.abb.com/hvdc.

[97] ABB. Ultra high voltage dc systems, 2009. ttp://www.abb.com.

[98] B. Kelly. Nexant parabolic trough solar power plant systems analysis, 2005. http://www.nrel.gov/csp/troughnet/pdfs/40162.pdf.

[99] B. Kelly. Nexant parabolic trough solar power plant systems analysis task 3: Multiple plants at a common location, 2005. http://www.nrel.gov/csp/troughnet/pdfs/40164.pdf.

[100] Hydro. Floating windmills, 2005. http://www.hydro.com/en/Press-room/News/Archive/2005/November/16878.

[101] United States Geological Survey. Potash statistics and information, 2009. http://minerals.usgs.gov/minerals/pubs/commodity/potash.

[102] Steffen Thorsen. Sunrise and sunset calculator, 2008. http://www.timeanddate.com/.

[103] Gordon J. Aubrecht. Energy - physical, environmental, and social impact ch 21 extension 4, 2005. http://wps.prenhall.com/wps/media/objects/2513/2574258/pdfs/E21.4.pdf.

[104] Skre et. al. Solar cells, 2008. http://org.ntnu.no/solarcells/pages/PV.php.

[105] Jessika Toothman and Scott Aldous. How solar cells work, unknown. http://science.howstuffworks.com/solar-cell.htm.

[106] A. Tipler and A. Llewellyn. Modern physics fourth edition, 2003. W.H Freeman ISBN 0-7167-4345-0.

[107] A. Daniels. Introduction to electrical machines. macmillan publishers., unknown. http://en.wikipedia.org/wiki/File:Transformer3d_col3.svg.

[108] William B. Stine and Michael Geyer. Power from the sun, 2001. http://www.powerfromthesun.net/book.htm.

[109] Duffie and Beckman. Solar engineering of thermal processes, 1980. John wiley and sons.

[110] Roland winston. Light collection within the framework of geometrical optics, 1970. JOURNAL OF THE OPTICAL SOCIETY OF AMERICA VOLUME 60 NUMBER 2.

[111] A.B. Meinel and M.P. Meinel. Applied solar energy: An introduction, 1976. Addison-Wesley isbn13: 9780201047196.

[112] Solar Millenium AG. Picture of the andasol plants, 2009. http://www.solarmillennium.de.

[113] German Aerospace Center (DLR). Picture of the andasol plants, 2009. http://www.dlr.de/en.

[114] German Aerospace Center (DLR). Picture of nevada solar one, 2009. http://www.acciona-na.com.

[115] European Climate Foundation (ECF). Volume 1 - technical and economic analysis, appendix b-e - grid, 2009. http://www.roadmap2050.eu/downloads.